FORSCHUNGSZENTRUM JÜLICH GmbH

KFA

Institut für Chemie und Dynamik der Geosphäre 3: Atmosphärische Chemie

Distribution of C_1 - C_2 Aldehydes in the Free Troposphere

D.W. Arlander U. Schmidt D.H. Ehhalt

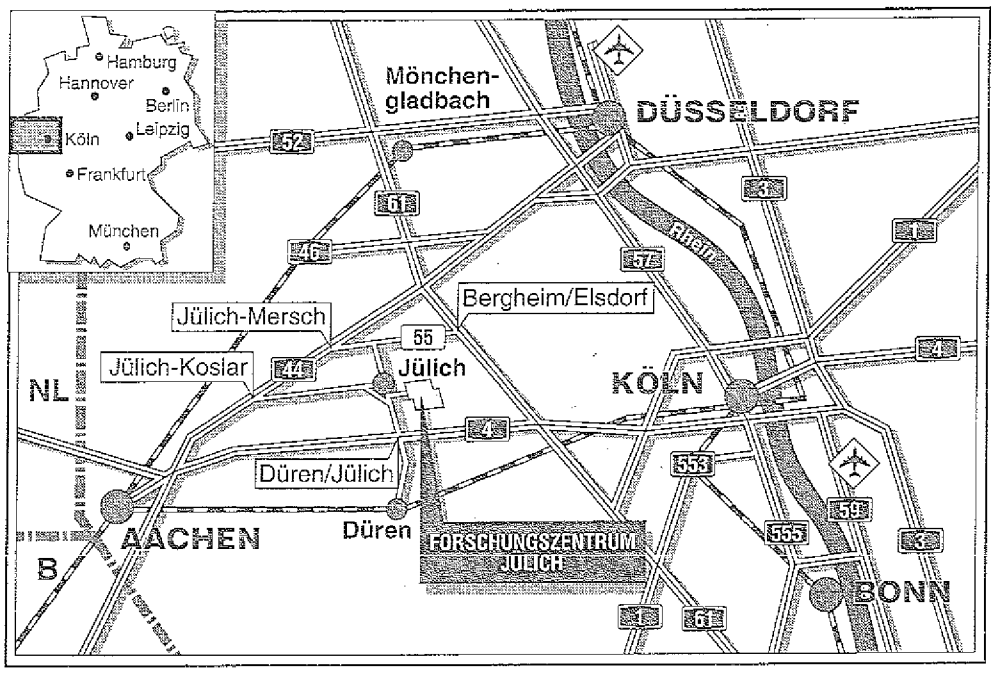

Berichte des Forschungszentrums Jülich ; 2650
ISSN 0366-0885
Institut für Chemie und Dynamik der Geosphäre 3: Atmosphärische Chemie Jül-2650
D 38 (Diss. Universität Köln)

Zu beziehen durch: Forschungszentrum Jülich GmbH · Zentralbibliothek
Postfach 1913 · D-5170 Jülich · Bundesrepublik Deutschland
Telefon: 02461/61-6102 · Telefax: 02461/61-6103 · Telex: 833556-70 kfa d

Distribution of C_1 - C_2 Aldehydes in the Free Troposphere

D.W. Arlander* U. Schmidt D.H. Ehhalt

* Dissertation

Abstract

A sensitive and selective measurement technique for the determination of tropospheric formaldehyde and acetaldehyde in background air is described. The method is based on the derivatization of aldehydes with 2,4-dinitrophenylhydrazine (DNPH). The derivative aldehyde hydrazones are then seperated using high performance liquid chromatography (HPLC) and detected at 355 nm using a conventional HPLC-UV/VIS absorbance detector.

Aldehydes were collected with Waters Sep-Pak C-18 DNPH-coated cartridges using a portable sampling system. The apparatus proved to be easy and convenient to operate, even in remote clean air locations where aldehyde mixing ratios and their natural variations are likely to be of special interest in air chemistry.

The method was used for ground-based measurements of formaldehyde and acetaldehyde during an uninterupted two-week period in August 1990 in Jülich. Ground level measurements in Jülich for formaldehyde and acetaldehyde were shown to vary from 0.5 to 7 ppb and 0.1 to 2.0 ppb, respectively. Diurnal mean mixing ratios of formaldehyde and acetaldehyde were 2.8 +/- 1.5 ppb and 0.7 +/- 0.4 ppb respectively. Significant diurnal patterns were observed with maximum mixing ratios in the early afternoons, and minimum mixing ratios shortly before sunrise. A potential interference from organic hydroperoxides is also discussed.

Aircraft measurements up to nearly 5 km over the Eifel region in Germany from Summer 1990 to November 1990 showed the potential of cartridge-based methods for aldehyde measurements in the free troposphere. These test flights indicated that formaldehyde vertical profiles can be dependent on inversion height and cloud frequency. In-cloud formaldehyde measurements tended to be lower than gas-phase measurements. This effect is

most likely due to efficient absorption of formaldehyde into the droplets followed by rapid aqueous-phase oxidation.

The above mentioned sampling and analysis techniques were also used to determine mixing ratios of tropospheric formaldehyde up to 10 km altitude and acetaldehyde up to 5 km in January 1991 during the TROPOZ-II measurement campaign from 70^{o} N to 55^{o} S latitude aboard the French Caravelle 116 CEV (Centre d' Essais en Vol) research aircraft. Numerous vertical profiles were obtained which yielded a first ever characterization of formaldehyde and acetaldehyde distributions throughout the free troposphere. Above the mixing layer, aldehyde mixing ratios typically decreased with increasing altitude. Lowest values (ca. 50 ppt) of formaldehyde were detected in the upper troposphere. At this altitude, the practical detection limit of the method is reached.

Comparison of formaldehyde measurements with model results indicate that although methane is a very significant formaldehyde precursor, the inclusion of naturally emitted nonmethane hydrocarbons (NMHCs; C_2 to C_6) and possibly industrial sources are necessary in order to predict tropospheric formaldehyde mixing ratios more accurately.

Zusammenfassung

Es wurde eine Meßmethode zum spezifischen und empfindlichen Nachweis von Formaldehyd und Acetaldehyd in Reinluftgebieten weiter entwickelt und verwendet. Für die Probennahme und Anreicherung der Aldehyde wurden Kartuschen eingesetzt, die mit einer 2,4-Dinitrophenylhydrazin-beschichteten C-18 Packung verwendet wurden. Anschließend wurden die Hydrazonderivate durch Hochleistungsflüssigkeits-chromatographie (HPLC) getrennt und mit einem UV/VIS-Detektor bei 355 nm nachgewiesen.

Im August 1990 wurden in Jülich während einer zweiwöchigen Meßkampagne Formaldehyd- und Acetaldehyd-mischungsverhältnisse in Bodenluft gemessen. Sie zeigten deutliche Tagesgänge für Formaldehyd (0.5 bis 7 ppb) und Acetaldehyd (0.1 bis 2.0 ppb). Tagesmittelwerte für Formaldehyd and Acetaldehyd lagen bei 2.8 +/- 1.5 ppb und 0.7 +/- 0.4 ppb. Maximale Mischungsverhältnisse wurden normalerweise am frühen Nachmittag beobachtet und minimale Werte kurz vor Sonnenaufgang. Eine mögliche Störung der Formaldehydbestimmung wird ebenfalls diskutiert.

Flugzeugmessungen bis etwa 5 km Höhe wurden im Zeitraum von Juli 1990 bis November 1990 über der Eifelregion durchgeführt, um die Anwendbarkeit der Aldehydsammelkartuschen zu überprüfen. Die Messungen zeigten eine deutliche Höhenabhängigkeit für Formaldehyd. Oberhalb der planetarischen Grenzschicht nahmen die Formaldehydmischungsverhältnisse stark ab. Messungen innerhalb Wolken deuteten niedrigere Mischungsverhältnissen als außerhalb. Als Ursache dafür kommt die Absorption von Formaldehyd in den Tröpfen und nachfolgende Reaktionen in Betracht.

Ein erstmaliger Überblick der troposphärischen (1 bis 10 km und 70° N bis 55° S) Verteilung von Formaldehyd und Acetaldehyd wurde durch die TROPOZ-II Flugzeugexpedition an Bord der Caravelle 116 der CEV (Centre d' Essais en Vol) im

Januar 1991 ermöglicht. Meßdaten und Modellergebnisse dieser Meßkampagne weisen auf die Bedeutung der Nichtmethan-kohlenwasserstoffe (NMKW) als wichtige photochemische Quelle für Formaldehyd neben Methan hin.

C O N T E N T S

1.1 Introduction

Although the atmospheric aldehydes, formaldehyde HCHO, and acetaldehyde CH_3CHO, are known to have several anthropogenic sources, the oxidation of naturally emitted hydrocarbons represents the major source of these aldehydes in the remote global troposphere. Major anthropogenic sources of aldehydes consist of primary combustion emissions from industrial sources and automobiles. Aldehydes are also formed as secondary products of photochemical smog. Aldehyde mixing ratios in the vicinity of metropolitan areas have been reported as high as 100 parts-per-billion (ppb, 10^{-9} v/v) or higher (Grosjean, 1982; Altshuller and McPherson, 1963). Altshuller (1989) reported formaldehyde and acetaldehyde mixing ratios in the lower ppb range upwind of several large cities in the USA to an elevation of 1.5 km. These summertime measurements of formaldehyde and acetaldehyde at near mixing layer heights varied from < 1.0 ppb to 3.5 ppb, and below 0.9 ppb, respectively. More information on these measurements is contained in Westberg and MacGregor, (1987).

In comparison to the urban measurements, relatively few aldehyde measurements in remote areas or in the free troposphere have been reported. Previous measurements of formaldehyde in the free troposphere above the Eifel region in Germany up to nearly 7 km made by Lowe et al., (1981) showed that the vertical profile of formaldehyde can be highly dependent upon inversion height. Above inversions (> 2.5 km), formaldehyde mixing ratios quickly decline with increasing altitude (< 0.25 ppb) and should in many cases be representative of clean background air. In the absence of an inversion, formaldehyde mixing ratios in summer were relatively high (2 - 3 ppb) to an elevation of nearly 3 km due to vertical transport and active photochemical production.

Since aldehydes have atmospheric life times on the order of only several hours, mixing ratios in the free troposphere,

in remote areas, or in the marine troposphere are considerably lower (0.1 to 2.0 ppb) (Schmidt and Lowe, 1981; Arlander, 1988; Arlander et al., 1990, and references therein). In the case of formaldehyde, the oxidation of atmospheric methane CH_4 with an average global mixing ratio of about 1.7 ppm, is the major production mechanism. In the free troposphere or in remote areas, the oxidation of naturally emitted nonmethane hydrocarbons (NMHCs) such as ethane, ethene, propane, propene, isoprene, terpenes, among others via OH radical or ozone can represent a major source of aldehydes. Although the combined mixing ratios of the C_2 to C_6 NMHCs is only on the order of a few ppb (Rudolph and Ehhalt, 1981; Eichman et al., 1979), the alkenes and alkanes are photochemically more active than methane, and can therefore represent an important source of carbonyls throughout the free troposphere of nearly equal if not more significance than methane (Ehhalt et al., 1985).

Photochemical models which estimate ground level HCHO mixing ratios solely from the oxidation of methane by $OH^{\cdot}$ predict HCHO to be in the 0.1 to 0.45 ppb range in the background troposphere (Graedel, 1979; Calvert, 1980; Logan et al., 1981).

Predicted acetaldehyde values of about 0.02 ppb have been calculated with ethane as the precursor (Singh and Hanst, 1981). The underprediction of the models for both formaldehyde and acetaldehyde may be explained by the exclusion of the oxidation of additional NMHCs, and the possible error in the reaction rate constants used in the models.

1.2 Production mechanisms for tropospheric formaldehyde and acetaldehyde

Formaldehyde is naturally formed in the troposphere from the oxidation of hydrocarbons. Hydrocarbons react with OH radical and ozone to form HCHO and/or other aldehydes or

ketones as intermediates in a series of reactions that ultimately lead to CO, H_2, H_2O and CO_2 (Zimmerman et al., 1978, Calvert, 1980). The main photochemical source of HCHO in the natural atmosphere is from the oxidation of methane:

$$CH_4 + OH^{\cdot} \longrightarrow CH_3^{\cdot} + H_2O \quad (1)$$

$$CH_3^{\cdot} + O_2 + M \longrightarrow CH_3O_2^{\cdot} \quad (2)$$

$$CH_3O_2^{\cdot} + NO \longrightarrow CH_3O^{\cdot} + NO_2 \quad (3)$$

$$CH_3O^{\cdot} + O_2 \longrightarrow HCHO + HO_2^{\cdot} \quad (4)$$

However, in the case where the NO level is low (< 10 ppt) as in the remote marine troposphere, reaction (3) may be sufficiently slow so that reaction (5) may compete:

$$CH_3O_2^{\cdot} + HO_2^{\cdot} \longrightarrow CH_3OOH + O_2 \quad (5)$$

$$CH_3OOH + h\nu + O_2 \longrightarrow HCHO + HO_2^{\cdot} + OH^{\cdot} \quad (6)$$

In order to verify the efficiency of reaction (5), much more sensitive measurement techniques for the detection of organic hydroperoxides in the remote atmosphere need to be developed. Photolysis is expected to be the most efficient removal process for gas-phase CH_3OOH, which in turn leads to gas-phase HCHO production. Methyl hydroperoxide may be also heterogeneously removed and is an aqueous-phase source of formic acid in atmospheric water droplets.

$$CH_3OOH + OH^{\cdot} \longrightarrow CH_2(OH)_2 + OH^{\cdot} \quad (7)$$

$$CH_2(OH)_2 + OH^{\cdot} + O_2 \longrightarrow HO_2^{\cdot} + HCOOH + H_2O \quad (8)$$

As net effect from the above reactions, gas-phase removal of methyl hydroperoxide leads to HCHO production, whereas the aqueous-phase removal mechanism tends toward aqueous formic acid production. The aqueous-phase pathway should considered to be plausible only in the lower troposphere.

The photochemical production of formaldehyde and acetaldehyde in the gas-phase by the oxidation of ethene, propene, and propane are shown in detail by Grosjean (1990a). Acetaldehyde is formed as a major product of the reaction of ozone or OH· with all olefins bearing a methyl substituent, i.e., propene, 2-butene (cis and trans), 2-pentene, 2-methyl-2-butene. Dicarbonyl formation is also possible as a decay product of Criegee biradicals formed by the oxidation of 2-methyl-2-butene (Grosjean, 1990b). Acetaldehyde can then be formed by the photolysis of dicarbonyls. Acetaldehyde can also be formed via the OH-paraffin reaction, such as with propane, which proceeds by H-abstraction. A lengthy list of hydrocarbons which act as carbonyl precusors was compiled by Carlier et al., (1986). Compared to an atmospheric lifetime for methane of about 8 - 8.5 years, atmospheric lifetimes for the NMHCs can range from several hours to several weeks depending upon latitude, oxidant levels, altitude and hydrocarbon reactivity (Rudolph and Ehhalt, 1981). The production of formaldehyde and acetaldehyde by the oxidation of several hydrocarbons is shown schematically in Figure 1.1 (Schubert et al., 1988).

1.3 Removal mechanisms for tropospheric formaldehyde and acetaldehyde

Various processes contribute to the removal of tropospheric formaldehyde. The atmospheric lifetime of formaldehyde against gas-phase removal is on the order of several hours depending upon sunlight intensity and oxidant levels (Tables 1.1, 1.2 adapted from Finlayson-Pitts and Pitts, 1986). The major daytime loss mechanism for formaldehyde is photolysis (about 80%), of which two known pathways are shown:

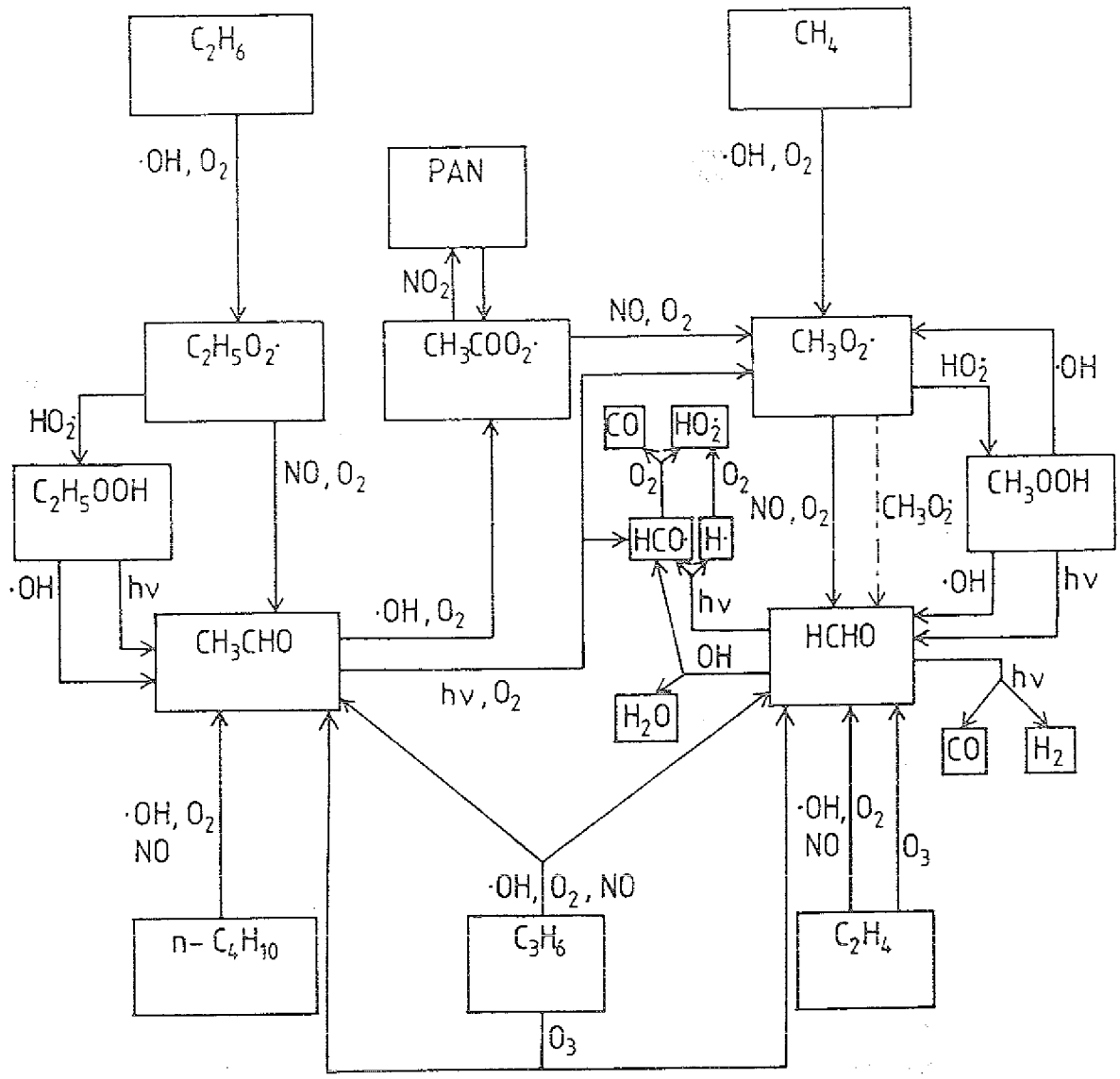

Figure 1.1

Hydrocarbon Oxidation Scheme

For the purpose of gaining a general overview, only the most essential reaction pathways are shown.

Table 1.1

Quantum Yield of Photodissociation of Formaldehyde

Absorption Cross Sections (σ) and Primary Quantum Yields (ϕ) for Reactions (a) and (b) for HCHO at 300°K and One Atmosphere Pressure

λ (nm)	Absorption Cross Section σ (10^{-20} cm^{-2} molecule^{-1})	Quantum Yields ϕa (H + HCO)	ϕb (H_2 + CO)
290	2.51	0.71	0.26
300	2.62	0.78	0.22
310	2.45	0.77	0.23
320	1.85	0.62	0.38
330	1.76	0.31	0.80
340	1.18	~0 (<0.1)	0.69
350	0.42	0	0.40
360	0.06	0	0.12

Table 1.2

Ground-Level HCHO Lifetimes

Lifetimes of HCHO with Respect to Photolysis and to Reaction with OH, HO_2 and NO_3 in Typical Relatively Clean and Polluted Atmospheres[a]

Loss Process	Estimated Lifetime
Photolysis	
Noon, January 1	8.6 h
Noon, July 1	3.8 h
Near sunrise/sunset, July 1 (θ = 86°)	174 h
Reaction with OH	
Relatively clean conditions	2.6 days
Moderately polluted conditions	6.2 h
Reaction with HO_2	
Relatively clean conditions	1.5 days
Moderately polluted conditions	3.7 h
Reaction with NO_3	
Relatively clean conditions	80 days
Moderately polluted conditions	8 days

[a] Concentrations under relatively clean conditions were taken to be as follows: [OH] = 5×10^5 cm^{-3}, [HO_2] = 1×10^8 cm^{-3}, [NO_3] = 2.5×10^8 cm^{-3}. Under moderately polluted conditions, each concentration was taken to be a factor of 10 higher.

$$HCHO + h\nu \longrightarrow H_2 + CO \quad (9a)$$

$$\longrightarrow H^{\cdot} + HCO^{\cdot} \quad (9b)$$

Other possible gas-phase formaldehyde removal mechanisms include reaction with $OH^{\cdot}$ and $NO_3^{\cdot}$, as shown in Table 2. The reaction with $OH^{\cdot}$ is fast enough under most circumstances in the lower troposphere to contribute to formaldehyde removal:

$$HCHO + OH^{\cdot} \longrightarrow HCO^{\cdot} + H_2O \quad (10)$$

$$HCO^{\cdot} + O_2 \longrightarrow HO_2^{\cdot} + CO \quad (11)$$

In reaction 11, the $HO_x^{\cdot}$ which was consumed in reaction 10 is regenerated. In addition, there is a net production of HO_x radicals. The photolytically produced radicals in reaction 9b are both quickly converted to $HO_2^{\cdot}$ via reaction 11, and the hydrogen atom quickly combines with O_2 in a three body reaction to form $HO_2^{\cdot}$. In the lower troposphere this process contributes to about 10 - 15% of the total HCHO removal, yielding 0.3 HO_2 radicals per CH_4 (or HCHO) molecule consumed. The oxidation of methane as well as other alkanes via this oxidation scheme serves as a significant source of atmospheric free radicals (Ehhalt, 1987). Reaction 9a serves as an important source of CO and H_2 in the remote troposphere.

Reaction with $NO_3^{\cdot}$ (Reaction 12) is much too slow in clean atmospheres, but may contribute to formaldehyde loss during the night when other chemical removal mechanisms are minimal.

$$HCHO + NO_3^{\cdot} \longrightarrow HCO^{\cdot} + HNO_3 \quad (12)$$

Laboratory studies reported by Burrows et al., (1989) have shown that HCHO reacts too slowly with $HO_2^{\cdot}$ to represent a significant sink for HCHO or as a source for HCOOH as was previously hypothesized.

Dry deposition of formaldehyde is recognized as a major sink during the night. Dry deposition of formaldehyde has been estimated to be 0.45 cm/s over a body of water (Thompson 1980; Zafiriou et al., 1980). Schubert et. al., (1988) reported an average value of 0.21 cm/s for formaldehyde, and 0.045 cm/s for acetaldehyde over water. Model predictions from the same study estimated 0.33 cm/s for both formaldehyde and acetaldehyde. The large discrepancy between measurements and predictions for acetaldehyde was attributed to low solubility, uncertainties in turbulent mixing above water, and chemical or biological decomposition in water.

Heterogeneous loss processes (wash out, rain out, aerosol nucleation) represent 5 to 10% of total formaldehyde removal in lower troposphere. The destruction of formaldehyde in the aqueous-phase occurs primarily through oxidation by $OH^{\cdot}$. Once solubilized, formaldehyde becomes hydrated, is oxidized, and acts as a possible source of atmospheric formic acid:

$$HCHO(g) \quad <---> \quad HCHO(aq) \quad <---> \quad CH_2(OH)_2(aq) \qquad (13)$$

$$CH_2(OH)_2 + OH^{\cdot} + O_2 \; ---> \; HO_2^{\cdot} + HCOOH + H_2O \qquad (8)$$

This sequence has been well studied (Chameides and Davis, 1983; Adewuyi et al., 1984), and is generally recognized as a significant source of formic acid in precipitation as originally observed by Galloway et al., (1982), Keene et al., (1983), and Chapman et al., (1986). The lifetime of aqueous-phase formaldehyde against $OH^{\cdot}$ oxidation as discussed in Lelieveld and Crutzen (1990, 1991) is on the order of 15 minutes.

Aqueous-phase removal mechanisms for acetaldehyde leading to the production of acetic acid are too slow to act as a significant source. The main loss mechanism for acetaldehyde is through reaction with OH radical as shown in reaction 14:

$$CH_3CHO + OH^{\cdot} \longrightarrow CH_3CO^{\cdot} + H_2O \quad (14)$$

$$CH_3CO^{\cdot} + O_2 \longrightarrow CH_3C(O)O_2^{\cdot} \quad (15)$$

$$CH_3C(O)O_2^{\cdot} + NO_2 \longleftrightarrow CH_3C(O)O_2NO_2 \quad (16)$$

$$CH_3C(O)O_2^{\cdot} + NO \longrightarrow CH_3C(O)O^{\cdot} + NO_2 \quad (17)$$

$$CH_3C(O)O^{\cdot} + O_2 \longrightarrow CH_3O_2^{\cdot} + CO_2 \quad (18)$$

The reaction scheme then continues via reaction 3 or 5. Acetaldehyde is weakly photolyzed yielding a methyl and a formyl radical (reactions 19b,c are relatively unimportant for wavelengths longer than 290 nm (Horowitz and co-workers, 1982a,b), which can contribute to a slight increase of atmospheric reactivity.

$$CH_3CHO + h\nu \longrightarrow CH_3^{\cdot} + HCO^{\cdot} \quad (19a)$$

$$CH_3CHO + h\nu \longrightarrow CH_4 + CO \quad (19b)$$

$$CH_3CHO + h\nu \longrightarrow CH_3CO^{\cdot} + H \quad (19c)$$

Further reactions of these photolysis products were previously shown to lead to the direct production of either formaldehyde or free radicals.

1.4 Scope of the thesis

From the above mentioned reactions it is clear that the production and destruction of formaldehyde and acetaldehyde are highly dependent on hydrocarbon concentrations, photon flux, and OH radical mixing ratios. As a result of the large diurnal, seasonal, latitudinal and altitudinal variability of these parameters, correspondingly large variations in formaldehyde and acetaldehyde mixing ratios are to be expected. The measurement of formaldehyde and acetaldehyde in remote regions is necessary in order to assess the natural contribution to the chemistry of the free troposphere as apart from anthropogenically influenced processes.

There is presently a lack of in-situ measurement methods which possess the required sensitivity and time resolution to determine mixing ratios of formaldehyde and acetaldehyde in the free troposphere. The aim of this work was the development of a measurement technique which is sensitive enough to permit a general survey of tropospheric distributions of formaldehyde and acetaldehyde to help define the role of these compounds in the global atmospheric cycles of carbon and oxidants such as ozone and the OH radical. Measurements obtained by this method can then be used for the testing and development of current theories of hydrocarbon oxidation in the free and upper troposphere and can assist in the development of more accurate global scale photochemical models.

2. Method development

Many of the present day formaldehyde measurement methods have been developed for the determination of formaldehyde or other carbonyls in urban conditions or at ground level, and consequently lack the sensitivity required for the

quantification of these compounds in the free troposphere. Two recently reported in-situ methods (O'Hara and Singh, 1988; Pierotti, 1990) have shown promise for the sensitive measurement of non-formaldehyde carbonyls via gas chromatography. These methods report detection limits in the 10 to 100 pptv (parts per trillion by volume; 10^{-12} v/v) range for C_2 to C_5 carbonyls. Applicabilty of these methods for formaldehyde is at present unlikely.

Since formaldehyde decomposes on a variety of surfaces, direct detection of picogram quantities of the molecule by standard gas chromatographic methods is virtually impossible. One way in which to increase the stability of formaldehyde is through derivitization. Not only is HCHO then stablized, but detectability is also greatly enhanced. An effective derivatization reagent should react with HCHO under mild conditions with a high yield, possess a high extinction coefficient as derivative, display a reproducibly low background, and be resistant to interferences. The derivatives can then be directly measured using standard high quality HPLC detectors, thus indirectly measuring the amount of aldehyde originally sampled. The most commonly used derivitization methods are reviewed in detail by Sawicki and Sawicki (1975), Carlier et al., (1986), and Otson and Fellin (1988).

In this work several derivatization reagents were thoroughly tested and compared. Derivatization reagents which yield fluorescent reaction products were chosen and tested due to their potentially higher selectivity over many UV/VIS methods. Among the reagents tested were 3-methyl-2-benzothiazolane hydrazine (MBTH) (Hauser and Cummins, 1964) (MBTH determined by HPLC-IR), 2,4 pentadione (Nash, 1953), 5,5-dimethyl-1,3-cyclohexanedione (Dimedone) (Mopper et al., 1983), 1,3-cyclohexanedione (CHD) (Stahovec and Mopper, 1984), diethyl acetonedicarboxylate (DEAC) (Pesez and Bartos, 1972), and dansyl hydrazine (DH) (Johnson et al., 1981; Bächmann et al., 1989). Table 2.1 lists the above mentioned reagents, and

2,4-dinitrophenylhydrazine (DNPH), and their respective absolute HCHO (in-column) detection limits which were achieved using reversed-phase high performance liquid chromatography.

Table 2.1

Absolute Formaldehyde Detection Limits

Reagent	Absolute Detection Limit
MBTH	500 pg (IR)
2,4 Pentadione	300 pg
Dimedone	0.5 pg
CHD	0.8 pg
DEAC	350 pg
DH	10 pg
DNPH	10 pg (UV/VIS)

My laboratory comparisons showed that due to impurities in most reagents or derivative instability, sufficiently low background levels could not often be obtained which could enable the required method sensitivity. From the above mentioned fluorescence reagents, dansyl hydrazine showed the most consistent and lowest background values when used in sampling cartridges. A very high sensitivity for formaldehyde with a detection limit near 10 picograms was obtained. In spite of this, direct comparison of the DNPH and DH methods under the same sampling conditions showed greater reproducibility and similar to better detection sensitivity for the DNPH method. For this reason, the DNPH method was finally chosen for use during most of the mentioned field measurement campaigns. For the past 10 to 12 years, the majority of atmospheric HCHO measurement methods have been based upon the derivatization reaction with DNPH.

Since DNPH derivatives possess high extinction coefficients, and are reproducibly and quantitatively produced, HPLC-UV/VIS has become the universal method of analysis. The DNPH derivatives are very strong absorbers in the near UV and VIS regions with extinction coefficients on the order of 20,000 [liters/mole · cm] or more, allowing detection to the 10 picogram (HCHO) range.

Originally, water was used as the sampling medium due to the high collection efficiency of the highly polar HCHO molecule. Accordingly, various "impinger" geometries and denuder systems were developed (Lowe 1981; Lowe and Schmidt 1982; Cofer and Edahl, 1986; Lazrus et al., 1988; Dasgupta et al., 1988); Carlier et al., 1990 (using acetonitrile). These methods have proven to be sensitive enough for background continental and marine air. The Lowe method, Lowe (1981), was also used for obtaining vertical formaldehyde profiles up to nearly 7 kilometers. Unfortunately at this altitude and above, aqueous sampling solutions can freeze rendering the samples unusable. The chemical equilibrium of the hydrazone derivatives in aqueous solution is highly temperature and pH dependent. For long-term aircraft campaigns, the liquid-phased sampling methods are simply impractical due to storage problems or cumbersome sampling equipment.

With the development of cartridge-based collection methods, many of the shortcomings of impinger methods have been alleviated. Cartridges can be easily stored before and after collection, are stable for several months in dry ice, and sampling systems are very portable and simple to operate. Various DNPH cartridge-based methods are now well documented: Beasley et al., (1980); Fung and Grosjean (1981); Matthews and Howell (1982); Grosjean and Fung (1982); Kuwata et al., (1983); Guenier et al., (1984); Lipari and Swarin (1985); Tejada (1986); Tanner et al., (1988); Druzik et al., (1990); Zhou and Mopper (1990); and Arlander et al., (1990). The majority of these studies were conducted in urban or near

urban locations. Westberg and MacGregor (1987), and Altshuller (1989), reported the first known aircraft based measurements using a cartridge method which we had developed for measuring aldehydes in the lower ppb range upwind of several major urban areas in North America. The DNPH reagent in conjunction with C-18 sampling cartridges has proven itself to be reliable and applicable in a wide range of field conditions. C-18 non-polar packing material is produced by chemically bonding C-18 paraffinic groups onto micron-sized silica-gel spheres, and is identical in form to present-day HPLC reversed-phased packing. Laboratory tests of the DNPH/C-18 sampling cartridge method have yielded a detection limit for formaldehyde in the sub-40 pptv range in 10 liters STP. Such a detection limit is required in order to enable formaldehyde measurements in the 40 to 100 ppt range expected throughout the free troposphere with reasonable temporal and spatial resolution.

Optically-based measurement methods such as DOAS (Differential Optical Absorption Spectrometry, Platt and Perner, 1980) typically need path lengths of several kilometers and are therefore unsuitable for aircraft expeditions. Recent improvements in the measurement of HCHO via TDLS (Tunable Diode Laser Spectroscopy, Harris et al., 1989) has shown much potential for aircraft applications. Due to time, cost and space constraints, the development of a TDLS method was deemed impractical for the present work.

2.1 Reaction of 2,4-dinitrophenylhydrazine with carbonyls

The method is based upon the well known reaction of carbonyl compounds (formaldehyde and acetaldehyde) with 2,4-dinitrophenylhydrazine (DNPH):

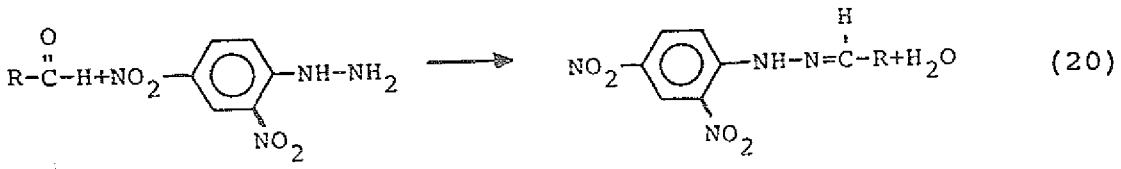

(20)

which proceeds by nucleophilic addition on the carbonyl followed by 1,2-elimination of water and the formation of the 2,4-dinitrophenylhydrazone. The DNPH reagent is very specific for carbonyls and derivatives are formed at high yields in the liquid or solid phase (Waters C-18 Sep-Pak sampling cartridges). Since DNPH is a weak nucleophile, often a small amount of acid is added to the DNPH reagent which promotes the protonation of the carbonyl, thereby accelerating the reaction.

For quantitative sampling and analysis of atmospheric aldehydes in the trace range, it is necessary that the DNPH solution be prepared using high purity DNPH crystals. The DNPH crystals were produced by recrystallizing 99.0% DNPH (Merck, pro analysi, no. 3081) three times in high purity 99.8% HPLC grade acetonitrile (Merck LiChrosolv) between 30 - 50^{o} C. The crystals are then stored in a closed vessel at room temperature in a helium atmosphere protected from light. The concentration of the DNPH solution used for cartridge coating was typically between 55 to 80 ug/ml in acetonitrile, which yields approximately 20 ug DNPH in the C-18 cartridge after coating and drying (coating procedure listed in Section 2.6a). For all field measurements described in the present work, a minimum molar ratio of at least twentyfold of DNPH to HCHO was maintained. These results are in accordance with previous work

(Arlander, 1988), which showed that a molar ratio of at least 10 must be maintained for optimal aldehyde quantification.

2.2 Analysis by high performance liquid chromatography

Quantitative desorption of the hydrazones from the Waters C-18 Sep-Pak cartridges was achieved with 1.2 ml Merck LiChrosolv HPLC grade acetonitrile pushed slowly through the cartridges with a Hamilton 5.0 ml Luer-Lock syringe (1005LT) into another Hamilton 5.0 ml syringe containing 0.3 ml high purity Merck LiChrosolv HPLC grade water, ensuring that laboratory air never comes in contact with samples. The sample solution is then stable at 5^{o} C for at least 24 hours enabling repeated analysis. For the analysis of the cartridges, a BIOTRONIK HPLC system equipped with two HPLC pumps (model 8100) and a model 8200 HPLC UV/VIS detector was used. The mobile phases (water and acetonitrile) were degassed for 30 minutes prior to mixing with 6.0 high purity helium to remove dissolved gases which are detrimental to chromotographic efficiency. The mobile phases are then mixed on the high-pressure side (downstream of the HPLC pumps) in a Knauer dynamic mixing chamber. A 50 microliter sampling loop was installed into a VICI-Valco C6UN60 injection valve. The 50 microliter sampling loop combined with the 1.5 ml cartridge total elution volume yields a "cartridge-to-column" dilution factor of 30. 0.5 ml of sample is injected for each analysis. After each analysis, 0.5 ml of high purity acetonitrile is injected and analyzed to remove or detect any possible residual artifact present in the HPLC system. Back-to-back analyses of the same sample yields a reproducibility of about 1%, independent of column loading. Detection of the hydrazones is carried out at 355 nm, 0.001 absorption units (full scale). The BIOTRONIK model 8200 UV/VIS detector contained a deuterium lamp light source with an effective range of 190 to 400 nm,

band width of 8 nm, integration time constant of 3 seconds, and a 8 ul flow cell with a 10 mm pathlength. Peak integration was performed by a Merck D-2000 integrator, and a Laumann chart recorder as back up.

DNPH-formylhydrazone standard solutions were used to test the linearity of the detector over a wide range of concentrations (13 pg to 77 ng HCHO in-column). The highly stable hydrazone derivatives were prepared according to Shriner et al., (1980), where successive dilutions were made in a 80/20 v/v mixture of acetonitrile and water. Although the detector shows a very high linearity over the entire range (R = 1.000), the linearity of the detector response starts to deteriorate at very near the detection limit (below 15 picograms HCHO in-column, R = 0.999). R or K, the correlation coefficient is defined as a measure of linearity between two variables, whereby a value of 1 or -1 indicates a perfect direct or indirect relationship, respectively. In practice, the blank cartridges from TROPOZ-II contained typically between 20 and 30 pg (HCHO in-column), and therefore the lowest concentrated samples were slightly above the non-linear region of the detector response. Further non-linearity corrections were not needed for low level samples.

The hydrazone derivatives were separated by using a reversed phase column (250 x 8 x 4.6 mm, Kromasil 5-micron C-8, CS Chromatographie, Langerwehe, Germany) maintained at 35^{o} C in a column oven (Techlab Chromatographie) to eliminate retention time drift. A suitable separation was obtained using an isocratic mobile phase mixture of 55% acetonitrile and 45% water at 1.0 ml/min. As a typical chromatogram, one run of a TROPOZ-II air sample and the corresponding cartridge blank are shown in Figure 2.1. The amount of HCHO in-column in the shown air sample corresponds to approximately 95 picograms, whereas the blank contains ca. 15 picograms HCHO.

Figure 2.1

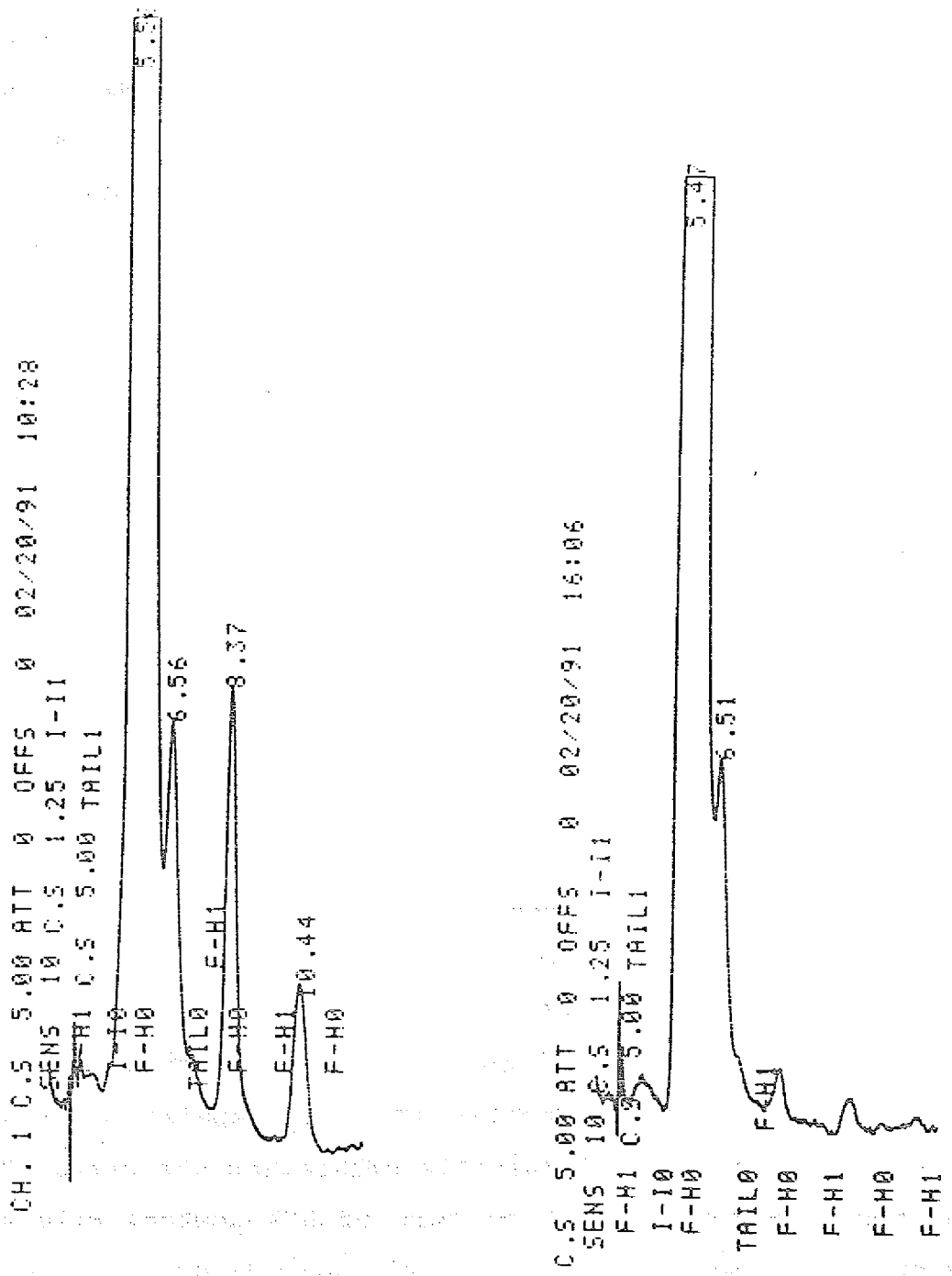

Typical liquid chromatogram of an air sample and corresponding blank from the TROPOZ-II campaign. DNPH-Peaks at 5.5 and 6.6 mins; formaldehyde-DNPHzone at 8.4 min; acetaldehyde-DNPHzone at 10.4 min.

In Table 2.2, several important chromatographic parameters are listed:

Table 2.2

HPLC Chromatographic Parameters

Component	R_t	k'	a
Solvent Front	2.8	-	-
2,4-DNPH	5.5	1.0	-
HCHO-zone	8.4	2.0	2.1
CH_3CHO-zone	10.4	2.7	1.4

- R_t (retention time in minutes)
- k' (solute partition ratio, optimal between 1 and 8)
- a (relative retention, optimal between 1 and 2)

2.3 Air sampling technique

For the collection of atmospheric aldehydes it is important that a homogeneous, stable surface be chosen which facilitates highly efficient collection, is as resistant as possible to interferences, does not hinder derivatization, and be cost effective. In the literature, silica gel, florisil, and C-18 are the most commonly used materials for cartridge-based aldehyde sampling. For reasons explained previously or in the following sections, the Waters Sep-Pak C-18 cartridges were chosen. Waters C-18 cartridges contain 0.5 g +/- 5% of packing material in a HD/UHMW polyethylene casing. The packing is held on both ends with HDPE 35 micron frits.

A schematic of the complete sampling/flow system is shown in Figure 2.2. The flow system consists of a Vacuubrand ME-8C

4-Head Teflon membrane pump, a Brooks 5850 TR Flow controller and a Brooks 5850 TR Flow meter/integrator. A buffer volume of 1 liter is placed behind the pump to ensure stable flow to the flow meter. Before each sampling interval, leak tests are performed to a pressure of 100 mb. The system is then brought up to atmospheric pressure in 5.0 dry N_2. During sampling, leaks can be detected by monitoring the pressure gauge. After the sampling interval and before cartridge removal, the system is returned to atmospheric pressure in N_2 by the manipulation of the four valves.

2.4 Sampling cartridge characteristics

Previous DNPH sampling methods have traditionally used an acid to catalyze the derivitization reaction. In order to minimize contamination, the presently described sampling method was used without an acid. Although the reaction is somewhat slower without the addition of an acid, the overall sensitivity of the method is significantly increased (15 to 25 times); (acids may possibly oxidize the cartridge housing leading to slight aldehyde contamination). Without the addition of an acid, the reaction surface in the Waters C-18 Sep-Pak sampling cartridge is slightly basic (pH= 8.5). The in-cartridge reaction time between DNPH with formaldehyde under these conditions was tested in order to determine if the derivatization process is efficient enough for use in air sampling applications. For these sets of experiments, a series of C-18 DNPH cartridge samples of VICI-HCHO calibration gas (Section 2.5) were taken with identical sampling intervals, and then analyzed by HPLC with differing in-cartridge reaction time intervals from 0 to nearly 120 minutes after sample collection. Reaction completion is determined to be 100% if the signal increase between successive cartridges is insignificant compared to the reproducibility of the method.

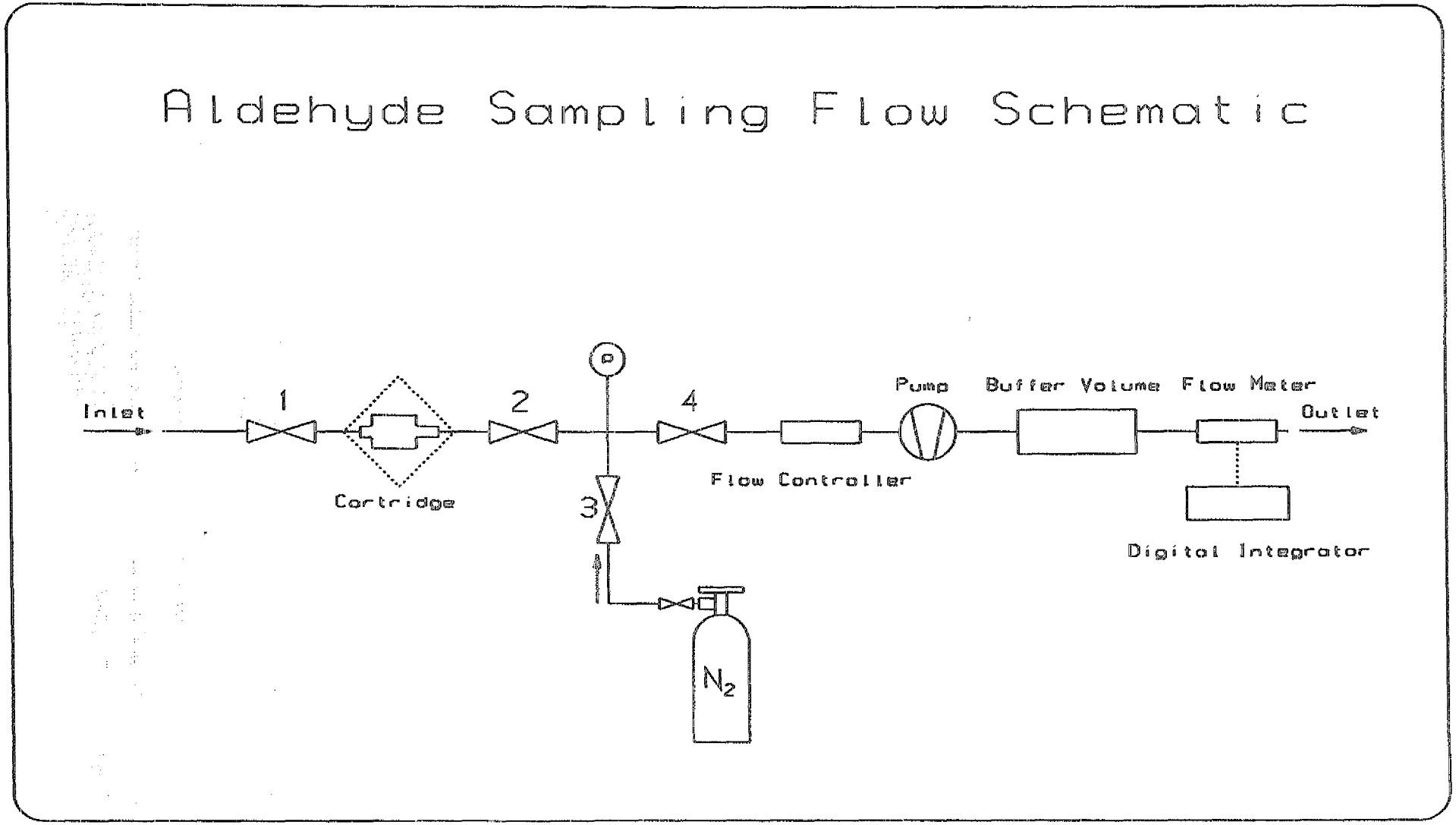

Figure 2.2 (Sampling/Flow System)

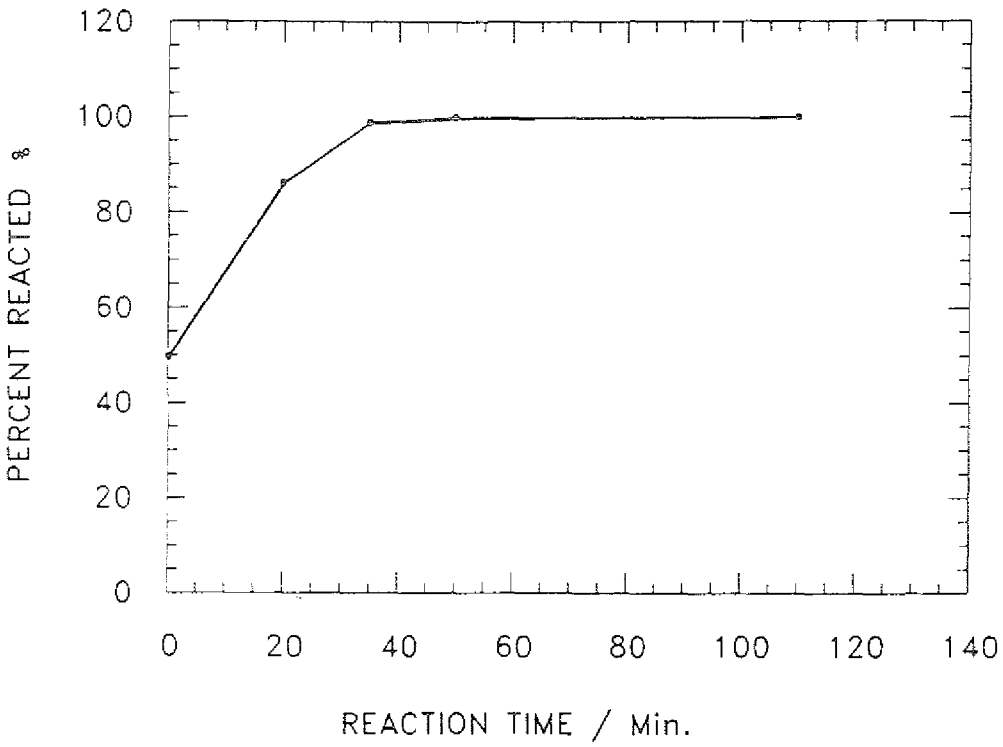

Figure 2.3 Reaction Time (1.5 ug HCHO Loading)

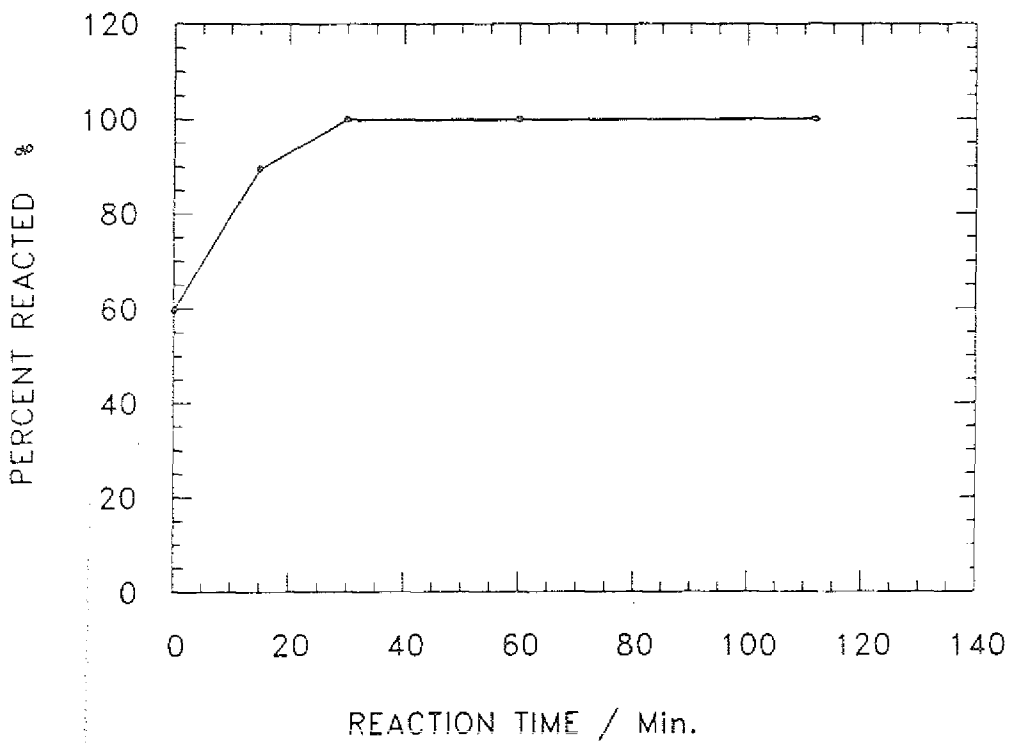

Figure 2.4 Reaction Time (28.4 ng HCHO Loading)

Reaction time required for 100% in-cartridge yield of DNPHzone at 22° C for two HCHO cartridge loadings.

For near 100% reaction completion, 35 minutes at 22° C are required for formaldehyde in 10 L STP calibration gas as shown in Figure 2.3 for 341 ppb at 0.4 Lpm (cartridge loading ca. 1,470 ng HCHO). The reaction time is very similar for cases where cartridge loading was much lower (22.1 ppb, 0.4 Lpm, 28.5 ng HCHO on cartridge) Figure 2.4. Due to steric effects, the reaction time for acetaldehyde is approximately 15% longer for similar loadings. In practice, the aldehyde is reacted out during sample collection, or shortly afterwards before storage.

The HCHO collection efficiency of the DNPH C-18 cartridges was tested for the flow range of 0.4 to 2.4 Lpm STP using 1.3 ppb HCHO calibration gas (10 to 15 L STP). For these experiments, two cartridges were placed in series C_1 in-front and C_2 in-back for each flow rate and then analyzed by HPLC. A blank cartridge (B) was treated identically as the test samples (without flow) and also analyzed by HPLC. Collection efficiency (e), is then calculated according to the following equation:

$$e = [(C_1 - B) - (C_2 - B)/(C_1 - B)] \times 100\% \qquad (1)$$

As shown in Figure 2.5, the collection efficiency for formaldehyde remains high for the entire range (99% to 87% at 22° C). The inherent high sensitivity of the method enables efficient aldehyde collection for most all sampling conditions using low sample volumes (5 to 15 L STP) at low flow rates (0.5 to 1.0 Lpm). Using low sample volumes also lowers the chance of interference. A possible decrease in collection efficiency by sampling at higher temperature is offset by slightly faster derivatization. Laboratory tests conducted at 35° C (cartridges were placed in a Techlab column oven during sampling) using the same sampling procedures yielded signals which were within experimental error to tests at 22° C. Although 100% reaction completion for acidified C-18 DNPH

Figure 2.5

Collection Efficiency of Formaldehyde and Acetaldehyde

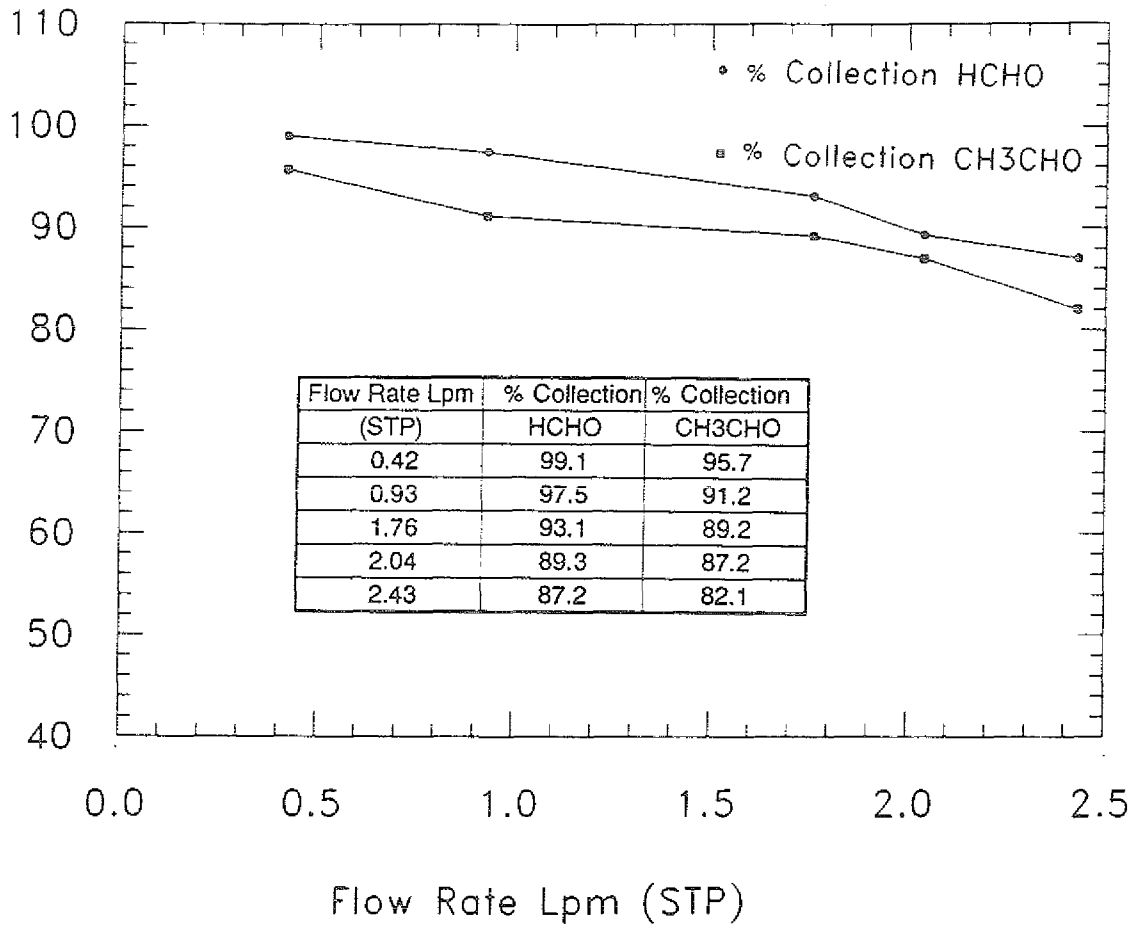

Flow Rate Lpm (STP)	% Collection HCHO	% Collection CH3CHO
0.42	99.1	95.7
0.93	97.5	91.2
1.76	93.1	89.2
2.04	89.3	87.2
2.43	87.2	82.1

Collection efficiencies of formaldehyde and acetaldehyde as a function of flow rate. Sampling for these tests was conducted at 22° C.

cartridges occurs within minutes after sampling, a significantly higher signal or collection efficiency was not evident. Similar tests for acetaldehyde have shown a similar but slightly lower collection efficiency than for formaldehyde using laboratory air (approx. 0.6 ppb CH_3CHO). Over the flow rate range of 0.4 to 2.4 Lpm, the collection efficiency for acetaldehyde ranged from 96% to 82%. At reduced atmospheric pressures, the contact time of the aldehyde on the C-18 packing is shorter. At an altitude of 9 to 10 km, the ambient pressure is typically 260 to 230 hPa. Due to diminished pump performance at low ambient pressures, the maximum flow rate achievable at this ambient pressure is about 0.4 Lpm STP. Collection efficiencies at these low pressures were reduced by about 5% at 0.4 Lpm as determined by laboratory simulation tests.

2.5 Calibration

For calibration purposes, a VICI Metronics Dynacalibrator Model 340 (Santa Clara, Ca.) was used to produce HCHO calibration gas over a wide range of mixing ratios in dry nitrogen. This calibration source is traceable to an N.B.S. (National Bureau of Standards) formaldehyde standard method. The system consisted of two permeation tubes with permeation rates of approximately 10 and 120 ng/min at 70° C, which enabled production of stable HCHO mixing ratios from 600 ppt to 350 ppb depending on amount of nitrogen dilution. The HCHO permeation rates were determined by weighing the tubes on a regular basis (1-2 times per month). The tubes are continually stored at 70° C in a flowing nitrogen atmosphere.

For the development of the calibration curve, a series of cartridge measurements at several mixing ratios (600 ppt, 1.1 ppb, 1.7 ppb, 3.6 ppb and 8.9 ppb) were sampled at ca. 0.4 Lpm in 12 liters of 5.0 dry nitrogen. Respective HCHO in-column

Figure 2.6

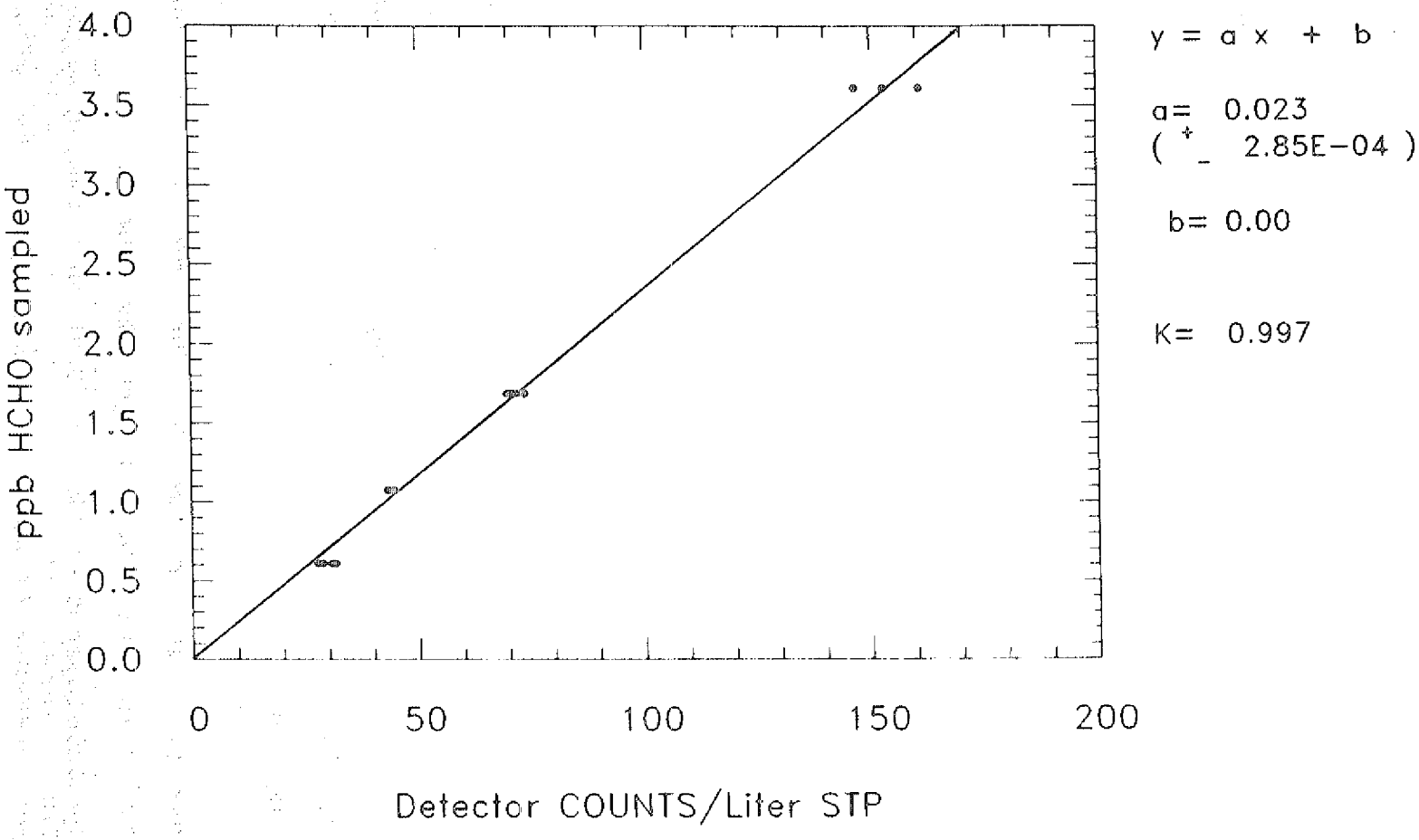

A calibration curve was constructed which directly relates the HPLC detector response divided by the sample volume (Liters STP) to the VICI-HCHO calibration gas mixing ratio in ppb.

loadings for the above mentioned mixing ratios are as listed: 294 picograms, 539 picograms, 833 picograms, 1,764 picograms, and 4,362 picograms. Especially in the lower calibration range, a stabilization time of several hours at constant flow rate is needed to obtain a reproducibility on the order of 7%. Over the range tested (600 ppt to 8.9 ppb), the VICI calibration system exhibited linear behaviour (R = 0.994). For samples collected during TROPOZ-II, a calibration curve was used for the range between 600 ppt to 3.6 ppb, which covered the upper range of collected samples. For the TROPOZ-II calibration, the calibration curve (R = 0.997, N = 16) was forced through the origin (Figure 2.6) in order to quantify samples in the lower ppt-range and to avoid negative mixing ratios. Since the Y-intercept of the calibration curve was very close to the origin, any possible error can be quantified. This matter is discussed further in Section 2.7 (Error analysis).

Since an acetaldehyde permeation source was not available for calibration, atmospheric mixing ratios of acetaldehyde were calculated as a function of the relative response to formaldehyde hydrazone as determined from the formaldehyde and acetaldehyde hydrazone standard solutions. The relative absorption for acetaldehyde hydrazone was seen to be approximately 5% higher than for formaldehyde hydrazone. Taking into account the slightly lower collection efficiency for acetaldehyde was also necessary.

In order to test the long term stability of the UV/VIS detector, dissolved hydrazone standards were repeatedly analyzed during sample analysis. Standard hydrazone solutions (300 picogram aldehyde in-column) were analyzed in periodic intervals, bracketing 3 atmospheric samples. Sample concentrations could then be directly corrected if time dependent changes in detector sensitivity were significant.

The VICI gas-phase HCHO calibration source was chosen over the liquid phase hydrazone standards for the actual

calibration and calculation of the air samples. As also observed and reported by Kirschmer (1989), the use of liquid-phase hydrazone standards can lead to a positive bias of 10% - 11%. Since calibration with liquid phase standards inherently neglects the gas-solid phase interactions which occur in the sampling cartridges during sample collection and VICI-calibration, it does not represent the complete sampling and measurement procedure. This bias is most likely due to the combined effects of hydrazone derivative reaction yield (in-cartridge) and collection efficiency, both of which may under certain circumstances be slightly less than 100%.

A series of intercomparison measurements for formaldehyde were made in conjunction with the Max Planck Institute of Atmospheric Chemistry (MPI), Mainz, Germany. Measurements of the calibration gas used for the calibration of the MPI Tunable Diode Laser Spectroscopy system (TDLS) were taken over a time range of 3 to 10 minutes. The samples were analyzed and compared to similarly loaded samples using our VICI calibration system. On average, the measured HCHO from the MPI permeation tube (approx. 100 ng/min) calibration system was within 10% of previous calibrations carried out in Mainz using an independent calibration method (Chromotrophic acid). During the Tropoz-II campaign, (9) 3-minute measurements of the MPI calibration gas were made to test the day-to-day stability of the MPI HCHO permeation source, and to assist in comparisons of the two HCHO TROPOZ-II data sets.

2.6 Interference tests

There are several possible ways in which the sampling method can be influenced, thus leading to slightly erroneous aldehyde mixing ratios.

a) Physical interferences

Laboratory tests have shown that a significant and variable source of aldehyde contamination in the picogram range is from the cartridge itself. In order to achieve reproducible and low level blanks, the cartridges need to be pretreated with DNPH before use. The following steps are needed to obtain low level and reproducible sampling cartridges and blanks:

1) Cartridges are coated with 1 ml DNPH solution and dried with flowing high purity 6.0 helium.
2) Time is allowed for the DNPH to react with in-cartridge aldehydes (35 minutes at room temperature).
3) Cartridges are then eluted with 1 ml acetonitrile and dried with flowing helium.
4) Cartridges are then recoated with 1 ml DNPH, again dried in flowing helium, sealed, and stored in dry ice.

Freshly made cartridges prepared in this manner yield a background signal which is very near the detection limit of the detector (ca. 10 picograms HCHO in-column, or ca. 300 picograms HCHO in-cart). For a standard 10 L STP sample volume, a detection limit of approximately 30 ppt HCHO can be achieved under ideal conditions. Several types of acetonitrile were tested during the development of the method. For air sampling at ground level concentrations, normally only one coating procedure is required. When freshly prepared cartridges and samples are stored in a refridgerator for longer than several weeks (0-5^{o} C), formaldehyde and acetaldehyde contamination in the trace level can occur. Materials used for the construction of refridgerators can yield above-ambient levels of aldehydes, whereby permeation through the cartridges during storage can occur. In order to minimize this problem, the cartridges are stored in dry ice at

-78° C. The cartridges are then kept in an aldehyde-free CO_2 atmosphere, and temperature-dependent permeation is also hindered. Several tests indicated that cartridges stored in 1dry ice showed only a slight increase in aldehyde contamination in the lower picogram range (10 to 20 pg in-column) for up to nearly two months. This time-dependent increase is in practice "cancelled-out" if samples and their corresponding blanks, of the same age, are both analyzed within a day of each other. Background levels of formaldehyde and acetaldehyde for blanks stored at 0-5° C in a refridgerator were typically 4-5 times higher (ca. 100 picograms HCHO in-col) at the end of the test period. Since both the cartridge casing and DNPH are photolytically sensitive, sample and blank cartridges should be kept out of direct sunlight. This problem can be alleviated by covering the cartridges with aluminum foil especially when sampling outdoors.

b) Chemical interferences

Under polluted conditions there are several airborne substances which could be co-sampled and have possible effects on the DNPH sampling method.

In clean tropospheric air, however, and coupled with the low sample volumes which are needed, the list of possible interferences is limited. In spite of this, a series of interference tests were conducted which included many typical compounds commonly observed in polluted air which may affect aldehyde quantification.

i) Sulfur dioxide

Sulfur dioxide is known to bind with formaldehyde in the aqueous phase. The recovery of HCHO remained quantitative up

to a gas phase mixing ratio of 1.0 ppm sulfur dioxide (Lipari and Swarin, 1985).

ii) Hydrogen peroxide

Although reactions between H_2O_2 with either DNPH or HCHO are not likely, the possibility of surface catalyzed breakdown of H_2O_2 in the cartridge leading to OH_x radical production needed to be considered. In the moderately polluted troposphere, H_2O_2 mixing ratios can reach 10 ppb. The MPI calibration system (Section 2.5) also contained 3.6 ppm of gas phase hydrogen peroxide. These tests showed that at high levels of H_2O_2, HCHO quantification remained unaffected. Reaction with DNPH was also not evident.

iii) Humidity

The effect of humidity on the collection of aldehydes on C-18 cartridges is discussed by Kuwata et al., (1983); Lipari and Swarin, (1985); and Druzik et al., (1990). No adverse effects were observed at normal relative humidities as well as at high humidities when kept at low sampling volumes (i.e., below 20 L STP). Total humidity does not play an important role above an elevation of 3-4 kilometers. In the lower troposphere (below 2.5 Km), sample volumes are normally 5-10 L STP due to higher HCHO mixing ratios. Extreme low humidity such as in the upper troposphere is also not expected to affect aldehyde collection. Calibration of this method was conducted in dry N_2, and is therefore expected to be represenative of conditions in the mid- to upper troposphere.

iv) Ozone

The possibilty of ozone acting as a negative interference for the silica-gel cartridge DNPH method was first reported by

Arnts and Tejada, (1989). They reported that when ozone mixing ratios exceeded 120 ppb (in 120 L STP), a significant loss of formaldehyde hydrazone occurs in silica-gel cartridges when compared with other measurement techniques. They proposed that ozone reacts primarily with DNPH and then with the hydrazone derivatives to a much lesser but still measureable degree. When ozone reacts with DNPH, radicals are formed on the silca-gel substrate which can propagate DNPH and hydrazone consumption. From the same work, identical tests were conducted with C-18 cartridges which showed no such interference for ozone at 120 ppb (120 L). It was suggested that the radicals produced from the ozone/DNPH reaction are rapidly scavenged by the C-18 packing material before being able to react with the hydrazones. Ozone is much more likely to interact with the highly polar OH-groups on the silica-gel surface than with the non-polar C-18 n-paraffinic surface.

From the literature and experimental observation, four possible effects in order of decreasing probability can appear due to excessive ozone:

1) Possible reaction between ozone and HDPE cartridge housing. This effect was observed in laboratory tests and in the upper troposphere region. The laboratory tests consisted of flowing aldehyde-free ozone (O_3; 40 to 70 ppb) through C-18 DNPH cartridges at 0.5 Lpm for different time intervals from 10 to 60 minutes (experimental set-up, H. Fark, 1991). Reaction products consist mainly of propionaldehyde, some acetaldehyde, and a very trace amount of formaldehyde. The formed aldehydes (in lower picogram range) then react with DNPH leading to a positive interference. Sampled ozone amounts are highly correlated to respective yields of propionaldehyde, acetaldehyde, and formaldehyde. In turn, from this correlation it is possible to correct formaldehyde mixing ratios as a function of propionaldehyde peak heights ($R = 0.996$ for propionaldehyde versus formaldehyde). It is in this case

assumed that where ozone is significant in the upper troposphere, atmospheric mixing ratios of propionaldehyde are negligible.

2) Possible reaction between ozone and DNPH can be easily detected by a significant decrease in the height of the DNPH peak. This effect was observed in laboratory tests, but was not significant in field measurements.

3) Ozone can under certain conditions react with aldehyde hydrazone derivatives. Laboratory tests have shown that this effect only becomes significant when DNPH is already nearly 90% removed. Atkinson and Carter, (1984) and Smith et al., (1989) reported that the ozone/DNPH reaction is much faster than the ozone/hydrazone reaction. There was no evidence of aldehyde hydrazone oxidation during the mentioned field campaigns.

4) From the reaction between ozone and DNPH (#2 above) it is possible that DNPH oxidation products are formed which have similar retention times as the aldehyde hydrazone derivatives. As reported by Smith et al., (1989), this effect can be circumvented by altering the HPLC elution parameters. For the TROPOZ-II analyses, a very similar elution scheme was chosen in order to prevent coelution of possible DNPH oxidation products. This effect presents a problem mainly for higher aldehyde analogs only.

From the above list of possible ozone interfences, the first is the only one which was shown to have a potentially significant bias on calculated formaldehyde mixing ratios. In order to alleviate this problem for future measurements, it is advisable to use cartridges constructed entirely from glass or teflon instead of HDPE. Such cartridges are already commercially available but are considerably more expensive and

not constructed so that they could be easily used during extensive field campaigns.

v) Organic hydroperoxides

Organic hydroperoxides have been previously reported as a possible positive interference for formaldehyde when sampled in acidic aqueous solutions (Schubert et al., 1988). Some organic hydroperoxides i.e., CH_3OOH, are known to breakdown in solution to formaldehyde under acidic conditions, which then react with DNPH to build formaldehyde hydrazone. This effect is only briefly mentioned here, but is described in more detail in Section 3.1 with emphasis on ground level measurements taken during the July/August 1990 OH-Campaign in Jülich.

vi) Nitrogen dioxide

As with the case for hydrogen peroxide, no direct reaction between HCHO and NO_2 was expected. In spite of this, possible effects such as physisorption need to be investigated before being ruled out. As mentioned in Section 2.5, a HCHO intercomparison study was performed with the Max Planck Institute Mainz (MPI). The MPI HCHO calibration gas contained 800 ppb NO_2 without exhibiting any effect on HCHO quantification. A similar test using NO_2 with mixing ratios up to 550 ppb which gave similar results was reported by Lipari and Swarin, 1985. Although NO_2 mixing ratios in polluted air can reach 100 ppb, it is still well below the levels used in the calibration. Elevated NO_2 mixing ratios observed in the upper troposphere (up to 400 ppt) due to aircraft are also well below the levels used in the mentioned studies and expected to be inconsequent for HCHO sampling.

vii) Carbon monoxide

Carbon monoxide at 2.0 ppm was co-sampled with formaldehyde using the MPI calibration system without noticeable degredation of HCHO quantification. Typical atmospheric CO mixing ratios can range up to 300 ppb at ground level, well below the mixing ratio used in this test. Physisorption of CO onto the sampling surface could be ruled out.

2.7 Error analysis

Both systematic and random errors influence the mixing ratios of formaldehyde and acetaldehyde determined by the technique.

a) Systematic errors

i) In the system there is no inherent differentiation of aldehydes between the gas- and aerosol-phases. As reported by Klippel and Warneck, (1980), in clean background air, approximately 1% of the total atmospheric formaldehyde exists in the aerosol-phase, whereas in highly polluted air, as much as 4% of total atmospheric formaldehyde can exist in the aerosol-phase. Since all values in this work are reported for the gas-phase, and in relatively clean air, a minor correction of approximately -1% could be applied.

ii) As previously mentioned in Section 2.4, the collection efficiency for formaldehyde ranged from nearly 100% to approximately 92% for the field campaigns mentioned in this work. Differences in collection efficiencies were corrected for, although they were negligible under most sampling conditions. For acetaldehyde, a collection efficiency of 90% was assumed which led to a maximum error of ca. +/- 10%.

iii) As previously described in Section 2.5, a VICI Metronics permeation tube system was used for the calibration of formaldehyde (for the range 600 ppt to 4.0 ppb). The HCHO permeation rates of the tubes are certified by the manufacturer to be within 10% of the rated value. For the calibration used for TROPOZ-II it was necessary to extrapolate the calibration curve through the origin in order to quantify the sub-600 ppt samples. When not forced through the origin, a Y-Intercept of -36 ppt +/- 42 ppt (R = 0.997, N = 16) is obtained. The percent-error increases as the signal approaches the origin. A maximum error for samples in the 50 ppt range is about 40%, or 19.5 ppt. For a sample with 200 ppt, the error is 15%, or 30 ppt.

b) Random errors

i) Repeated HPLC analysis of dissolved aldehyde hydrazone standards yielded a reproducibility of approximately 1%, independent of column loading. This is also true for repeatedly analyzed ambient air samples.

ii) The reproducibility of the sampling and analysis method using HCHO calibration gas at each mixing ratio used for the the calibration curve from 600 ppt to 4 ppb was 7%. Parallel measurements of ambient air in Jülich/KFA typically also yielded reproducibilities of 7%.

iii) An error of 1.5% is attributed to incertainty in the calculation of sample volumes into STP conditions. The error is mainly dependent upon the quality of the instrumentation which measure ambient temperature and pressure.

Total errors are calculated for several different cases depending on proximity to origin of the calibration curve, and

total amount of systematic and random error. Based on propagation of error calculations, the error increases with altitude due to typically lower mixing ratios, slightly lowered collection efficiencies, and possible ozone interferences. A typical HCHO sample taken at 9.5 km with minimal ozone interference and a mixing ratio of 50 ppt would contain a total error of 41%, or 21 ppt. The total error for a 200 ppt sample at an elevation of ca. 2 kilometers is 17%, or 34 ppt. A ground-based HCHO value of 2 ppb would have an total error of 12.5%, or 249 ppt.

Due to greater incertainty with the calibration, slightly larger total errors are expected for acetaldehyde. At the 50 ppt level, a 44% error, or 22 ppt is given. At 200 ppt acetaldehyde, 21%, or 42 ppt error is given. For 300 ppt, acetaldehyde would have a 19% error, or 56 ppt.

3. Field test results

During the development of a method for the measurement of formaldehyde and acetaldehyde in the free troposphere, two small-scale measurement campaigns were conducted. The purpose of the first campaign was to determine the applicability of the DNPH-Cartridge method for ground-based measurements in semi-urban summer conditions in Jülich. The second test campaign consisted of a series of 4 flights up to nearly 5 km over the northern Eifel region in Germany. These flights were the first time that a cartridge-based aldehyde measurement method had been used at this altitude. Both test campaigns were extremely useful for the development of the aldehyde method which was eventually used during the TROPOZ-II campaign.

3.1 Measurements of Formaldehyde and Acetaldehyde during the Jülich 1990 OH Campaign (Field test one)

Introduction

An institute-wide two-week OH-Radical measurement campaign was conducted in Jülich from 30' July 1990 to 13' August 1990. The DNPH-HPLC method was used for the duration of the campaign for the measurement of formaldehyde and acetaldehyde. As previously mentioned, oxygenated organics play a major role in the atmospheric cycle of the OH radical. Their measurement assists in the testing and development of chemical models for the prediction of OH radical mixing ratios. A list of other supporting measurements is included in Table 3.1. As the results of several other supporting measurements were not available at this time, the interpretation of the aldehyde results is limited.

Table 3.1

Measured Parameters	Method
HCHO, CH_3CHO	DNPH-HPLC (3.5 m)
NMHC, PAN, CH_4, CO, CO_2	ECD/FID GC (2.5 m)
SO_2, HCHO, OH'	DOAS1 (High Resolution)
SO_2, HCHO	DOAS2 (Wide Band)
NO, NO_2, $J(NO_2)$	Chemiluminescence (5m)
ROOH (Total Peroxides)	Fluorescence (3.5 m)
Aerosols (CN)	Aerosol counter (50 m)
O_3	Dasibi (50 m)
Temp., Press.,	T,P-Transducers (20 m)
Wind Direction, Speed	Anemometer (120 m, 20 m)

Experimental Procedure

A total of 420 DNPH cartridge samples were taken in 30 minute intervals around-the-clock for the entire two weeks. Sampling was conducted 20 meters next to the ICH-3 building at 3.5 meters above ground level. The sampling cartridges were mounted inside a rainproof funnel at the end of a retractable sampling boom. The pump and flow system were kept in the ICH-3 sampling container. Sample flow rates were typically 0.5 Lpm STP, yielding sample volumes of approximately 15 L STP. Samples were analyzed by HPLC-UV/VIS as mentioned in Section 2.2. The cartridges were prepared in batches of 8, of which one was used as a blank. Before and after sampling, the cartridges were refridgerated at 0-5^{o} C. For typical ground-level mixing ratios the cartridges can be refridgerated for several weeks, but should be analyzed as soon as possible to minimize contamination. Because of the large number of samples, analysis lasted until mid-October 1990 and approximately 49 of the 420 samples were discarded due to storage contamination as seen by increased formaldehyde and acetaldehyde levels in the blank cartridges (discussed in Section 2.6a). For future studies, storage in dry ice is preferable.

Results and discussion

Daily variations of formaldehyde, acetaldehyde and supporting measurements during the entire OH campaign are shown in Figure 3.1 in Universal Time (UT). Local time was 2 hours ahead of UT. Frequency distributions are shown for both aldehydes in Figures 3.2 and 3.3. HCHO mixing ratios ranged from 0.5 to 7 ppb, with a mean of 2.8 +/- 1.5 ppb (N = 371). CH_3CHO showed similar diurnal patterns as HCHO, but ranged between 0.1 to 2.2 ppb, with a mean of 0.7 +/- 0.4 ppb (N = 366). The mean diurnal variation for formaldehyde was 2.7 +/-

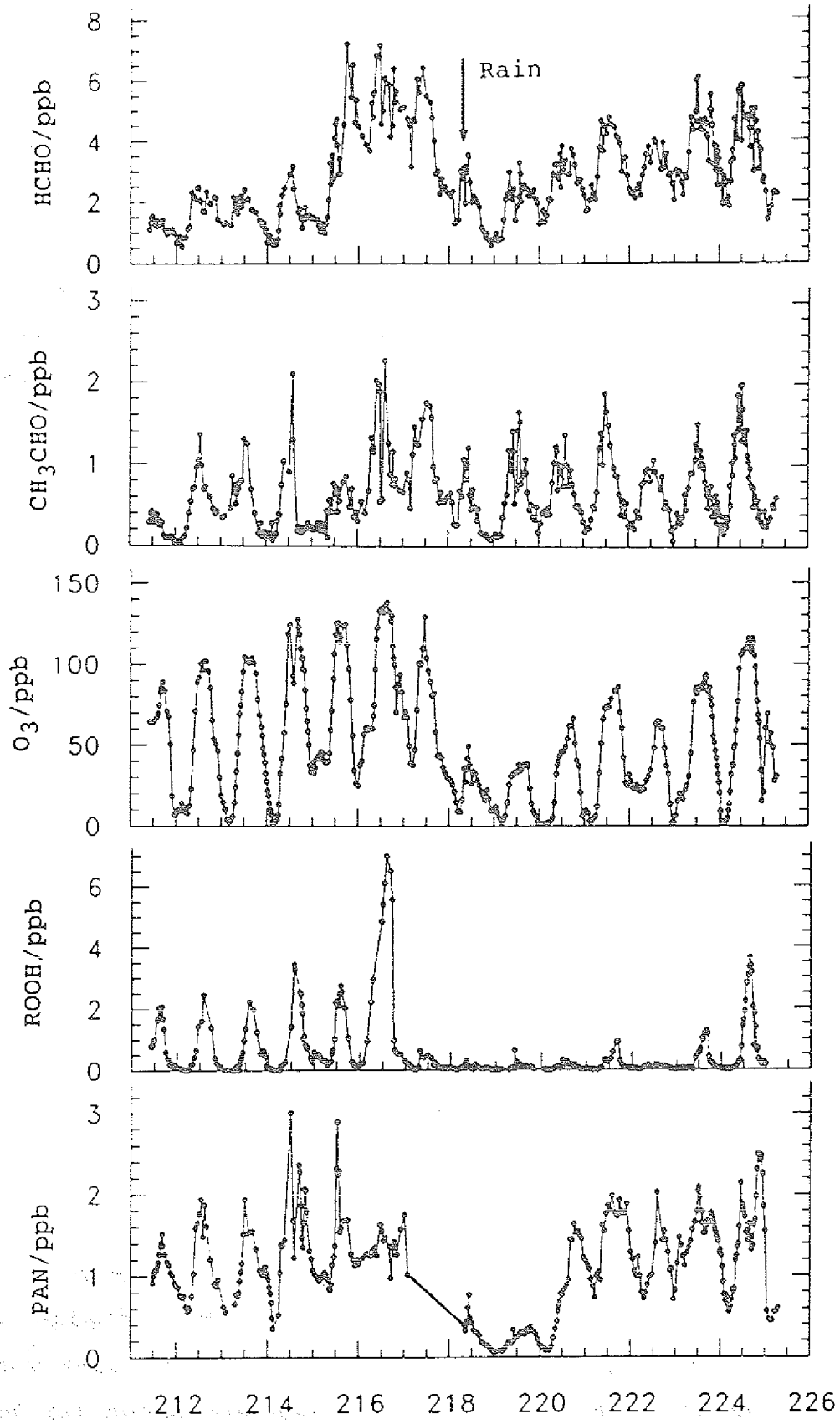

Figure 3.1

Diurnal Variations of Measured Parameters

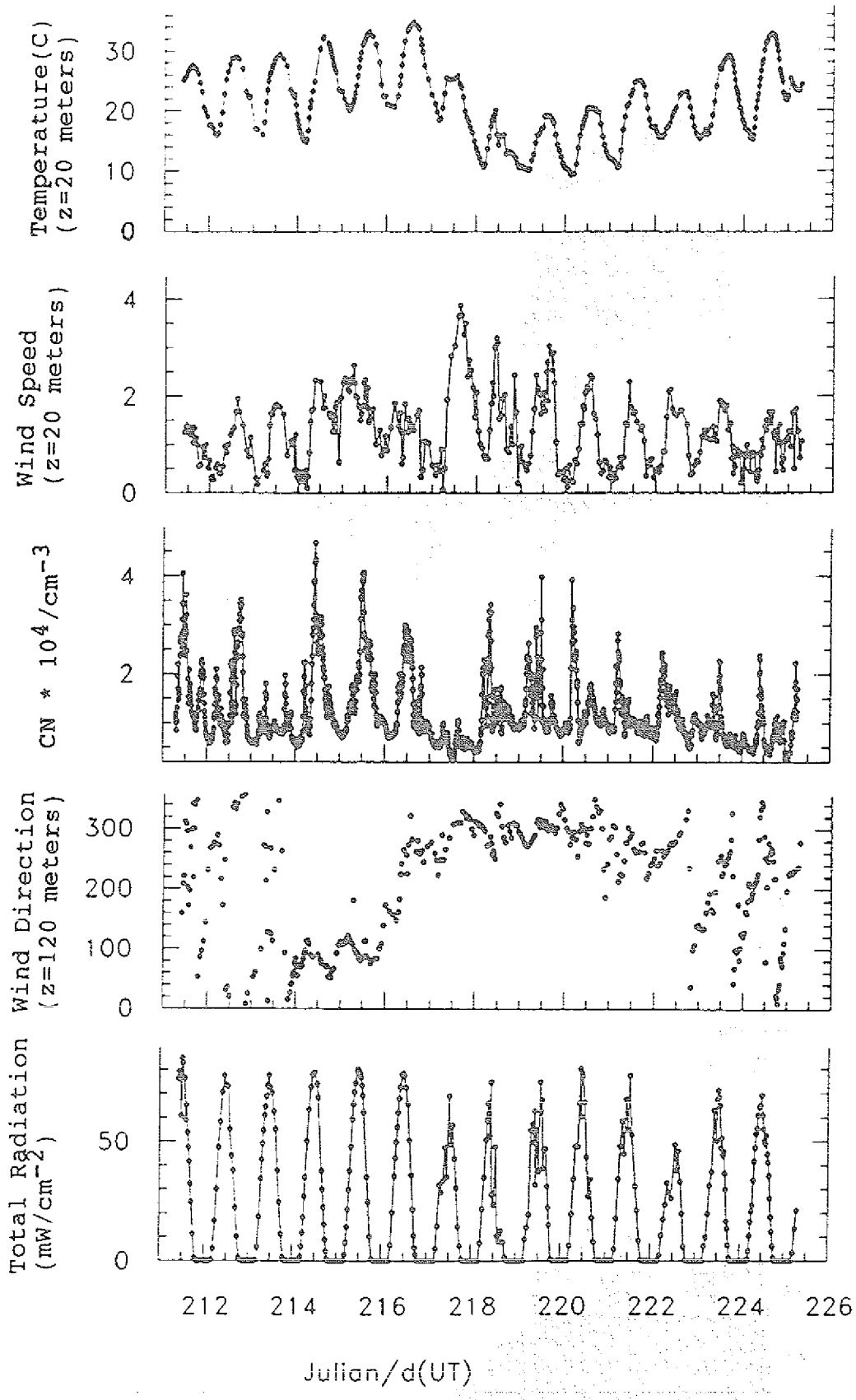

Figure 3.1

Diurnal Variations of Measured Parameters

Figure 3.2

Formaldehyde Frequency Distribution (ppb)

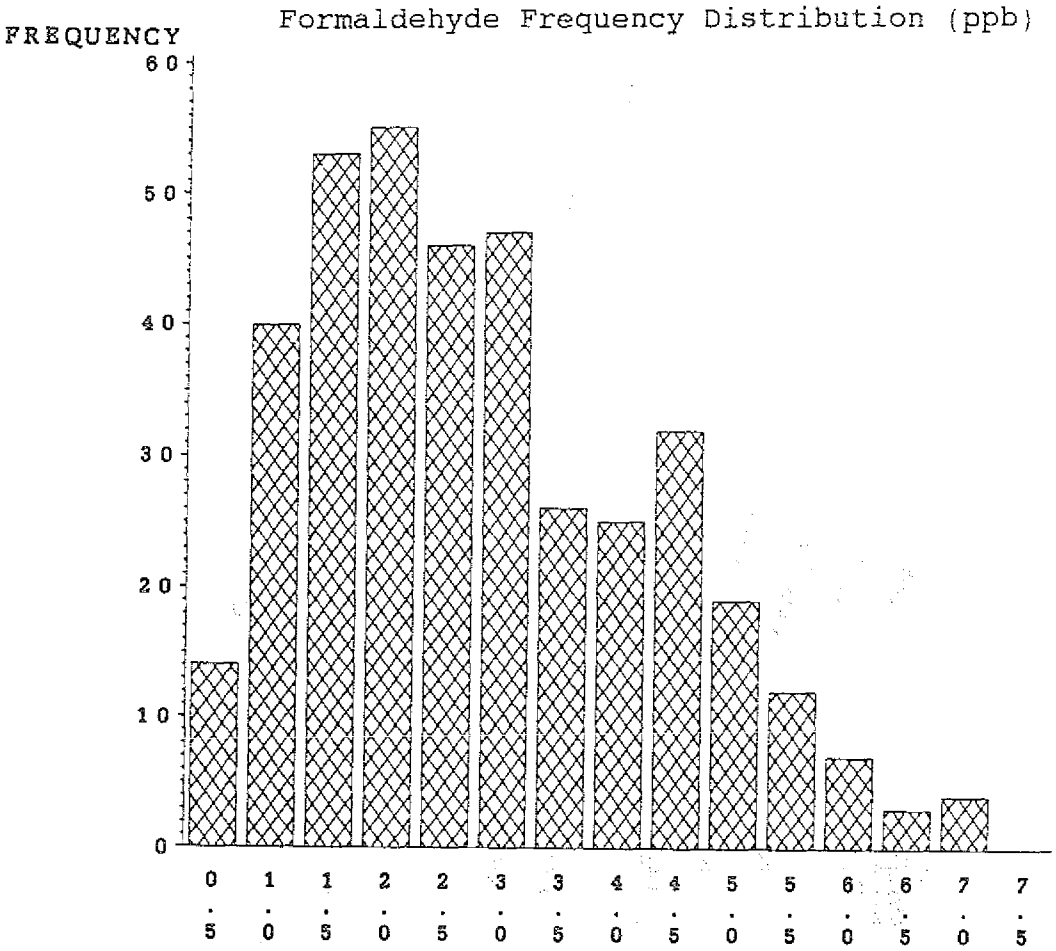

Figure 3.3

Acetaldehyde Frequency Distribution (ppb)

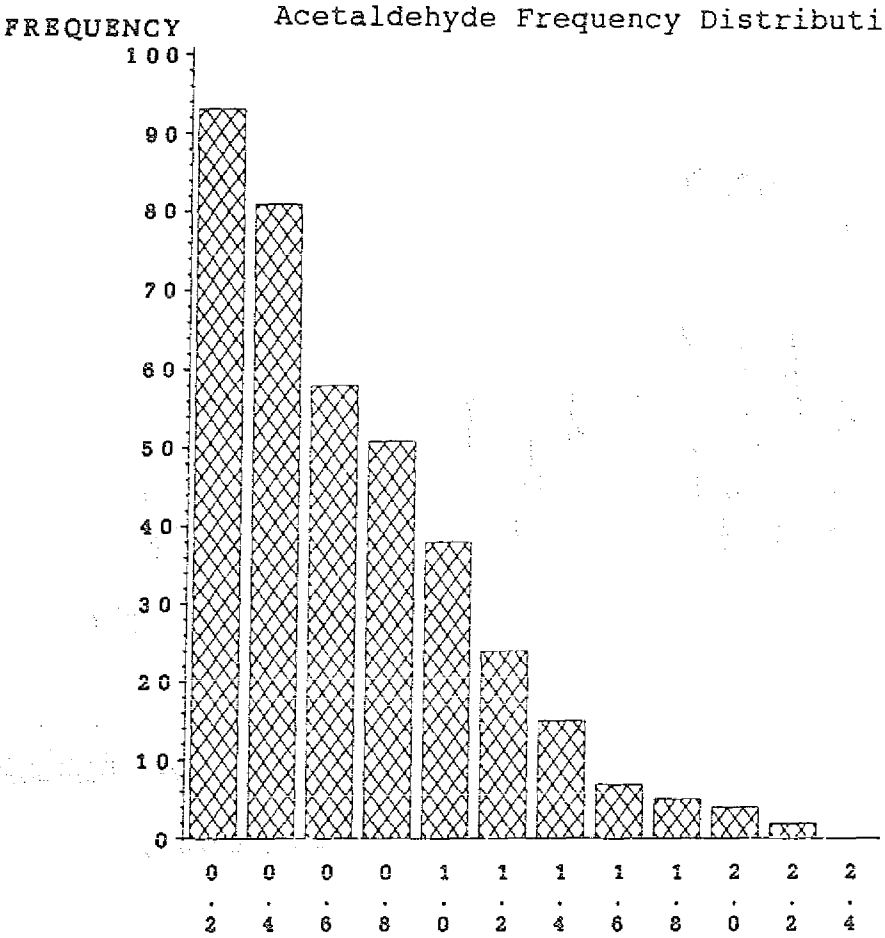

1.4 ppb, and for acetaldehyde 1.1 +/- 0.5 ppb. Previously reported August aldehyde values at this location (Schubert et al., 1988) ranged from 3.5 to 6.4 ppb for formaldehyde (uncooled sampler, N = 16), and 2.3 to 5.1 ppb (N = 16) for acetaldehyde with relatively little diurnal variability for this two-day sampling period in 1984. Wind directions were predominantly easterly, and evidence of anthropogenic influences were present (possibly from Cologne, located ca. 60 km to the east).

The entire 1990 campaign consisted of several weather dependent phases. The first 4-5 days were characterized by increasing temperature (up to 35^{o} C), increased ambient pressure (1015 hPa), increased mixing ratios of all major atmospheric constituents, bright sunlight, and westerly wind (Jülich and natural emissions located to the west), changing to easterly during 3/4 August (Julian dates 215/216). This period was followed by a very strong precipitation episode in the early afternoon of 6 August (Julian 218) between 11:00 and 11:10 (UT). Minimum mixing ratios of nearly all major compounds were observed in this time lasting through the night (Julian 218/219) and were very similar to values observed during and directly after rain episodes in Schauinsland, Germany (June 1984) as reported by Schubert et al., (1988). This period was also characterized by decreased atmospheric pressure and temperature. Thereafter, temperature and pressure began to increase, with winds changing back to westerly. During this period, the daily maximums of many atmospheric compounds gradually increased and began to level off. Average aldehyde mixing ratios are listed with respect to wind directions in Section 6.1. Lowest mixing ratios were seen during northerly and southerly winds, with highest values from the east (Cologne), which is in agreement with Schubert et al., (1988). At an elevation of 120 meters, wind speeds ranged from 4 to 9 m/s, which when a HCHO lifetime of approximately 5 hours is considered, possible transport of anthropogenic

emissions and precursors from Cologne could be likely. Several high values were also seen during westerly winds, and could probably be attributed to local vegetative sources or transport from Jülich.

To assist with the interpretation of aldehyde mixing ratios, correlations with several other pertinent photochemically dependent trace gases and local meteorological conditions were made. In Figure 3.4, formaldehyde is plotted over acetaldehyde. Approximately 95% of the data fits within a slope range of 1.4 to 7.8, with an average weighted slope of 2.5. The Y-Intercept is at 0.6 ppb HCHO, which is also in rough agreement with previous measurements made at this location and could indicate that methane represents the main HCHO source up to 0.6 to 0.8 ppb HCHO. A wide range for the slope should be expected due to the extreme variabilty of source strengths and respective oxidation lifetimes of the numerous other precursor hydrocarbons. Comparing aldehydes with other intermediate oxygenated organic species can yield information about the extent of hydrocarbon oxidation in a given location. For this purpose, total ROOH and PAN were also plotted in Figure 3.1 for the entire campaign. As seen in Figure 3.5, total hydroperoxides (ROOH), 20 to 30% of which presumably consists of organic hydroperoxides, are present at very low amounts until HCHO reaches approximately 1.0 ppb. Rough calculations show that under these atmospheric conditions, the steady state mixing ratio of formaldehyde due exclusively to the oxidation of methane (up to 1.85 ppm) can begin to approach 1 ppb. At this point, it is suspected that the oxidation of higher NMHCs starts to become significant for the production of organic-ROOH as well as HCHO. A very similar trend is also seen between ROOH and acetaldehyde in Figure 3.6. In this case the offset occurs at a lower aldehyde mixing ratio, which points to the fact that both of these compounds are very heavily dependent upon the source strengths and oxidation of higher hydrocarbons. Once again, a very similar

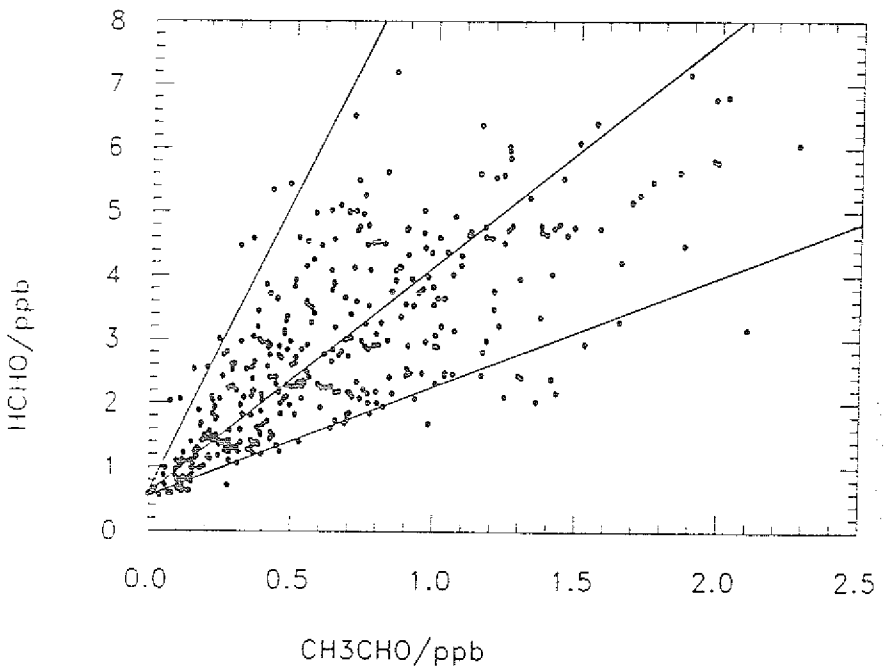

Figure 3.4

Formaldehyde versus Acetaldehyde

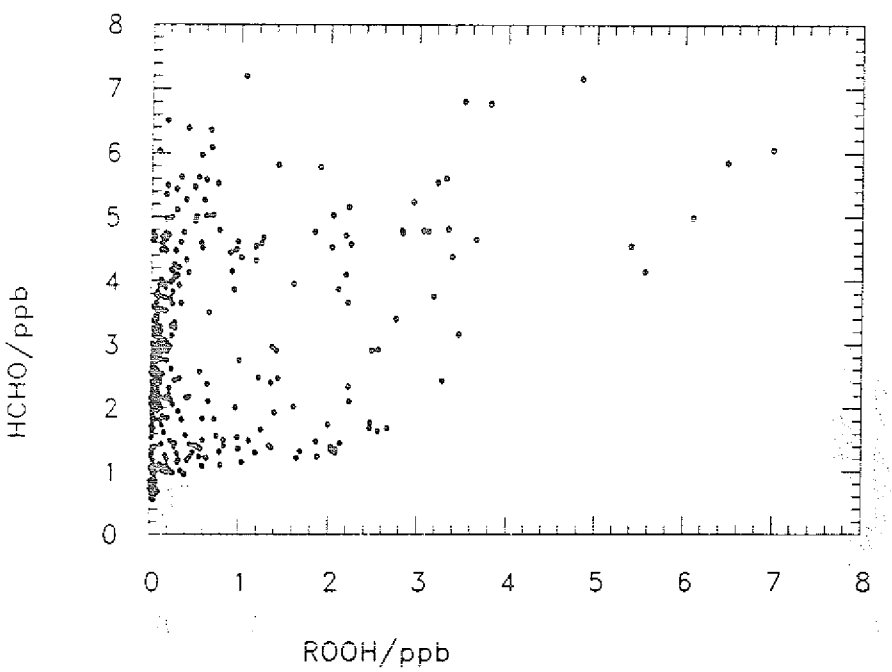

Figure 3.5

Formaldehyde versus ROOH

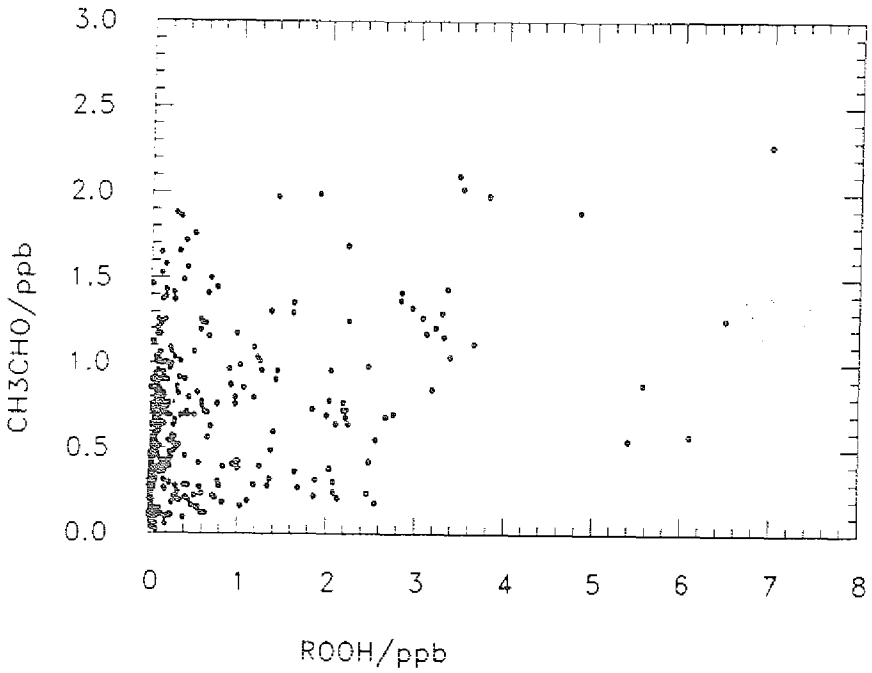

Figure 3.6

Acetaldehyde versus ROOH

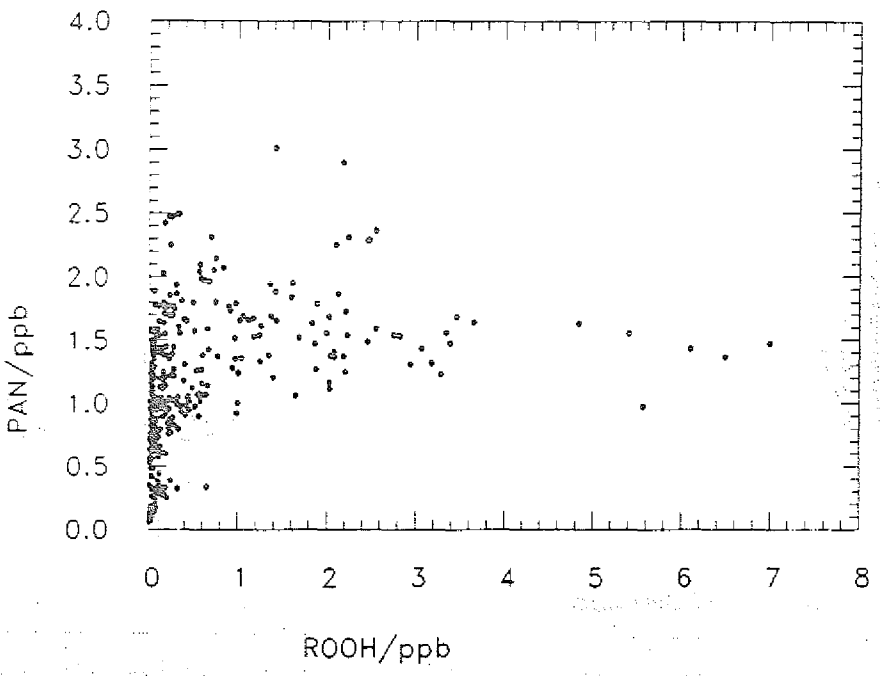

Figure 3.7

PAN versus ROOH

effect is seen when PAN is plotted against ROOH (Figure 3.7). ROOH remained very low up to 1 to 1.5 ppb PAN, at which very high ROOH values were observed (up to 7 ppb). At higher PAN values, ROOH values remained for the most part elevated.

Although a thorough comparison of HCHO between the DNPH method and the two optical-DOAS methods is not presently possible, a preliminary comparison to the DOAS#1 (High Resolution, average elevation 80 meters) indicates that the ground-level in-situ DNPH method delivered consistently higher results. Both of the long-path optical methods (DOAS) need to be compared to determine if they deliver similar and consistently lower HCHO mixing ratios than the in-situ DNPH method. Whether this difference is due to a mixing ratio gradient, differing wind directions, a calibration offset or another effect is yet to be shown. Previous sampling campaigns in Jülich have shown that air mass compositions and wind directions can differ greatly over short distances. Measurements reported by Altshuller, (1983) and calculations by Liu et al., (1987) show that concentrations of naturally emitted species can quickly decline within 20 meters of a given natural source. Large vertical concentration gradients can then form near regions of ground level sources due to rather slow upwardly directed mixing. Such an effect would then be only expected under stable atmospheric conditions.

A positive formaldehyde interference from organic hydroperoxides using a cooled (5^{o} C) aqueous acidic DNPH absorber solution was reported by Schubert et al., (1988) to occur most likely in summer months near areas of significant vegetative emissions of organic compounds. It is possible that the decay of organic hydroperoxides to formaldehyde is hindered when collected onto a "uncooled" basic surface. Since organic hydroperoxides were not directly measured during any of the mentioned measurement campaigns, only as total ROOH during the 1990 OH campaign, it is difficult to estimate the magnitude of a positive bias for formaldehyde for the present

method. For further ground based measurements in areas where organic hydroperoxide mixing ratios could according to prediction reach several ppb, interference tests should be conducted using an aldehyde-free organic hydroperoxide calibration source.

As also reported by Kleindienst et al., (1988), maximum HCHO and H_2O_2 mixing ratios were observed in the early-mid afternoon, with minimum values shortly before sunrise. Kleindienst et al., (1988) reported large diurnal flucuations measured with two side-by-side HCHO methods (TDLS and DNPH) at a semi-rural location in North Carolina, USA (36^o N) during June 1986. The techniques were well correlated over a range of 1 to 10 ppb HCHO. A very high correlation between H_2O_2 and formaldehyde using both TDLS-HCHO and DNPH-HCHO methods was also reported. Although this study did not hint to a organic hydroperoxide contamination for the DNPH cartridge method, the occurence of such an interference for the Jülich data should perhaps not be completely ruled out for cases where ROOH reaches maximum values. Since total ROOH mixing ratios remained normally quite low during the entire campaign (less than 1.5 to 2 ppb) this effect would not be expected to be significant although a short-term maximum of 7 ppb was observed. Maximum values of ROOH were not systematically coincident with maximum HCHO values. The ROOH method reported 6 points which were over 4.0 ppb (all during westerly winds), three of which may be consistent with higher HCHO. Direct measurement of vegetative emissions from nearby wooded areas were most likely during westerly winds. Measurements of short-lived NMHCs such as isoprene which can produce HCHO in-situ and possibly CH_3OOH need to be made to estimate the magnitude of a vegetative source. Anthropogenic emissions from Jülich with westerly winds may represent another source of higher values for both compounds. In any case, convincing evidence of a ROOH interference on this DNPH method is not present. For measurements in the free troposphere, where organic

hydroperoxide mixing ratios are minimal, it is assumed that such an effect should be negligible.

3.2 Vertical Measurements of Formaldehyde above the northern Eifel (Field test two)

Introduction

A series of four test flights in a twin engine Piper Seneca-II aircraft were conducted up to an altitude of nearly 5 kilometers over the northern Eifel region in Germany (50 - 51^{o} N) to test the applicability of cartridge-based airborne aldehyde sampling methods under different weather conditions. Three of the flights were conducted during the summer of 1990, and the forth in November 1990.

Experimental Procedure

For these tests, a cartridge-based dansyl hydrazine method as briefly mentioned in Section 2.0 was used. A similar method using dansyl hydrazine for the measurement of carbonyls in urban air is described in detail by Schmied (1988); Bächmann et al., (1989); and Przewosnik (1989). For these measurements, Sep-Pak C-18 cartridges coated with dansyl hydrazine in dichloromethane solution were used. Measurements of near ambient mixing ratios of HCHO calibration (1.5 ppb) gas yielded a reproducibility of about 10%.

The sampling line consisted of a 1.3 meter teflon tube which was placed through the front windshield of the aircraft, well above and in front of the engines on the wings. Engine exhaust was directed to the back and downwards under the wings. The likelihood of sampling engine exhaust was very minimal. The flow system was identical to that described in Section 2.3. Typical sample volumes were 10 to 25 liters STP,

in sampling times varying from 10 to 20 minutes. Before and after sampling, the cartridges were stored in dry ice, and were analyzed in the laboratory within 24 hours after each flight. Analysis was performed by reversed phase HPLC using a fluorescence detector - excitation wavelength 340 nm, emission wavelength 530 nm, Merck LichroCart (50839) 250-4 RP-select B C-8, 5-micron column with a mobile phase isocratic mixture of 65/35 Acetonitrile/Water at 1.0 ml/min.

As these flights were planned only for the purpose of testing this measurement method, and because of lack of space and power in the aircraft, no other chemical species were measured. In spite of this, interpretation of the data with respect to the weather conditions can yield much insight to the measured mixing ratios. Weather information was obtained from the Deutscher Wetterdienst (German Weather Service) in Essen, Germany.

Results

Mixing ratios of formaldehyde for each of the four flights are shown in Figure 3.8. Flight 1 shown by circles, flight 2 with squares, flight 3 with triangles, and flight 4 with diamonds. The sampling conditions, protocol and results are tabulated in Section 6.2, and should be read in conjunction with the figure to see under what condition the samples were taken. Sampling plateaus were flown at elevations of 1.4 to nearly 4.5 km. Since it is not experimentally possible in an airplane to sample a cloud at a given point, every attempt was made during sampling to determine if and when the aircraft entered or exited a given cloud bank. Sampling was always conducted in the late-morning to mid-afternoon, when photochemical processes were assumed to be most active.

Figure 3.8

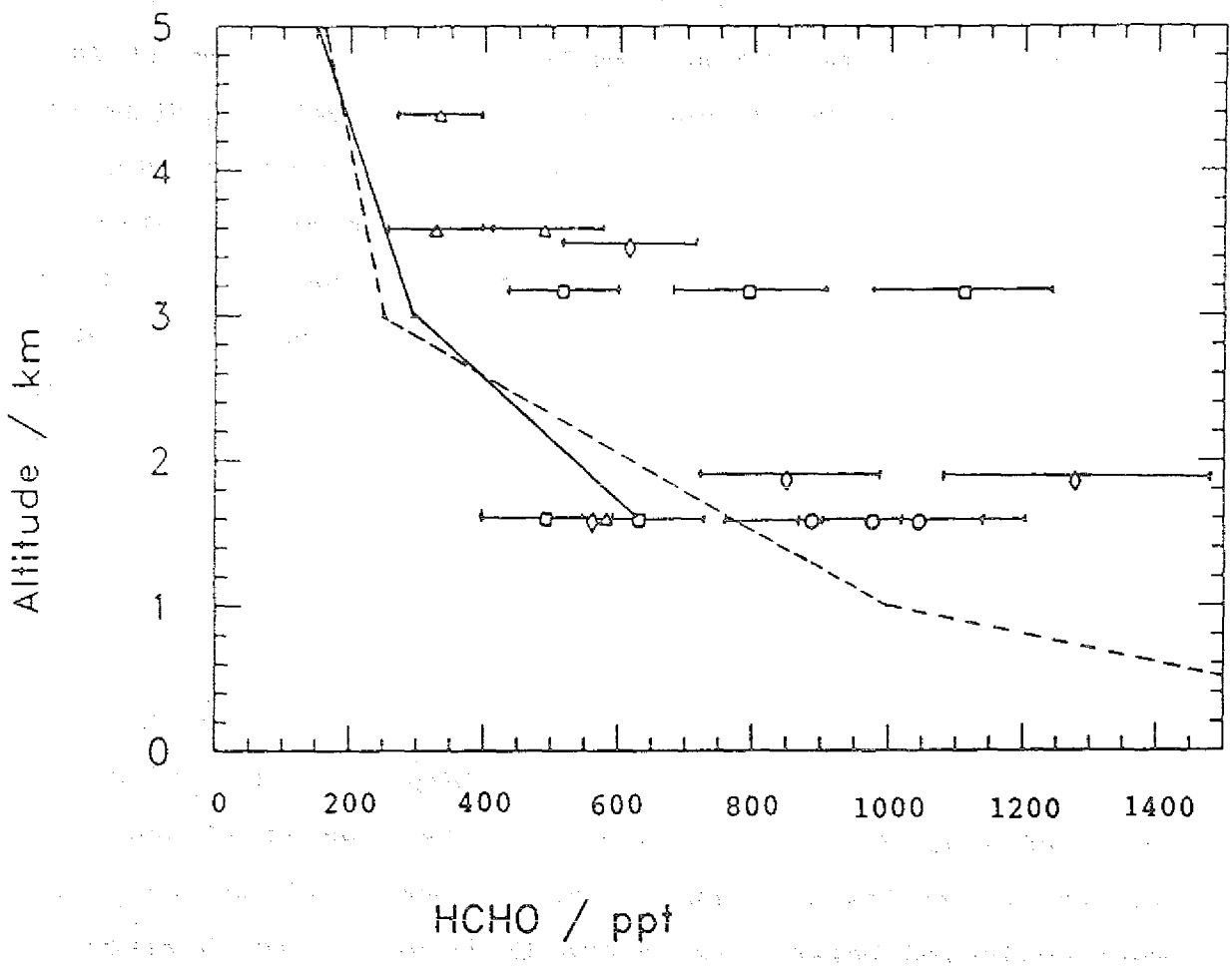

-Circle, Flight one, 11'June
-Square, Flight two, 19'June
-Triangle, Flight three, 25' August
-Diamond, Flight four, 7' November
---------- Model Profile, McKeen et al., 1991
———————— Model Profile, Hough, 1991

Tropospheric HCHO measurements above the northern Eifel region in Germany, 1990. The measurement error interval (ca. 15%) is given for each sample at each flight level.

Discussion

Flight 1:

The first flight was flown on 11' June 1990 at a constant altitude of 1.5 km. Three samples were taken from 11:28 to 12:35 local time. The temperature at this level ranged between 2.5 and 3.5^{o} C. A high pressure system over northern Scotland brought NW winds to the entire region. Shown mixing ratios are representative for cloudless, inversionless summer conditions, and are comparable to values reported by Lowe (1981) under similar conditions. Possible anthropogenic emissions from industrialized coastal areas in the Netherlands should be considered as a potential source region.

Flight 2:

Flown on 19' June 1990, flight plateaus were made at 1.5 km (Temp. = 5 to 6^{o} C) and 3.1 km (Temp. = -3 to -4^{o} C). Two in-cloud samples at 1.5 km were made between 11:30 and 12:13, and three samples (one out of cloud, one in-cloud, one mixed) were collected between 12:25 and 13:31 at 3.1 km. A strong low pressure system south of Iceland brought WSW winds. No inversion was detected. Several samples were collected near coal-fired power plants, which could explain high values at the 3.1 km level. Possibly due to vertical transport, up to 1.1 ppb gas-phase HCHO was observed at 3.1 km. Scattered cumulus clouds at 3.1 km made mixed sampling at this level possible. The in-cloud samples at 1.5 km were similar to in-cloud values at 3.1 km.

Flight 3:

The third flight was flown on 25' August 1990 at 1.5 km (Temp. = 14^{o} C), 3.5 km (Temp. = 0^{o} C), and 4.3 km (Temp. = -

10° C). A strong low pressure system south of Greenland brought westerly winds at all levels to western Europe. No inversion was detected. The 1.5 km sample (17:22 to 17:37) was collected in-cloud, as well as 2 samples at 3.5 km (16:06 to 16:49). One sample at 3.5 km (16:51 to 17:11) and one sample at 4.3 km (15:49 to 16:04) were mixed (in and out of cloud).

Flight 4:

The final flight of this series was flown on 7' November 1990. A well developed, stable high pressure system over northern Scotland brought NNW winds at all levels to the flight region. An inversion was noted at the 800 - 850 hPa level. A very stable, homogeneous stratus cloud layer was observed between 1.3 km and 1.7 km for the entire Eifel region. The boundary layer below the cloud layer (inversion) was hazy. The sky above 1.7 km was completely cloudless and bright. Samples were taken in-cloud and immediately above the cloud layer. Formaldehyde measured above the cloud layer is assumed to be mainly due to transport from the north, and not from below. Four plateaus were flown at different levels and conditions. One sample at 3.4 km was taken out of cloud between 10:39 and 10:59, (Temp. = -4° C). Two samples were collected out of cloud at 1.8 km between 12:43 and 13:15, (Temp. = 3° C), and one in-cloud sample at 1.5 km (Temp. = -2° C) was collected from 13:22 to 13:36.

A total of 17 samples are reported here, 7 of which were sampled during cloudless conditions. The measured mixing ratios are in general agreement with previously reported measurements from the same region and under similar sampling conditions (Lowe, 1981). Recent model results for formaldehyde from ground level to 6 km published by McKeen et al., (1991) are in general agreement with these measurements. Formaldehyde was predicted to decrease with altitude from ca. 2.0 ppb at ground level, 1 ppb at 1 km, 250 ppt at 3 km, and ca. 160 ppt

at 5 km under cloudless but stable, high-pressure summer conditions. The model contained a full range of natural and anthropogenic NMHC precursor compounds. As a feature of the model, there is very little vertical transport of HCHO and HCHO precursors (NMHCs, NO_x) into the free troposphere. This could be in part responsible for the underprediction of formaldehyde above the boundary layer, and high mixing ratios (2 ppb) at ground level. The Harwell model (Hough, 1991) for the month of January at 52° N delivered similar HCHO values for the free troposphere as the McKeen model (630 ppt at 1.5 km, 350 ppt at 3 km, and 150 ppt at 5 km). Since the NMHCs are more reactive in summer, the Harwell values should be upwardly adjusted to match the time frame of the 3 summer flights. The November flight shows approximate agreement to both models. In general, the models fit very well with the low-end, in-cloud HCHO samples through the entire vertical profile. As calculated by a simple CH_4-Kinetic model (Section 4.1a), a diurnal HCHO variation at each vertical level is on the order of 30 to 40% of the maximum midday values, and becomes less significant with altitude.

Although these measurements are still preliminary and further conclusive work in this area is needed, it appears that samples which were sampled in-cloud tended to contain lower amounts of formaldehyde than gas-phase samples at similar elevations. The relatively high solubilty of formaldehyde coupled with the short aqueous-phase lifetime of formaldehyde, ca. 15 minutes for OH°-oxidation (Lelieveld and Crutzen, 1990, 1991), is the most probable explanation for the lower in-cloud values.

In regions of large SO_2 emissions, formaldehyde can also react with sulfite ion to form hydroxylmethanesulfonate in the aqueous-phase. This reaction is pH dependent, and is most efficient in non-neutral pH conditions and where oxidant levels, primarily H_2O_2, are low. Generally, SO_2 is effectively

oxidized by either H_2O_2, $OH^{\cdot}$, or O_3 before reaction with formaldehyde becomes significant.

Due to technical difficulties with the fluorescence detector and a noticed strong temperature dependent stability of the dansylhydrazones, the DNPH method was chosen for further measurement campaigns (TROPOZ-II). In spite of these difficulties, agreement within 15% was obtained for formaldehyde for the two methods based on the VICI permeation tube calibration system at 1.6 ppb.

4. Measurements of formaldehyde and acetaldehyde in the free troposphere during TROPOZ-II

Introduction

The DNPH/HPLC method was used for the measurement of formaldehyde and acetaldehyde during the 30-flight TROPOZ-II measurement campaign which was conducted from 09' January 1991 until 1' February 1991 aboard the French Caravelle 116 research aircraft. Measurements were taken up to a maximum elevation of 10.5 kilometers from 70^{o} N to 55^{o} S. The flight route is shown in Figure 4.1, with locations tabulated in Table 4.1. The purpose of the measurement campaign was to quantify major atmospheric chemical constituents which are recognized to have a significant influence on the global tropospheric balances of important oxidants such as OH radical and ozone. The TROPOZ-II campaign was a continuation in a series of global scale airborne research expeditions which included STRATOZ-III (June 1984) and STRATOZ-II (April-May 1980). The TROPOZ-II mission was conducted in winter so as to augment previous spring/summer measurements, and to determine seasonal fluctuations in the mixing ratios of major tropospheric trace gases in both hemispheres. A list of measured species and participating laboratories is given in

Figure 4.1

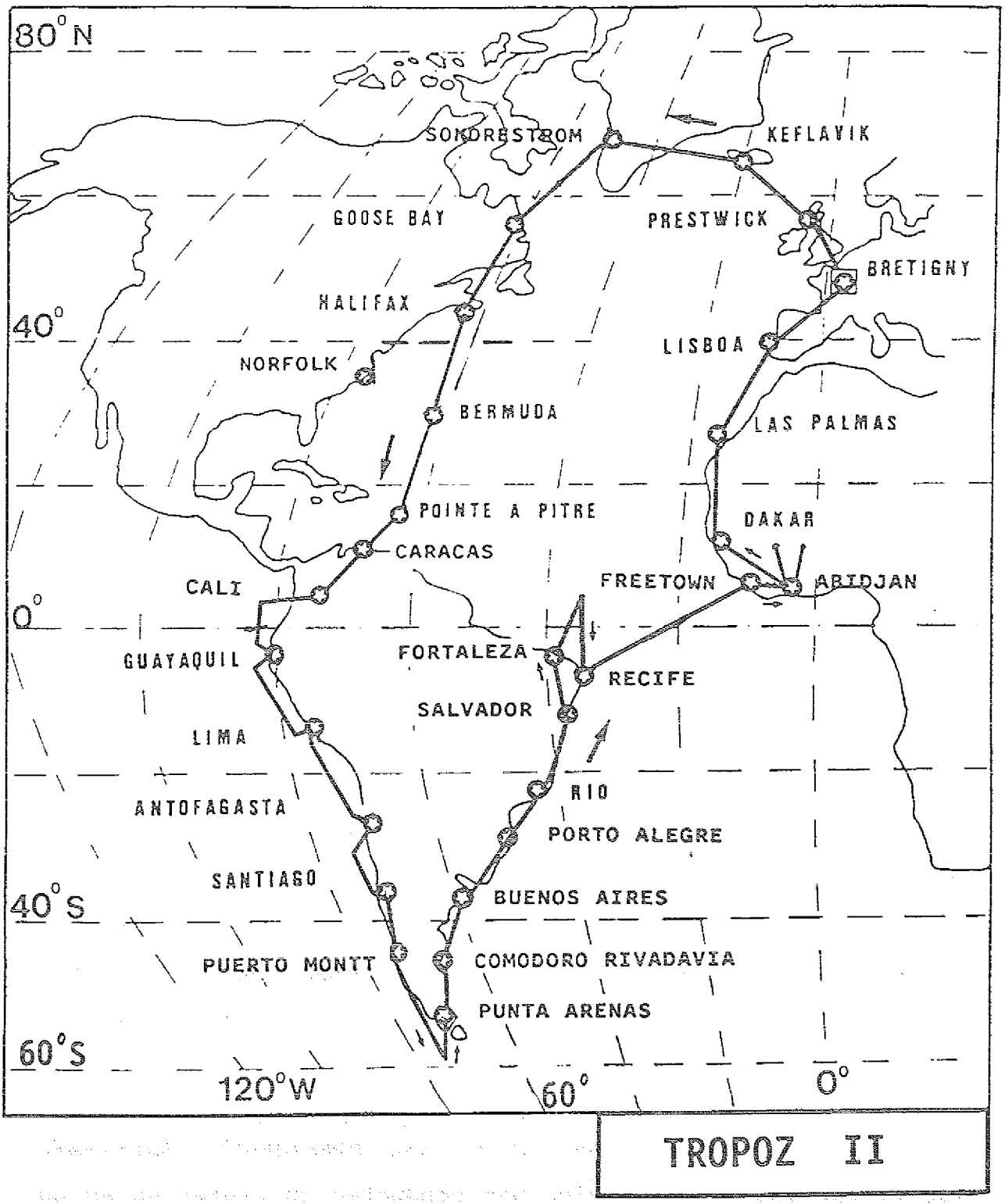

TROPOZ-II Flight Route

Table 4.1

TROPOZ-II Flight Information

Date	Flight Number	Locations	Latitude Range
09.01.91	1	Bretigny-Prestwick	48.5/53
09.01.91	2	Prestwick-Keflavik	55/64
10.01.91	3	Keflavik-Sondrestrom	64/67
11.01.91	5	Goose Bay-Halifax	53/45
11.01.91	6	Halifax-Bermuda	45/32
12.01.91	7	Bermuda-Pointe a Pitre	32/16
15.01.91	8	Pointe a Pitre-Caracas	16/10.5
15.01.91	9	Caracas-Cali	10.5/3
16.01.91	10	Cali-Guayaquil	3/-2
16.01.91	11	Guayaquil-Lima	-2/-12
18.01.91	12	Lima-Antofagasta	-12/-23.5
18.01.91	13	Antofagasta-Santiago	-23.5/-33.5
21.01.91	14	Santiago-Puerto Montt	-33.5/-41.5
21.01.91	15	Puerto Montt-Punta Arenas	-41.5/-57/-53
22.01.91	16	Punta Arenas-Comodoro Rivadavia	-53/-46
22.01.91	17	Comodoro Rivadavia-Buenos Aires	-46/-35
23.01.91	18	Buenos Aires-Porto Alegre	-35/-30
23.01.91	19	Porto Alegre-Rio	-30/-23
25.01.91	20	Rio-Salvador	-23/ -13
25.01.91	21	Salvador-Fortaleza	-13/-4
25.01.91	22	Fortaleza-Recife	-4/-7
29.01.91	25	Abidjan (Local Flight)	5
30.01.91	26	Abidjan (Local Flight)	5
31.01.91	27	Abidjan-Dakar	5/15
31.01.91	28	Dakar-Las Palmas	15/28
01.02.91	29	Las Palmas-Lisbon	28/39
01.02.91	30	Lisbon-Bretigny	39/48.5

Table 4.2

List of Measured Parameters during TROPOZ-II

Measured Parameter	Laboratory
HCHO, CH_3CHO (This Work)	ICH-3, KFA Jülich
NO_X, NO_y, $J(NO_2)$	ICH-3, KFA Jülich
NMHC, PAN	ICH-3, KFA Jülich
O_3, CO, CH_4, CO_2	Lab d'Aerologie, Toulouse
CO, H_2O_2, NO_2, HCHO	MPI Mainz
H_2O_2, PAN	LPCE Paris
Kr-85, NMHC, Rn-222	CFR Gif-sur-Yvette
SO_2	IMGF Frankfurt

Table 4.2. The TROPOZ-II campaign was the first of these campaigns whereby aldehydes were measured, and was a first ever attempt to measure formaldehyde and acetaldehyde in the global troposphere. Aldehyde distributions were interpreted with the aid of supporting meteorological data and relevant co-measured chemical species. A thorough interpretation of the data set is limited by the present unavailability of supporting results.

Experimental Procedures

Aldehydes were collected in DNPH coated cartridges in sample volumes ranging from 5 to 30 liters STP. Before and after sample collection, the cartridges were stored in dry ice in the aircraft. Leak tests were continually carried out during sampling in order to test for the possibility of system contamination. The inlet system was constructed entirely out of teflon tubing (1.5 meter, 0.64 cm OD) to prevent wall losses and possible sources of contamination. The air intake flange was extended approximately 10 cm outside of the aircraft to avoid contamination from the aircraft fuselage. Also to this purpose, the intake was positioned in front of the engines. Sampling was consequently commenced or curtailed directly outside of metropolitan areas or near airports to prevent contamination of the sampling system due to polluted air. Directly after the research flights, analysis of the cartridges via HPLC-UV/VIS was commenced. The elapsed time between cartridge preparation and sample analysis ranged from 2 to 7 weeks.

Analysis of the sample cartridges and calibration was performed as mentioned in Sections 2.2 and 2.5 respectively. For the TROPOZ-II campaign, the reproducibility of the blanks was approximately 15% and 20% for formaldehyde and acetaldehyde respectively on average for a given flight. This variability has a direct effect on the overall detection limit

for each flight. Detection limits for formaldehyde and acetaldehyde during the TROPOZ-II expedition were approximately 70 +/- 10 ppt and 50 +/- 10 ppt respectively for a typical 15 liter STP air sample. Detection limits were both sample volume and blank cartridge dependent, whereby 3-flight moving averages yielded an average of 4-5 blank values for each flight. The detection limits were calculated in accordance with the accepted convention. The detection limit is given as the sum of the mean plus three times the standard deviation based on a standard sample volume. Detection limits (HCHO DL) for each sample cartridge are listed in Section 6.3 (Appendix). Samples taken in the upper troposphere which were significantly affected by ozone interferences were discarded (ca. 10). In this case, ozone corrections yielded net signals which were below the detection limit as just described, and in Section 2.6b.

4.1 Tropospheric photochemical models for TROPOZ-II

The results of two different photochemical models were obtained in order to compare the present state of photochemical theory with the experimentally obtained values of formaldehyde and acetaldehyde from TROPOZ-II. The first model was written to run on a personal computer, and kinetically predicts steady state atmospheric formaldehyde mixing ratios using methane as the sole source. Results from the second model, obtained from the Harwell Laboratory, AERE, Oxfordshire U.K., computes both formaldehyde and acetaldehyde globally as a function of most major hydrocarbons (C_1 to C_7) which can lead to aldehyde formation.

The purpose of the comparison of experimentally obtained values with modelled results is three-fold:

1) Firstly, the kinetic CH_4-model was used to gain a representative picture of the HCHO distribution which is due to the oxidation of methane alone.

2) Secondly, the Harwell model results were used to identify differences in the formaldehyde distribution due to the inclusion of major higher hydrocarbons up to C_7 which can lead to formaldehyde formation.

3) Thirdly, comparison of experimentally obtained values with the above mentioned models can aid in determining if the formation of formaldehyde due to additional NMHCs and/or still undefined sources may be significant.

4.1a Description of the methane kinetic model

A zero-dimensional kinetic photochemical box model was developed to calculate steady state HCHO mixing ratios under cloudless conditions as a function of zenith angle (i.e., latitude, elevation, date, local time), OH radical mixing ratio, total ozone column density, altitude dependent HCHO photolysis rates, and methane mixing ratios used as the sole source of HCHO. The reaction of methane with OH radical is the rate-limiting-step. The purpose of the model was to develop a first-approximation point-for-point comparison of formaldehyde mixing ratios from TROPOZ-II using the most essential physical parameters. For formaldehyde, this CH_4-kinetic model is very similar in construction to the Logan et al., (1981) model, and delivers HCHO values which typically agree within 10 to 20% with the Logan model over most of the troposphere. A global tropospheric OH radical mixing ratio field to 10 km for the month of January was adapted from Hough (1991). Since methane mixing ratios measured during TROPOZ-II were not yet available, methane profiles from the STRATOZ-III campaign

conducted during June 1984 were used (Marenco et al., 1989). The seasonal difference in the global methane distribution is only on the order of 3%, which is not expected to represent a major source of error in the model. The annual tropospheric increase of methane is presently only on the order of 1.0%, and is also not a major source of error in the model. Due to the high variabilty of in-situ conditions, i.e., temperature and pressure, a total error for kinetically modelled formaldehyde values is on the order of 20%. Formaldehyde photolysis rates as a function of elevation in increments of 1 km and zenith angle were obtained using an algorithm developed by Röth (E.P. Röth, 1986, personal communication 1991). Solar radiation attenuation is calculated through the atmosphere due to several major stratospheric and tropospheric trace gases (O_2, Air - US Standard Atmospheres, NO_2 - LIMS Oct. 78 - May 79, O_3 - NASA Nimbus-7 TOMS) and aerosol loading (WMO 1986) according to their respective absorption or scattering properties. Ground albebo (0.16) and global temperature profiles (LIMS Oct.78-May 79) are also considered. The NASA TOMS Ozone column data was obtained (NASA-Goddard Space Flight Center, 1991) for each flight for the complete flight track in Dobson units, as shown in Table 4.3. The shape of the vertical profiles of the total ozone column densities are then fitted with respect to latitude and season. Because of the complexity of the algorithm, the calculations were obtained using the KFA-Cray X-MP system. An average of 30 Cray seconds were required for each flight profile. The calculated formaldehyde photolysis rates (J_{9a} and J_{9b}) were then used in the kinetic model with methane and OH radical concentrations. Calculated lifetimes of formaldehyde due to photolysis and OH radical oxidation along the flight track as a function of altitude at ground-level, 5 km and 10 km are also shown in Table 4.3. Steady state formaldehyde mixing ratios at STP (corrected for ambient temperature and pressure) were calculated for the entire troposphere using the following kinetic equation:

Table 4.3

Date	Flight Number	Locations	Latitude	Ozone Column	Calculated	HCHO	Lifetimes
			Range	Dobson Units	(0km)/Hrs	(5km)/Hrs	(10km)/Hrs
09.01.91	1	Bretigny-Prestwick	48.5/53	421	12.3	4.6	3.0
09.01.91	2	Prestwick-Keflavik	55/64	503	36.0	15.1	8.1
10.01.91	3	Keflavik-Sondrestrom	64/67	493	49.3	22.7	13.1
11.01.91	5	Goose Bay-Halifax	53/45	464	14.4	5.3	3.4
11.01.91	6	Halifax-Bermuda	45/32	454	7.8	3.1	2.3
12.01.91	7	Bermuda-Pointe a Pitre	32/16	267	3.7	1.8	1.5
15.01.91	8	Pointe a Pitre-Caracas	16/10.5	248	2.8	1.5	1.3
15.01.91	9	Caracas-Cali	10.5/3	246	2.8	1.5	1.3
16.01.91	10	Cali-Guayaquil	3/-2	250	2.5	1.4	1.2
16.01.91	11	Guayaquil-Lima	-2/-12	258	2.5	1.4	1.2
18.01.91	12	Lima-Antofagasta	-12/-23.5	261	2.3	1.3	1.2
18.01.91	13	Antofagasta-Santiago	-23.5/-33.5	274	2.3	1.3	1.2
21.01.91	14	Santiago-Puerto Montt	-33.5/-41.5	286	2.5	1.4	1.2
21.01.91	15	Puerto Montt-Punta Arenas	-41.5/-57/-53	303	2.8	1.5	1.3
22.01.91	16	Punta Arenas-Comodoro Rivadavia	-53/-46	309	2.8	1.5	1.3
22.01.91	17	Comodoro Rivadavia-Buenos Aires	-46/-35	286	2.5	1.4	1.2
23.01.91	18	Buenos Aires-Porto Alegre	-35/-30	279	2.4	1.4	1.2
23.01.91	19	Porto Alegre-Rio	-30/-23	268	2.3	1.3	1.2
25.01.91	20	Rio-Salvador	-23/ -13	271	2.3	1.3	1.2
25.01.91	21	Salvador-Fortaleza	-13/-4	268	2.3	1.3	1.2
25.01.91	22	Fortaleza--Recife	-4/-7	264	2.4	1.4	1.2
29.01.91	25	Abidjan (Local Flight)	5	265	2.4	1.4	1.2
30.01.91	26	Abidjan (Local Flight)	5	264	2.5	1.4	1.2
31.01.91	27	Abidjan-Dakar	5/15	261	2.7	1.5	1.3
31.01.91	28	Dakar-Las Palmas	15/28	284	3.4	1.7	1.4
01.02.91	29	Las Palmas-Lisbon	28/39	332	4.9	2.2	1.7
01.02.91	30	Lisbon-Bretigny	39/48.5	373	6.8	2.8	2.1

Tabulated for each flight are the latitude ranges, average ozone column densities and calculated atmospheric formaldehyde lifetimes at 0, 5 and 10 km.

$$[HCHO] = k_1*[CH_4]*[OH] \; / \; (J_{9a} + J_{9b} + k_{10}*[OH]) \quad (1)$$

whereby k_1 (Vaghjiani and Ravishankara, 1991) and k_{10} (Atkinson, 1990) are given as follows:

$$k_1 = 1.59* 10^{-20} * T^{2.84} * e^{-\{978/T\}} \; (cm^3 \cdot molec^{-1} \cdot s^{-1})$$
$$k_{10} = 1.25 * 10^{-17} * T^{2} * e^{\{648/T\}} \; (cm^3 \cdot molec^{-1} \cdot s^{-1})$$

The atmospheric lifetime of formaldehyde is then calculated using the sink terms in equation 1 (reaction with OH radical and photolysis):

$$t = 1/([OH] * k_{10} + J_{9a} + J_{9b}) \quad (2)$$

Photolysis is the predominant loss mechanism for formaldehyde in the troposphere. J_{9a} is typically 1.5 to 3 times faster than J_{9b} due to the higher actinic flux at wavelengths optimal for photolysis via J_{9a}. Reaction with OH$^\cdot$ may start to play a role in lower tropospheric polluted air in the winter hemisphere, but is then limited by a slower winter OH$^\cdot$ formation rate.

4.1b Description of the tropospheric Harwell model

For comparison purposes, calculations of the global tropospheric distributions for formaldehyde and acetaldehyde for the month of January from a two-dimensional global tropospheric model (Hough, 1989, 1991) which accounts for the contribution of NMHCs to formaldehyde and acetaldehyde mixing ratios in the free troposphere were obtained (Colin Johnson, AERE Harwell, personal communication, 1991). Global natural and anthropogenic emissions of major hydrocarbons (C_1 - C_7), isoprene, and terpenes based upon measurements and estimates

were applied in the model as functions of latitude and season. The model chemistry is nearly completely driven by time-dependent photolytic processes from 10 different source categories. The global average concentration of OH radical is $8.3 \times 10^{+5}$ cm^{-3}, and is in good spatial agreement with Penner et al., (1991) for the entire free troposphere. Vertical and horizontal transport is described in Hough (1989), and is based on comparison with measurements of the conserved tracers $CFCl_3$, CF_3Cl_2, ^{85}Kr, and water vapor throughout the troposphere.

Model output obtained in tabular form enabled a point-for-point comparison for measured and modelled values. For comparison purposes, however, it is important to realize that the chemistry (source strengths) in the two-dimensional Hough-Harwell model are averaged longitudinally over the entire globe at constant latitude and therefore a direct point-for-point comparison is not always realistic. This is especially true for flights 12-18 (southern region of South America) where there are nearly no other land masses (low source strengths) at these latitudes, and therefore modelled values should be somewhat lower. The Harwell results are plotted in the following section in 2-D form using the iterative Surfer program (Goldan Software).

4.2 Results and discussion

The flights began on 09' January 1991 from Bretigny sur l'Orge (30 km south of Paris, France) and were completed also in Bretigny on 01' February 1991. The maximum altitudes were approximately 10.5 km, lower than during STRATOZ-III (11-12 km), due to weight and safety limitations. For similar reasons, sampling was not conducted during flight 4 (Sondestrom to Goose Bay), flight 23 (Recife to Freetown), and flight 24 (Freetown to Abidjan). A total of 200 samples were

taken during 27 of the 30 flights, of which 124 were from the southbound section, and 76 during the northbound section. From the 200 samples, 51 were discarded due to either too low sample volumes (below detection limits), ozone interference, or evidence of contamination. For the southbound flights (5-15) a total of 52 formaldehyde and 25 acetaldehyde samples are reported. From the northbound flights (flights 1-3, and 16-30), 97 formaldehyde and 47 acetaldehyde samples are reported. The individual sampling point locations, aldehyde and ozone mixing ratios, and ambient conditions are listed in Section 6.3.

To assist in the presentation of the measurements, vertical 1-D profiles of formaldehyde are plotted with ozone, and potential temperature over the same sampling intervals (Figures 4.2a - i). Each plot contains data from 2-4 flights and can assist in detecting regional or vertical variations.

Globally, vertical profiles of formaldehyde generally showed a significant variability within the boundary layer followed by sudden to gradual decreases in the free troposphere. Minimum HCHO values were systematically detected at higher elevations. Ozone in the PBL was seen to be slightly higher in the northern hemisphere than in the southern hemisphere. In the northern hemisphere (to 50^{o} N), ozone typically ranged between 30 and 50 ppb throughout the troposphere yielding rather weak vertical gradients. In the southern hemisphere, ozone ranged between 10 and 30 ppb within the PBL and increased gradually with altitude.

In order to gain a better spatial overview of the data and to determine whether significant latitudinal or seasonal trends can be detectable, the southbound and northbound aldehyde data sets were plotted in 2-D form. Such a presentation of two-dimensional distributions on the basis of 149 formaldehyde samples and 72 acetaldehyde samples can only show the most fundamental features for each compound. A grid resolution of 10^{o} latitude by 1 km was chosen, whereby data

Figure 4.2a 48° N to 67° N

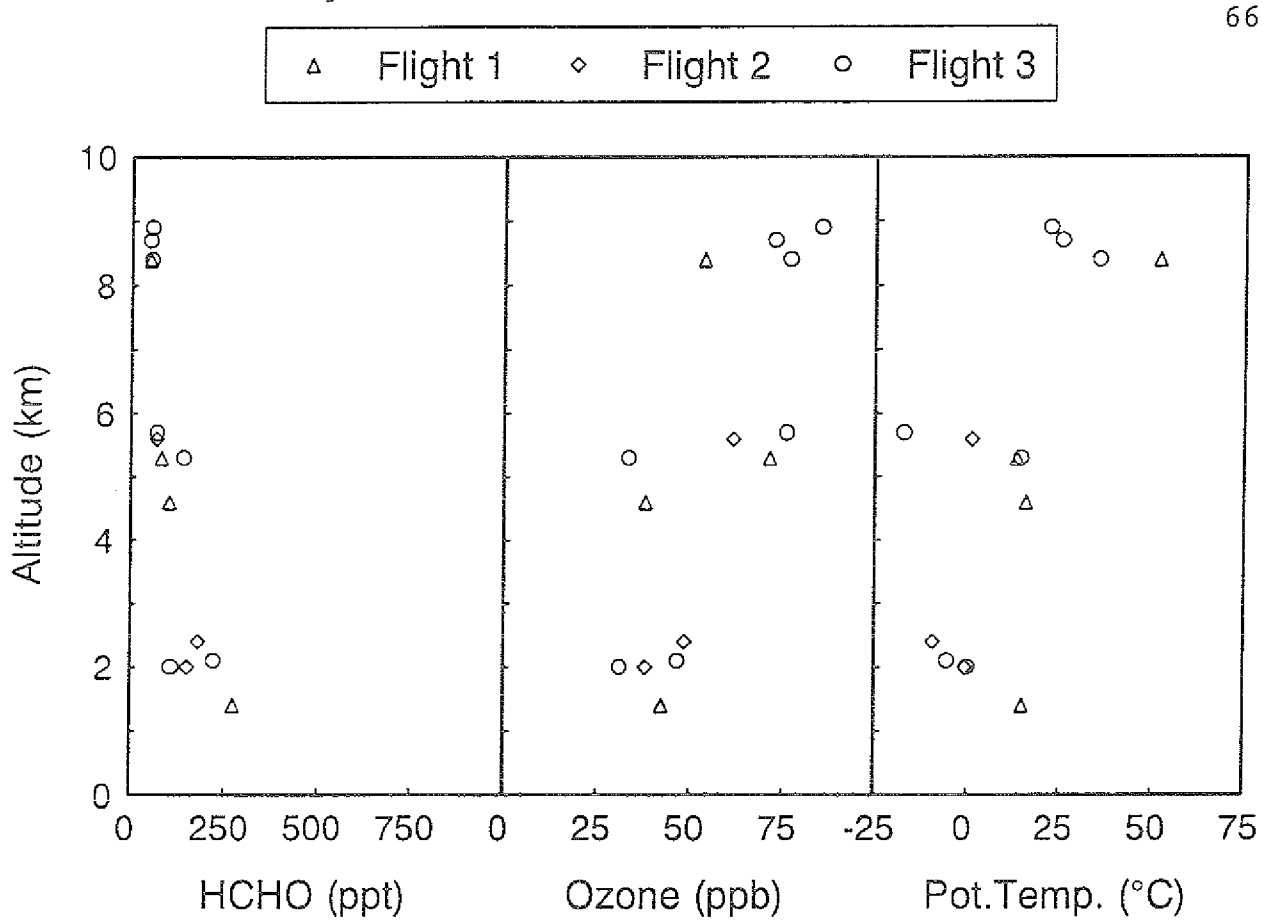

Figure 4.2b 53° N to 16° N

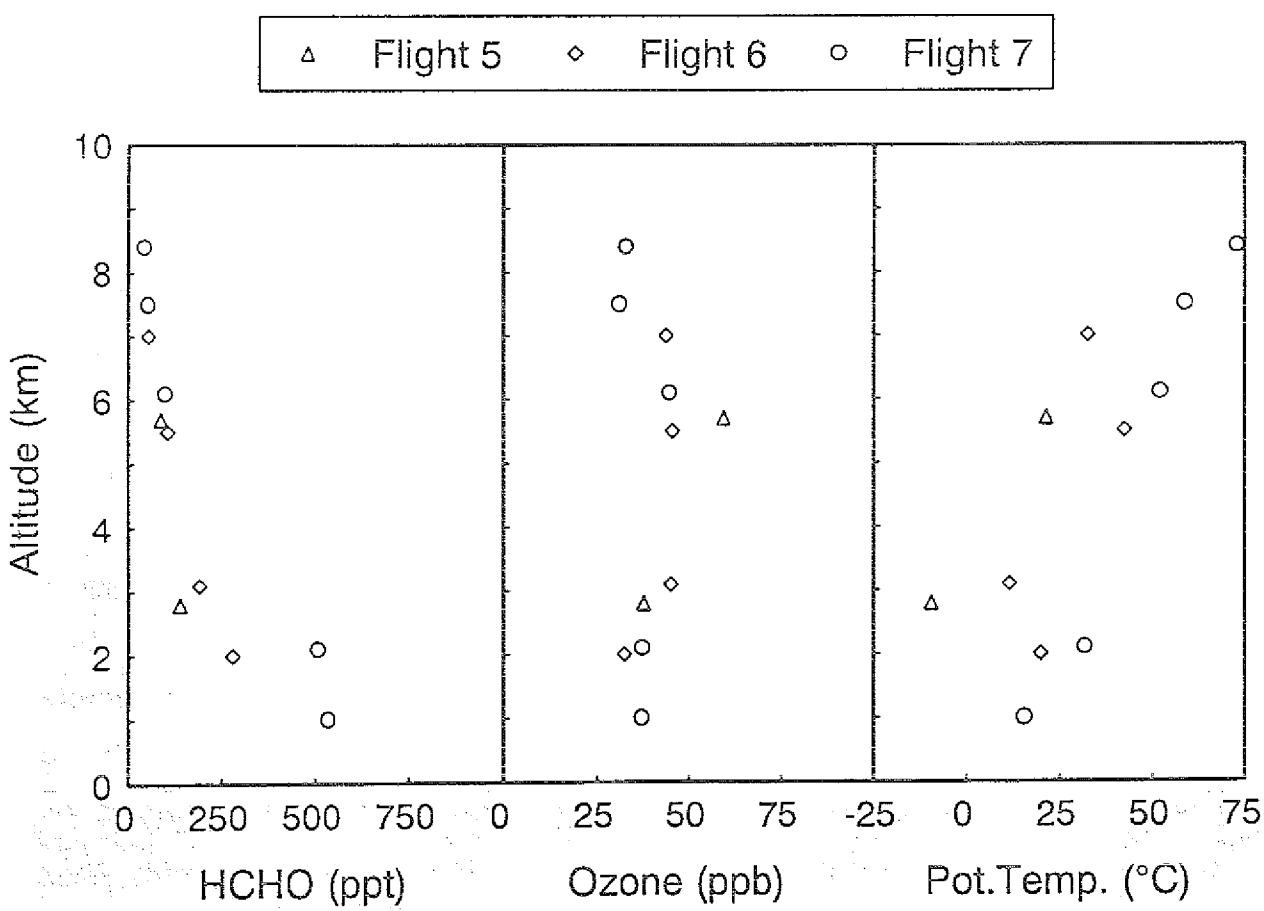

Figure 4.2c 16° N to 3° N

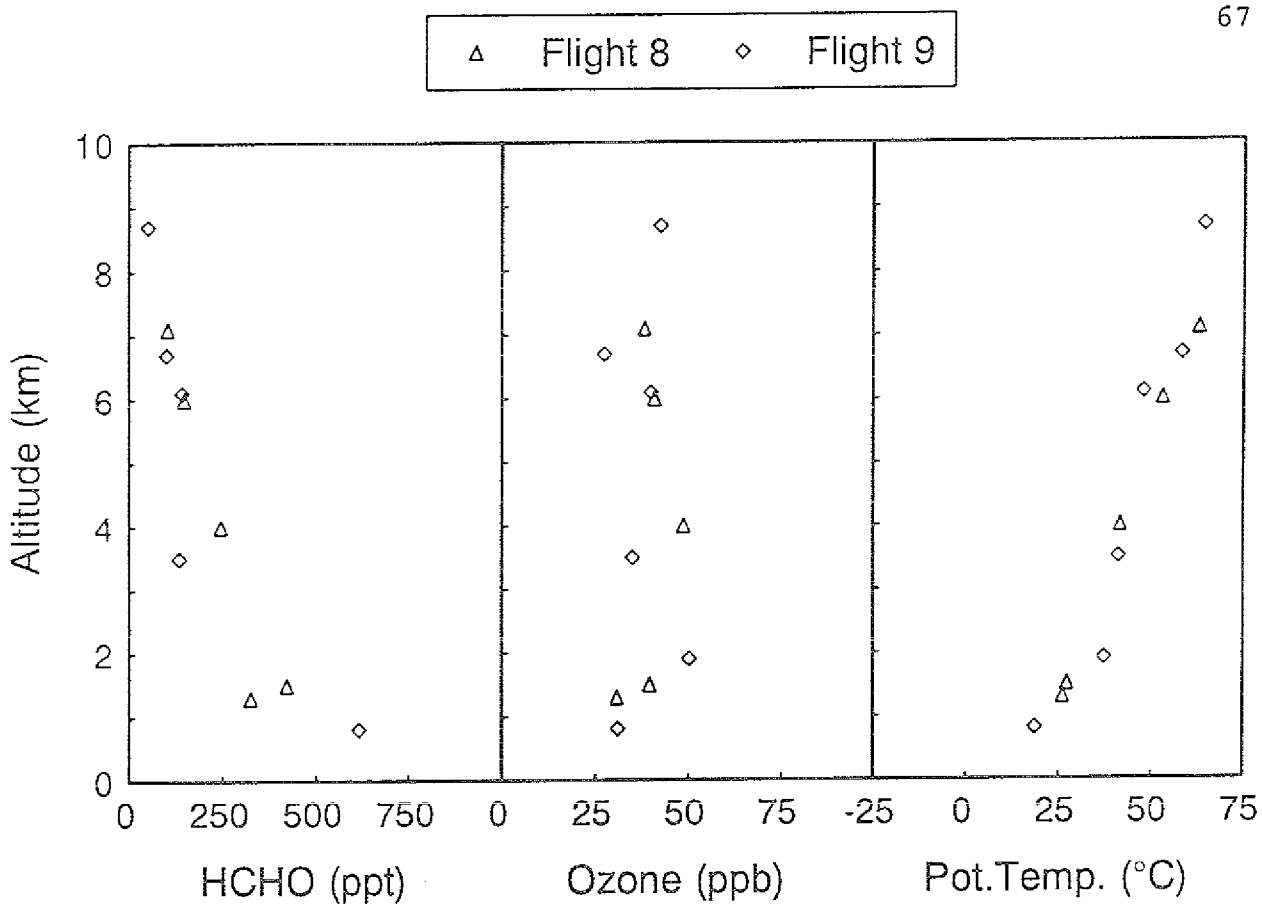

Figure 4.2d 3° N to 23° S

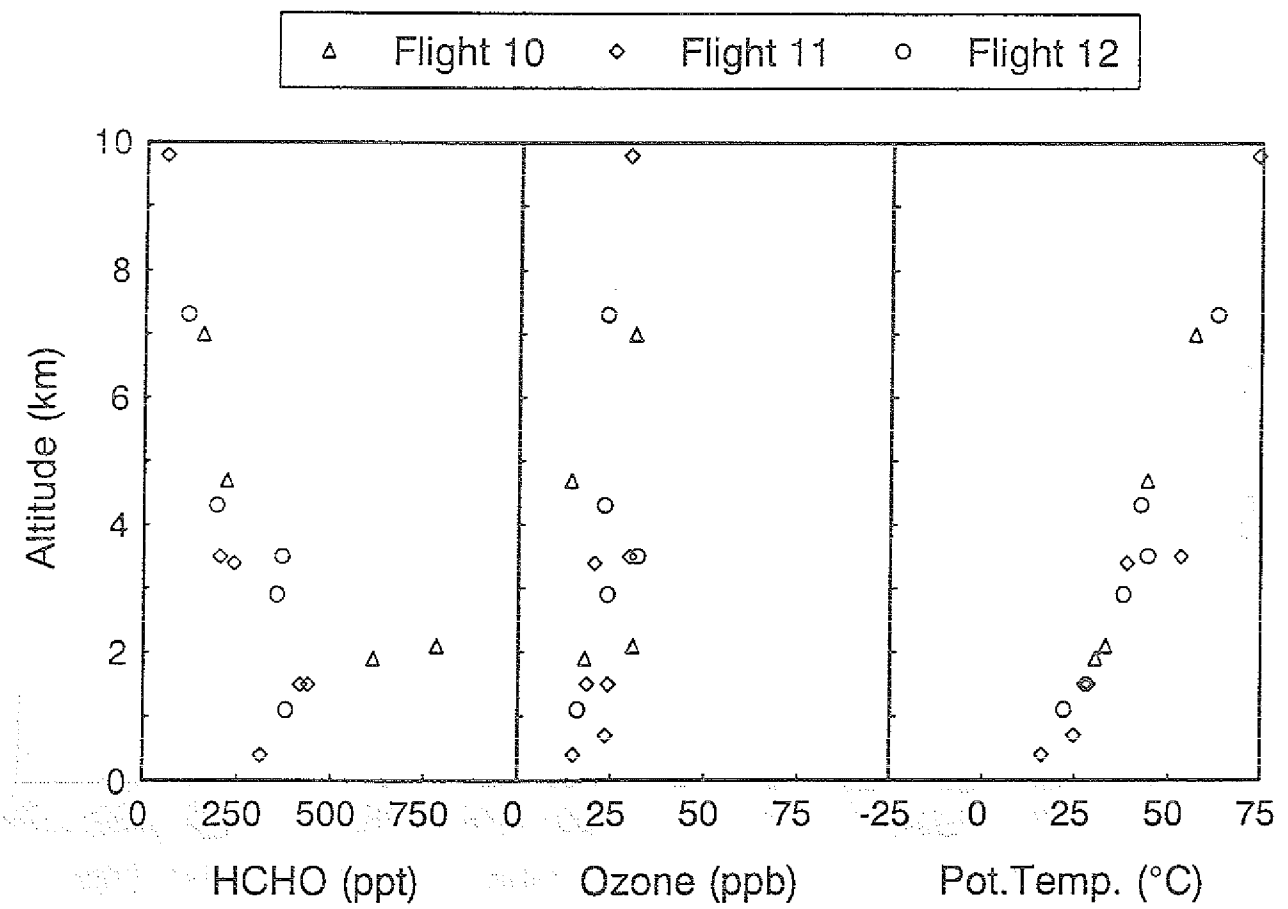

Figure 4.2e 23° S to 57° S

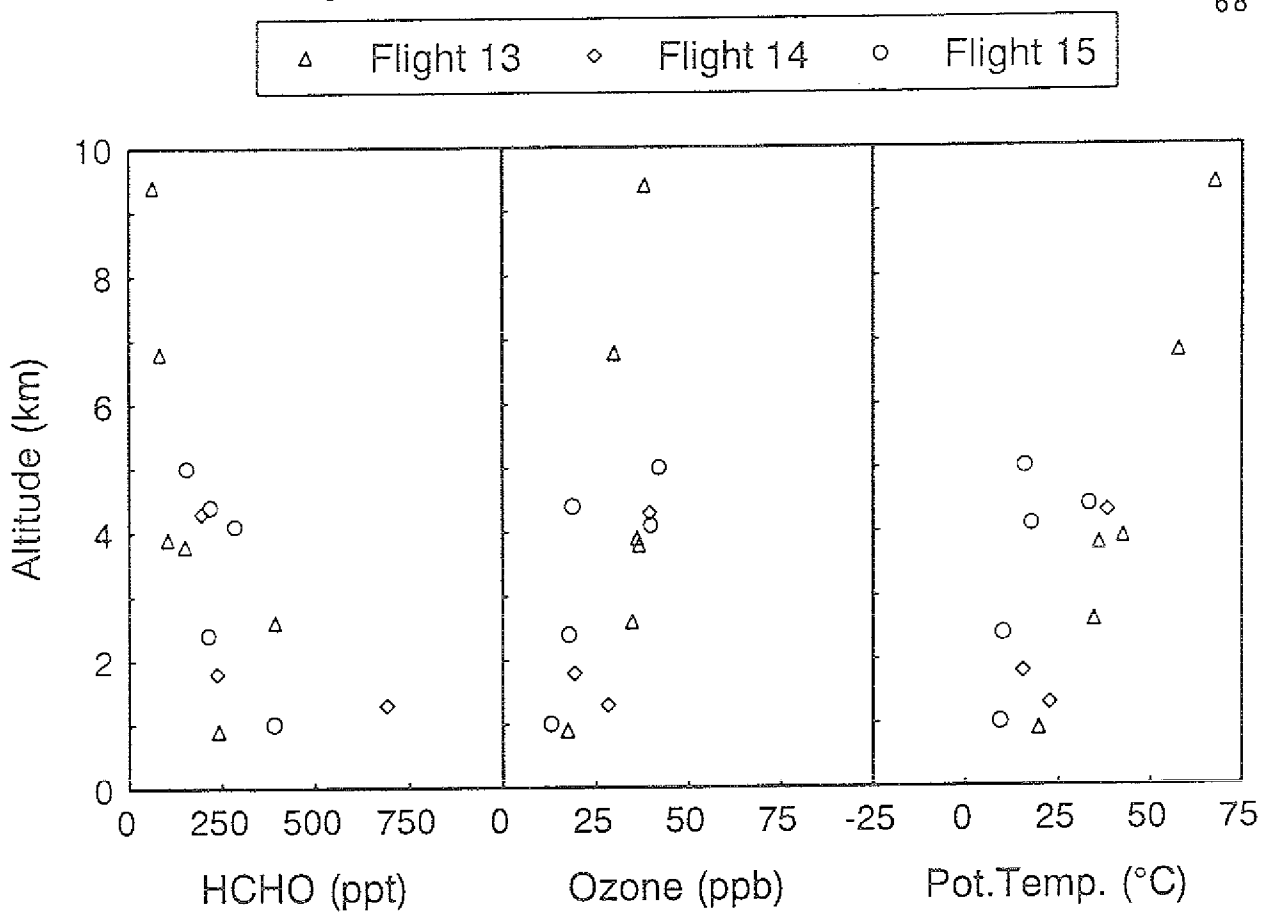

Figure 4.2f 53° S to 30° S

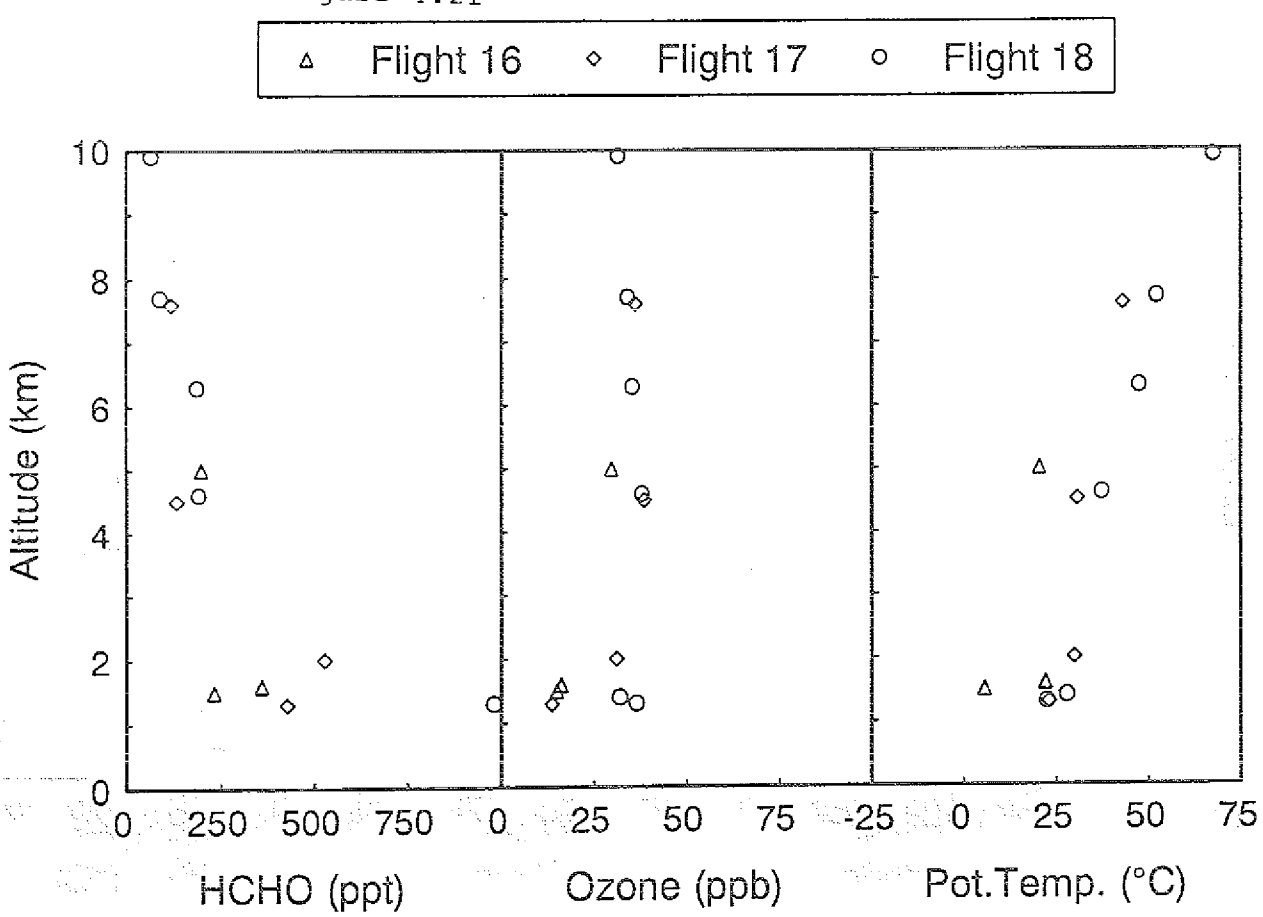

Figure 4.2g 30° S to 7° S

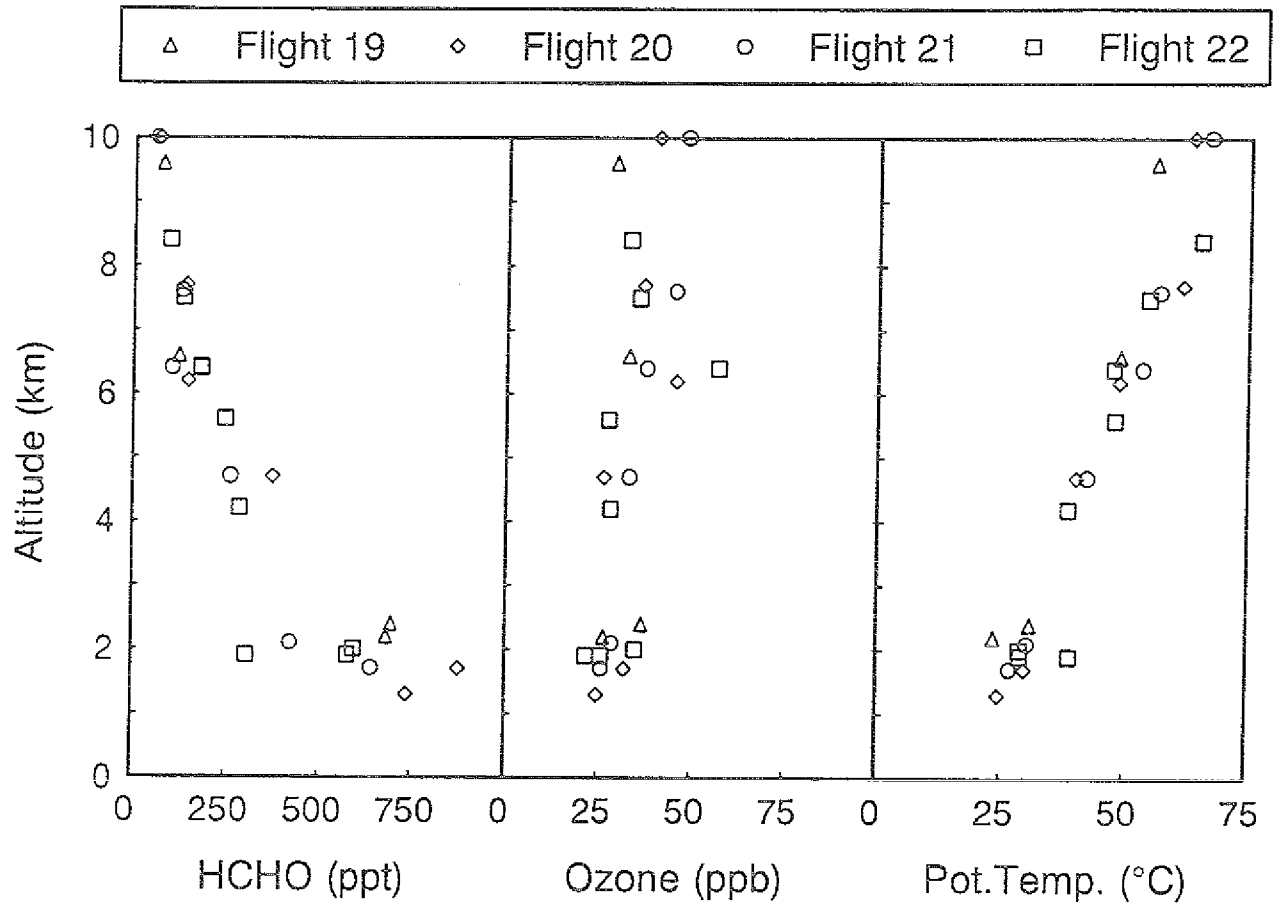

Figure 4.2h 5° N to 15° N

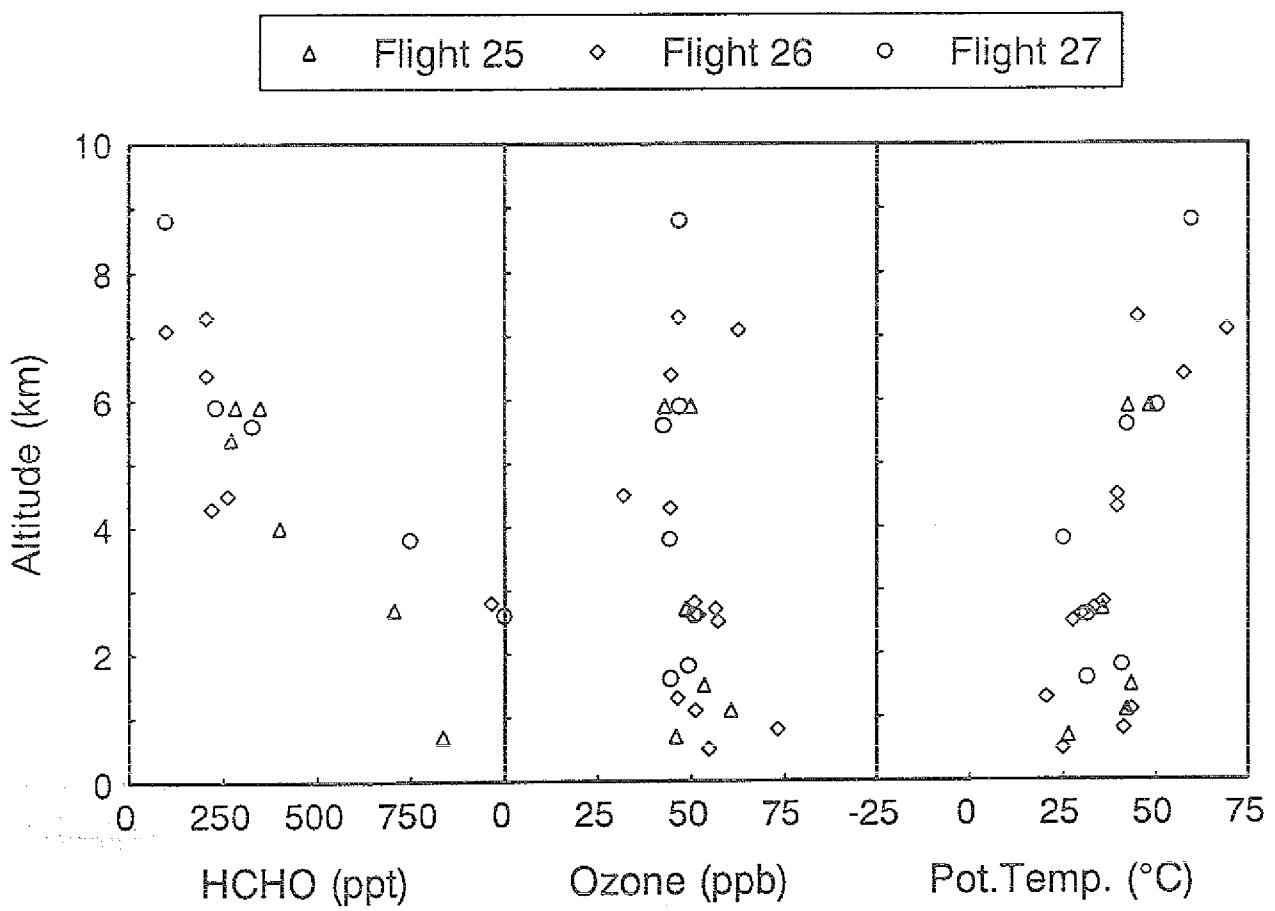

Figure 4.2i 15^{o} N to 48^{o} N

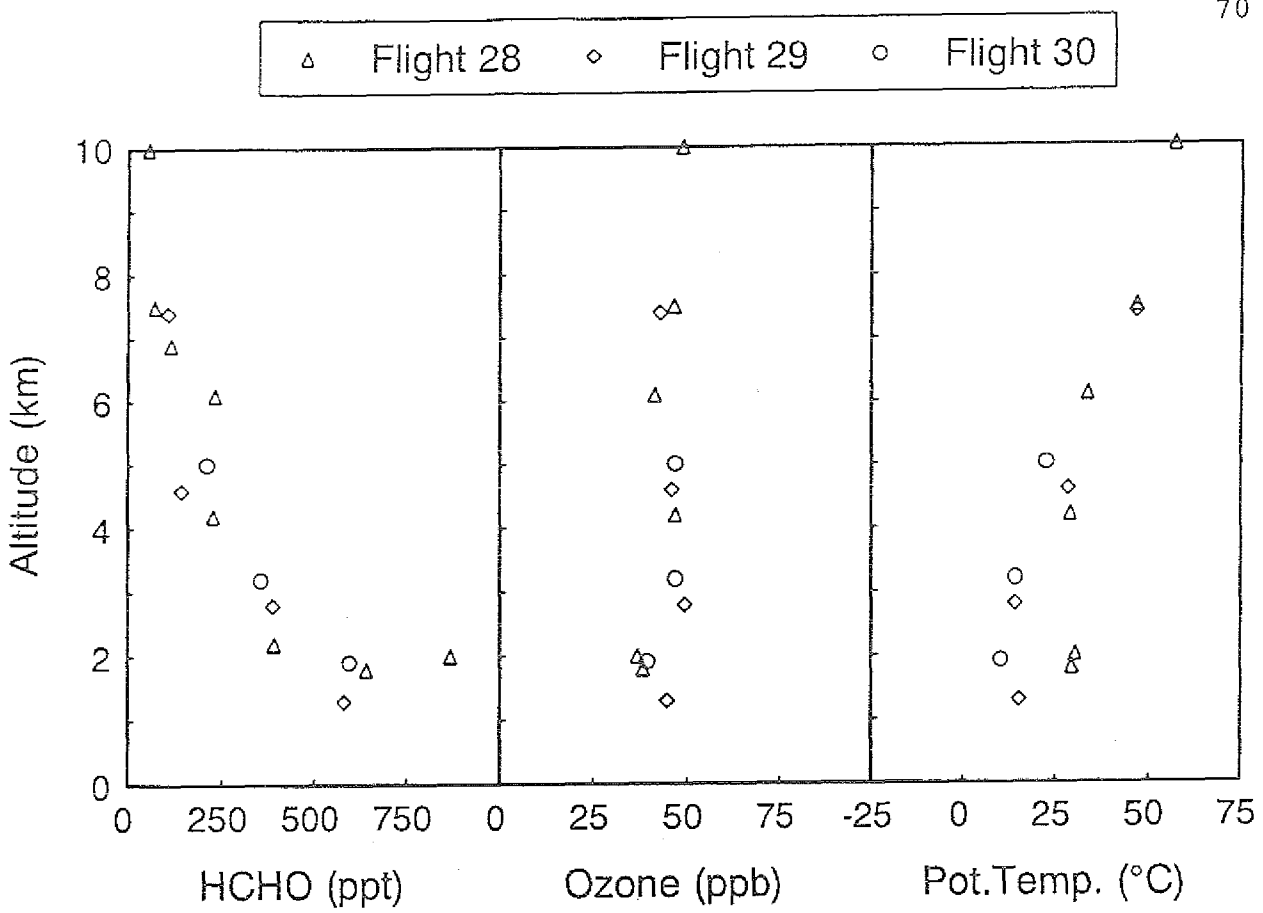

points were averaged within the boxes. Furthermore, it should be remembered that the observed altitude-latitude contours represent only a momentary snapshot of their respective distributions, and not necessarily a well-defined average. For the northbound plots, flights 1-3 are shown together with flights 16-30. Although there was a time span of nearly 3 weeks between these two sampling periods, it is not difficult to differentiate between them for interpretative purposes.

Presenting the data as meridional cross sections greatly assists the visual presentation of a rather large amount of information and provides a convenient basis for comparison with modelled values, meteorological parameters or distributions of other trace gases.

SOUTHBOUND FLIGHTS 5-15:

Due to the present lack of supporting data, a complete and thorough interpretation of measured formaldehyde and acetaldehyde is not possible. The following cursory discussions are based on the following preliminary data available in October 1991; wind direction, wind speed, atmospheric temperature, and ozone (A. Marenco, Personal Communication, 1991). Although measurements of NMHCs and NO_x from TROPOZ-II are presently not available, NMHC and NO_x measurements made during STRATOZ-III (Rudolph, 1988; Drummond et al., 1988; Ehhalt and Drummond, 1988) can be used to gain a rough overview of the tropospheric distributions of aldehyde precursors.

HCHO:

The higher elevations (> 8.5 km) in the northern hemisphere (20^{o} N to 55^{o} N) were typified by low temperatures (-50 to -65^{o} C), and short-termed elevated ozone mixing ratios

Figure 4.3

Measured Formaldehyde in ppt Southbound

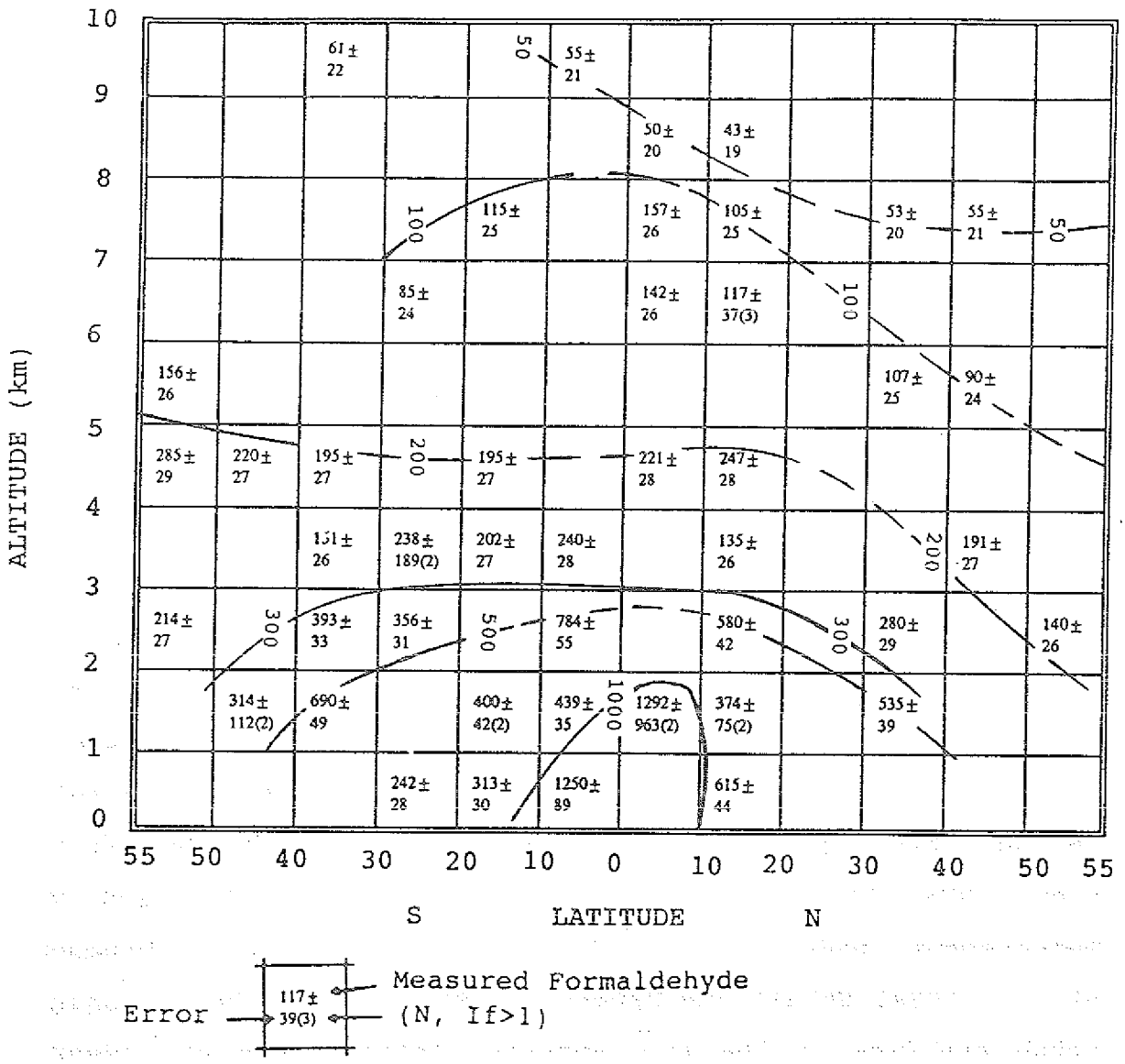

(200 - 350 ppb), indicating the possibility of slight intrusion of air from the stratosphere. Formaldehyde samples in this region during flight 5 which were not influenced by excess ozone interferences were seen to contain some of the lowest mixing ratios (ca. 50 ppt at 8.4 km) of the entire campaign. At present, information regarding their respective air mass origins is lacking. In general, as seen in Figure 4.3, HCHO mixing ratios in the higher elevations tended to range between 50 and 70 ppt for the duration of the southbound flights. The lower half of the troposphere showed fairly weak latitudinal dependencies except for the extreme north (slightly increased HCHO due to low photolysis rates) and equatorial regions (increased HCHO due to rapid hydrocarbon oxidation and/or increased vertical transport). At lower elevations (below 2.5 km), southern hemispheric values were slightly lower (487.1 +/- 310 ppt, range: 214 to 1250 ppt, N = 11) than northern hemispheric values (658.8 +/- 544 ppt, range: 280 to 1970 ppt, N = 8), but are in general accordance with previous shipboard HCHO measurements (200 to 300 ppt) over the remote southern Pacific Ocean (Arlander et al., 1990), implying a marine influence. In the lower troposphere, larger source strengths in the northern hemisphere could explain this slight hemispheric imbalance. For the reverse case, i.e., summer northern hemisphere with winter southern hemisphere, a still larger hemispheric imbalance could be expected. For these southbound southern hemispheric measurements, methane oxidation could alone nearly account for the observed HCHO levels. On the other hand, low elevation measurements in the northern hemisphere also resembled the northern hemispheric shipboard measurements (400 to 600 ppt). In both cases (airborne and shipboard) there is evidence of additional HCHO production from either in-situ oxidation of natural NMHCs or continental influences. A similar range of shipboard HCHO values were also found over the Atlantic Ocean by Schubert et al., (1988). For these southbound TROPOZ-II

flights, the wind directions were similar to the STRATOZ-III flights. This would further imply that the northern hemispheric measurements were possibly continentally influenced with sufficient NMHCs which could explain this slight latitudinal gradient at low altitude. A local maximum was observed near the equator (ca 1.5 km) in a small region of highly variable wind direction indicating possible continental influence. This effect was also observed during STRATOZ-III, indicated by highly localized maxima of several anthropogenic NMHCs at 1 km. Vertical transport from ground level in the ITCZ (ca. 0^{o} - 5^{o} N) may have contributed to slightly higher mixing ratios over this region.

The kinetic CH_4 model (Figure 4.5) shows very similar characteristics in the free tropopshere as the observations. This result confirms the importance of methane-OH radical reaction as a major formaldehyde source. Or, HCHO production rates in the far north were greatly reduced simply due to low $OH^{\cdot}$ availabilty. Due to the likely presence of abundant NMHCs in the northern hemisphere, significant differences are seen in the lower troposphere. Additional HCHO sources in the free troposphere of the northern hemisphere need to be considered. Formaldehyde production rates (Figure 4.4) were most significant in the southern hemisphere at low altitudes, and decreased significantly with altitude, and moving northward. Atmospheric lifetimes (Figure 4.4) for formaldehyde for each sampled location were also calculated for the respective in-situ conditions. Relatively little variation was seen for much of the mid- to upper troposphere, with most values ranging between 2.0 and 4.0 hours. The highest lifetime values, up to nearly 20 hours, were calculated in the northern hemisphere, and were due to significantly lower photolysis rates as a result of higher O_3 column densities in the stratosphere. This resulted, in turn, in a slight leveling-off in HCHO mixing ratios in the northern regions.

Figure 4.4

Formaldehyde Production Rates and Lifetimes Southbound

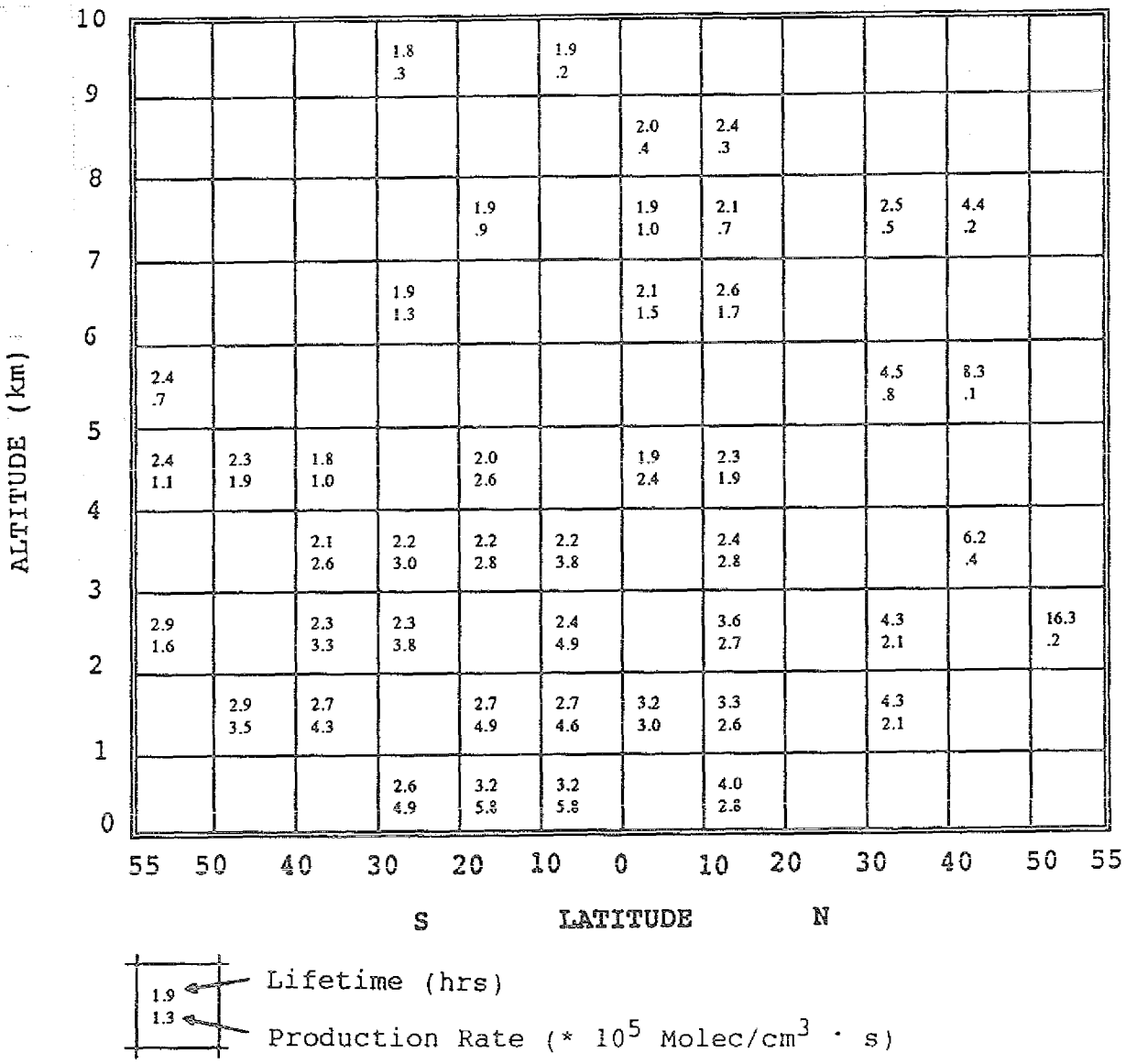

Figure 4.5

Kinetic Formaldehyde in ppt Southbound

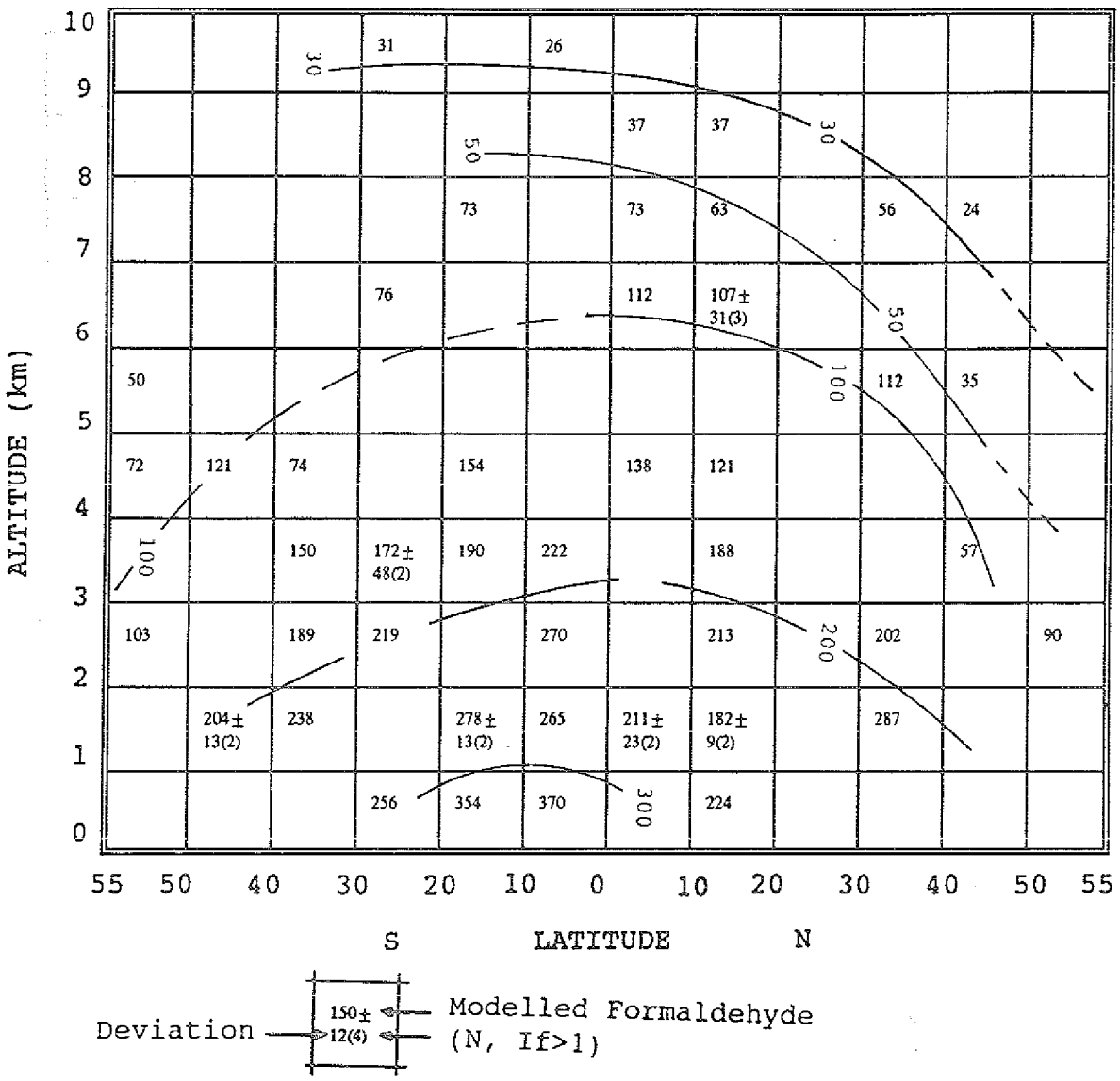

Figure 4.6

Harwell Formaldehyde in ppt

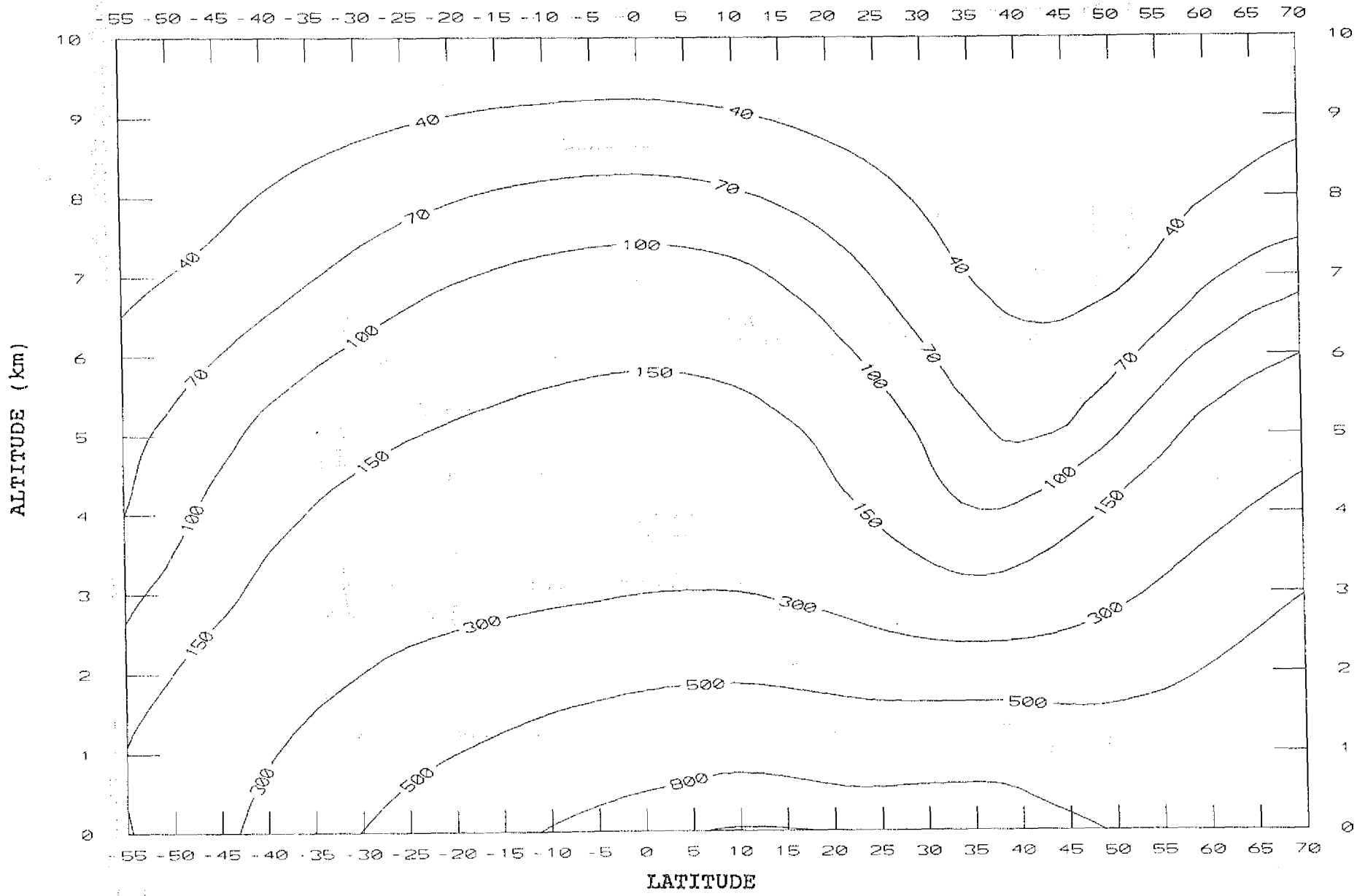

Figure 4.7

Formaldehyde Measurement : Model Comparisons (in ppt)

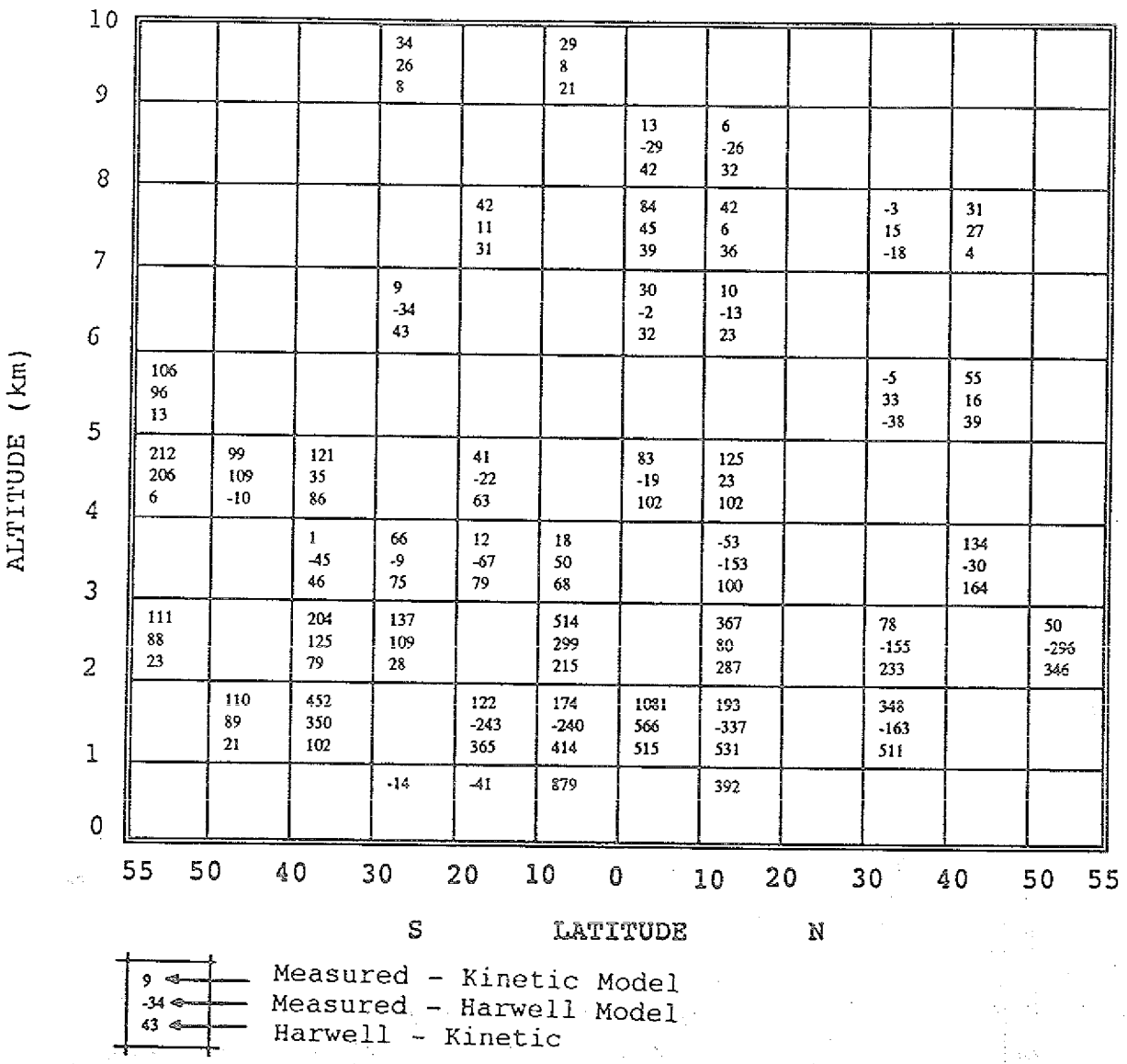

The January results of Harwell model from 70° N to 55° S for formaldehyde are shown (Figure 4.6) so as to include the entire flight track during the TROPOZ-II expedition. The distribution is characterized by typically higher ground-level HCHO mixing ratios in the northern hemisphere (nearly 1 ppb) due to the input of the NMHCs. In the winter hemisphere, the production of HCHO is highly limited above the boundary layer by the lack of OH radical. This effect is exhibited by lower HCHO mixing ratios in the free troposphere (above 3 km) between 35° N and 55° N. (In the free troposphere, OH radical concentrations are 10 to 20 times lower in the winter northern hemisphere than in the summer southern hemisphere; NMHC oxidation is hindered.) North of this region, HCHO once again begins to increase due to rapidly decreasing photolysis rates. In this region, the atmospheric lifetime of HCHO can increase to several days. This effect is also observed in the simpler kinetic model. Due to a higher availability of OH radical in the southern hemisphere, methane and NMHCs are efficiently oxidized to HCHO throughout the southern hemisphere. Throughout the free troposphere, OH radical is seen to be much more effective as a source of HCHO than as a HCHO sink. HCHO mixing ratios in the upper troposphere (ca. 9 km) are typically 40 ppt or less, depending upon location. Highest mixing ratios in higher altitudes occur in regions of maximum sunlight intensity, indicating the high photochemical dependence (higher OH radical production rates) of formaldehyde production. The only exception to this occurs in the far north, where photolysis rates are extremely slow and both natural and anthropogenic source strengths, i.e., direct emissions, can be very significant.

In most cases, the inclusion of the NMHCs as in the Harwell model is shown to overlap much of the difference between the observed values and the kinetic model results. A direct comparison between measured HCHO mixing ratios and the Harwell HCHO model shows good agreement for most of the

troposphere (Figure 4.7) when the measurement error is also considered.

The difference (in ppt) (Figure 4.7) in the modelled production of formaldehyde due to the inclusion of the additional nonmethane hydrocarbons (C_2 - C_7) compared to only methane-derived formaldehyde is shown to be significant to an elevation of 5 to 7 km. In the boundary layer alone, the contribution of the additional NMHCs can lead to a doubling of formaldehyde mixing ratios. For most of the global troposphere up to 7 kilometers, it is observed that the Harwell model typically predicted up to 2.0 times more HCHO than the kinetic model. The differences between measured results and the HCHO results obtained from the kinetic-methane model are seen to be considerably larger than the differences seen between measured results and the Harwell model results.

Air mass origin appeared to have an important role as indicated by typically higher aldehyde mixing ratios in regions which were continentally influenced. Also observed is the significant influence of the NMHCs in the industrial northern hemisphere. Due to both natural and industrial sources, abundant amounts of NMHCs can be present throughout the troposphere of the northern hemisphere. The effect of the NMHCs on HCHO production is seen to diminish moving southward as the source strengths decrease. As seen by NMHC measurements from STRATOZ-III (Rudolph, 1988), NMHCs appear to be more dependent upon latitude than altitude. Due to very efficient vertical transport processes and their sufficiently long lifetimes, the NMHCs can represent a significant source of aldehydes throughout the troposphere in a given latitudinal band. Formaldehyde on the other hand, as seen by both measurements and models, is somewhat more altitude dependent. (The latitude dependence appears to be slightly less significant.) Formaldehyde which is transported during the day to the upper troposphere will likely be photolyzed within 2

hours in most cases. Both models predict HCHO mixing ratios of ca. 40 ppt at the 9 km level as a global average.

Recent calculations of formaldehyde and acetaldehyde up to 6 km over the eastern US (McKeen et al., 1991), predicted decreasing mixing ratios with altitude for July 1986. A full suite of both anthropogenic and natural NMHCs were included which yielded profiles which could be considered as near upper-limit estimates for the aldehydes in the boundary layer. Ground level mixing ratios of 2 ppb and 800 ppt for formaldehyde and acetaldehyde decreased progressively to ca. 110 ppt and <10 ppt at 6 km. Due to the lack of vertical mixing in the model, modelled free troposphere aldehyde values are comparatively lower than northern hemispheric (winter) Harwell values.

CH_3CHO:

For these southbound flights, large latitudinal or vertical gradients were not evident as shown in Figure 4.8. To my knowledge there are no other previously reported above-boundary-layer measurements of acetaldehyde, which makes comparison difficult. Acetaldehyde mixing ratios were never over 100 ppt above 1.5 km, with the one exception at 3.5^{o} N at 1.5 km (ca. 170 ppt). As with formaldehyde, boundary layer (below ca. 2.0 km) values in the southern hemisphere (58.8 +/- 24.2 ppt, range: 27 to 105 ppt, N = 11) were slightly lower than northern hemispheric values (82.3 +/- 40.5 ppt, range: 46.1 to 173 ppt, N = 8). Wind directions in the northern hemisphere suggest slight continental influence. Shipboard acetaldehyde measurements over the mid-equatorial Atlantic (Schubert et al., 1988) showed 100 ppt for maritime air, and 200 ppt on average for possibly continentally influenced air. Other preliminary shipboard acetaldehyde measurements off the

Figure 4.8

Measured Acetaldehyde in ppt Southbound

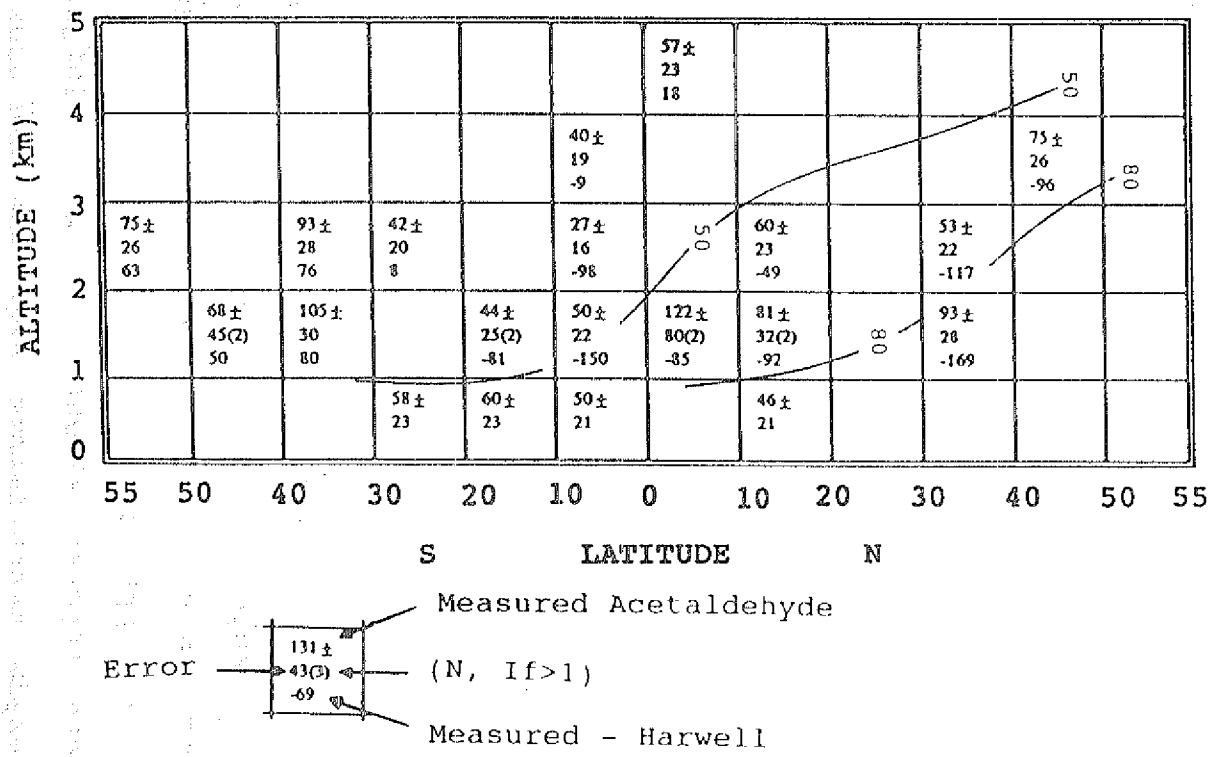

east coast of the United States averaged around 200 ppt (Zhou and Mopper, 1990), but air mass origin was not mentioned.

Wind directions throughout the equatorial region were highly variable up to ca. 2 km, and as with formaldehyde, a local maximum was observed around 2.0 km at 3.5° N near the ITCZ. From approximately 10° N moving southward between 2 and 5 km, nearly all sampled air was of predominantly marine origin (Pacific). Throughout this region, acetaldehyde levels were near the detection limit (ca. 30 ppt).

To a first-approximation, average formaldehyde mixing ratios in remote marine regions can typically approach 500 ppt. Due to the lack of NMHC oxidation, formaldehyde to acetaldehyde ratios should be fairly high. In clean air or background marine regions where CH_4 oxidation is the predominant source of HCHO, C_1/C_2 ratios typically ranged from 2.0 to 10 (Schubert et al., 1988) over the Atlantic Ocean. In cases where NMHC oxidation starts to become evident, this ratio begins to decrease. Unfortunately due to the relative low resolution of aldehyde C_1/C_2 ratio data in the lower troposphere, no conclusive arguments can be made concerning NMHC oxidation states. In spite of this, there are numerous occasions where low HCHO mixing ratios were coincident with C_1/C_2 ratios well above 2.0 in maritime conditions in both hemispheres.

Calculated acetaldehyde mixing ratios obtained from the Harwell model are shown (Figure 4.9) to be highly spatial dependent. There is a large imbalance in global source strengths which yielded significantly higher values in the northern hemisphere than in the southern hemisphere. On a global scale this prediction is probably correct. However, much of the southern hemispheric data collected during TROPOZ-II was near areas with potentially significant source strengths. Due to several common precursor hydrocarbons, acetaldehyde production follows that of formaldehyde, but on a smaller scale.

Figure 4.9

Harwell Acetaldehyde in ppt

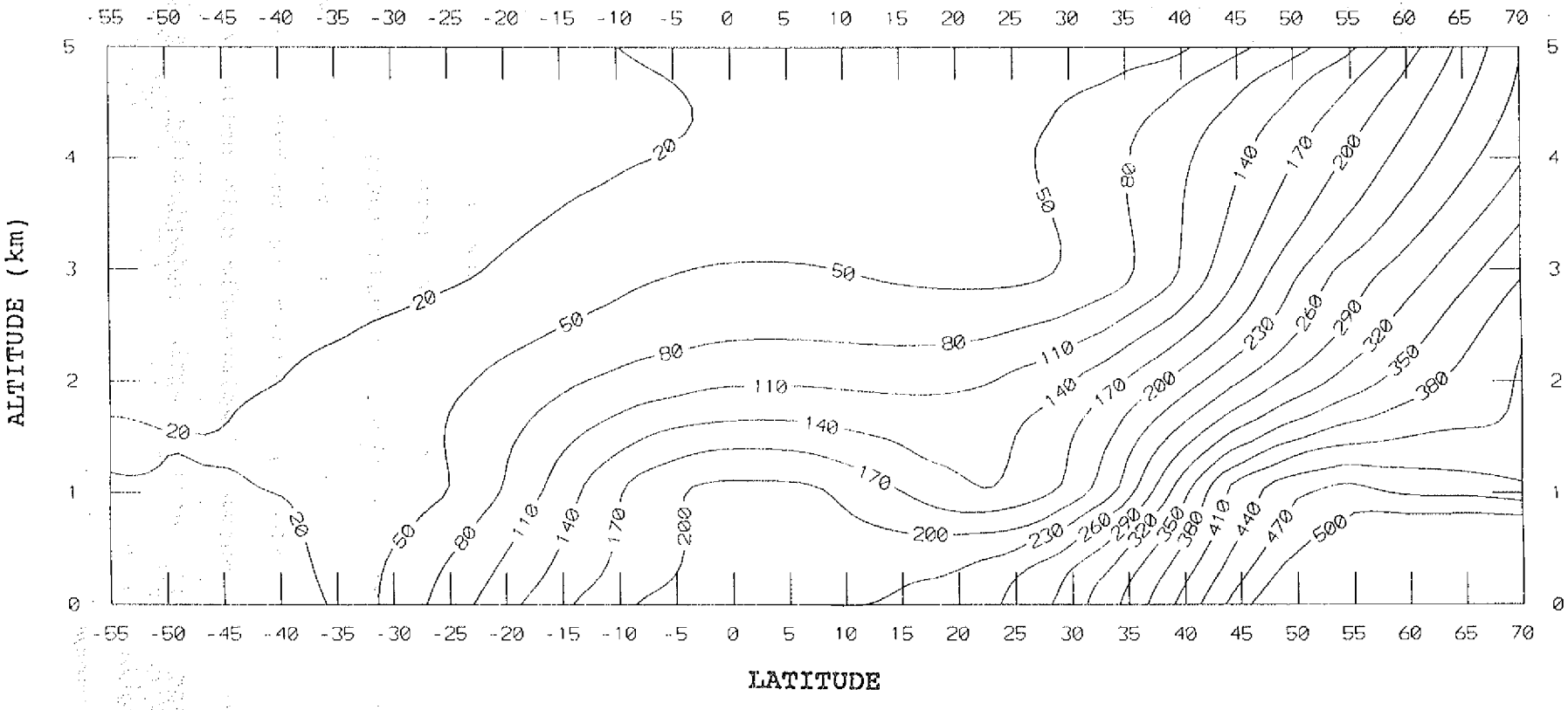

In general, the Harwell model tended to overpredict acetaldehyde in the northern hemisphere, and underpredict acetaldehyde in the southern hemisphere (Figure 4.8). From 30^{o} N to moving southward into the southern hemisphere, the lower troposphere was heavily influenced by marine air. Southern hemispheric samples were typically the lowest of the campaign. In this case, a justification for underprediction is clear. Since the model globally averages source strengths as a function of latitude, underpredictions near continental regions should be expected. Also due to changing wind directions in the lower troposphere and the high variabilty of acetaldehyde source strengths, marked discrepancy should be expected between measured and modelled acetaldehyde. In spite of these factors, the measured values are of similar magnitude as the Harwell values.

The atmospheric lifetime for acetaldehyde is on the order of 14 hours at ground level in mid-latitudes in summer. Sources of atmospheric acetaldehyde are more varied, albeit weaker, than for formaldehyde, resulting in a much more variable distribution. Although the gas-phase lifetime of acetaldehyde is approximately 2-3 times longer than formaldehyde, the total source strength of acetaldehyde precursors is considerably lower than for formaldehyde. Lower values for modelled acetaldehyde mixing ratios in the southern hemisphere are expected due to the abundance of OH radical, which serves as the major sink reaction initiator for acetaldehyde. As with formaldehyde in the far north, and coupled with a longer lifetime (due to low OH radical concentrations), modelled acetaldehyde appears to accumulate, leading to mixing ratios reaching 500 ppt or more at near ground level.

NORTHBOUND FLIGHTS 1-3, 16-30

The following discussion is in general quite similar to that just discussed for flights 5-15. For flights 1-3, and 16-30 only the main points and possible differences from the southbound flights will be mentioned.

HCHO:

Very similar trends are seen in Figure 4.10 for the northbound flights throughout the free troposphere. Upper tropospheric HCHO values were also not significantly different than during the southbound section. The error (maximum ca. 40%) associated with the upper level tropospheric samples is large enough so that clear distinctions cannot be made. The only exception to this is for samples taken during flights 1-3. The detection limits for these flights were somewhat lower (lower blank values), which enabled quantification of measureably lower mixing ratios (50 ppt) in the far north. For these 3 flights, ozone steadily increased above the PBL to a maximum of nearly 100 ppb at 9 km indicating slight stratospheric influence. Upper tropospheric mixing ratios were seen to resemble those from flight 5.

Wind directions indicated that air masses in the lower and middle troposphere were continentally influenced for much of the southern hemisphere. This is in contrast to the southbound section, whereby marine air was predominantly sampled. This may in part explain why HCHO mixing ratios tended to be slightly higher and more variable for the northbound flights (under 5 km). Above this altitude, continental effects began to have less importance. As with the southbound segment, ozone tended increase with elevation in the southern hemisphere.

Figure 4.10

Measured Formaldehyde in ppt Northbound

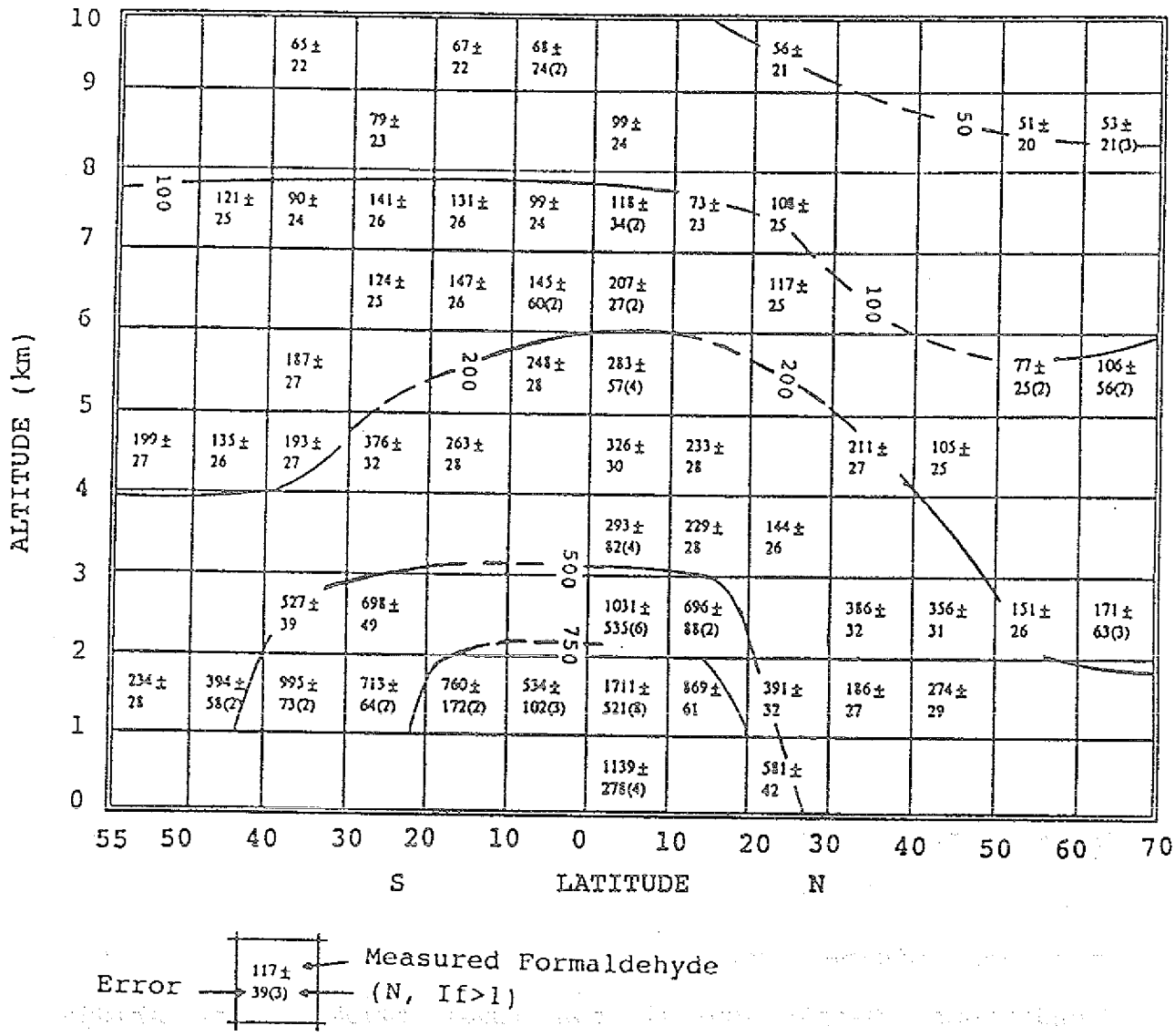

Sampling in the northern hemisphere was commenced in Abidjan, Ivory Coast (5^{o} N). Large variability for formaldehyde was observed within the PBL for this segment. Very preliminary data (F. Rohrer, personal communication, 1991) indicated that the boundary layer (0 to 2.5 km) was characterized by elevated NO_X mixing ratios. This is also confirmed by slightly elevated ozone (50 to 75 ppb) for all flights (flights 25, 26, and 27) near Abidjian up to an elevation of 2 to 2.5 km. From the other flights, typical boundary layer O_3 mixing ratios of 30 to 45 ppb were observed. Considerable cloudiness (orange to brown) was observed between 2 and 2.5 km possibly due to recent burning. HCHO mixing ratios up to 2.5 ppb range were observed, although no one single sample was taken entirely in the lower layer. Elevated ozone, HCHO, organic acids, and NMHCs also were observed over the northern Pacific Ocean in May 1987 due to a massive forest fire in northern China/Soviet Union where ca. 12 million acres (48,500 km^2) were burned over 21 days (Johnson et al., 1990; Arlander et al., 1990; Levine, 1990), eventhough the ship was located some 3,400 km from the fire and transport was not direct. Local photochemical production may have also had an important role. Above the boundary layer over Abidjan, HCHO and O_3 mixing ratios quickly returned to background conditions. Mainly due to the local flights near Abidjan, boundary layer HCHO samples taken in the northern hemisphere (986.9 +/- 685.5 ppt, range: 109 to 2430 ppt, N = 29) averaged somewhat higher than in the southern hemisphere (627 +/- 227.6 ppt, range 234 to 1010 ppt, N = 14). The air masses sampled during the remaining northbound flights were of mixed marine and continental origin, and tended to resemble the southbound section for this latitude band, i.e., HCHO in the free

troposphere tended to decrease with increasing latitude (20° N to 50° N). This decreasing tendency was mostly influenced by flight 29, (Las Palmas to Lisbon), which was flown over the ocean in westerly marine winds (above 2.0 km). For this flight, northbound HCHO values were slightly lower than southbound values for this latitude band (28° N to 38° N). In general, northbound samples which were continentally influenced tended to resemble southbound samples which were also continentally influenced. Several NMHCs measured during STRATOZ-III also showed similar distributions from 20° N to 50° N in the free troposphere for both southbound and northbound segments.

The kinetic CH_4 model shows very similar HCHO structure for both southbound and northbound segments (Figure 4.12). The northbound model is plotted to include flights 1-3 (50° N to 70° N). Any differences are mainly due to slightly different photolysis rates caused by variable ozone column densities along the flight track. Methane (STRATOZ-III) and OH radical mixing ratios (Penner et al., 1991) were essentially latitudinally identical for both flight segments. This in turn, yielded HCHO production rates which were very similar for both segments (Figure 4.11). Production rates in the far north were greatly reduced due to low OH^* concentrations. A slight increase in HCHO mixing ratios in the far north is due to decreased HCHO photolysis rates. In this northern latitude band, calculated HCHO lifetimes (Figure 4.11) are seen to increase significantly for flights 1-3, i.e., on the order of several days, compared to several hours, as in the southern hemisphere.

In several situations, especially in the lower troposphere from 50° S to 25° S and the local Abidjan flights flown near regions of biomass burning, the northbound flights tended to show slightly higher HCHO values than the southbound

Figure 4.11

Formaldehyde Production Rates and Lifetimes Northbound

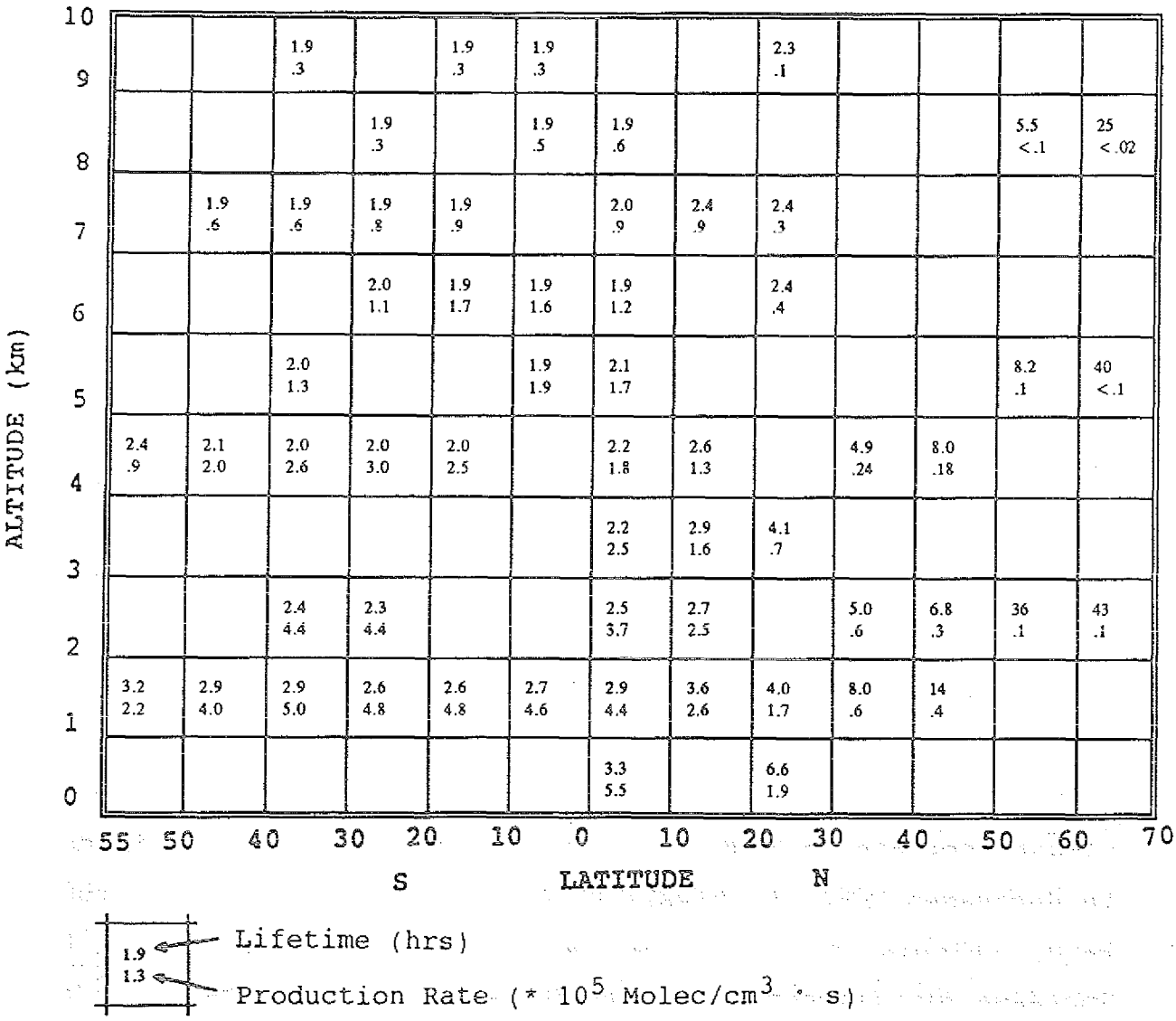

Figure 4.12

Kinetic Formaldehyde in ppt Northbound

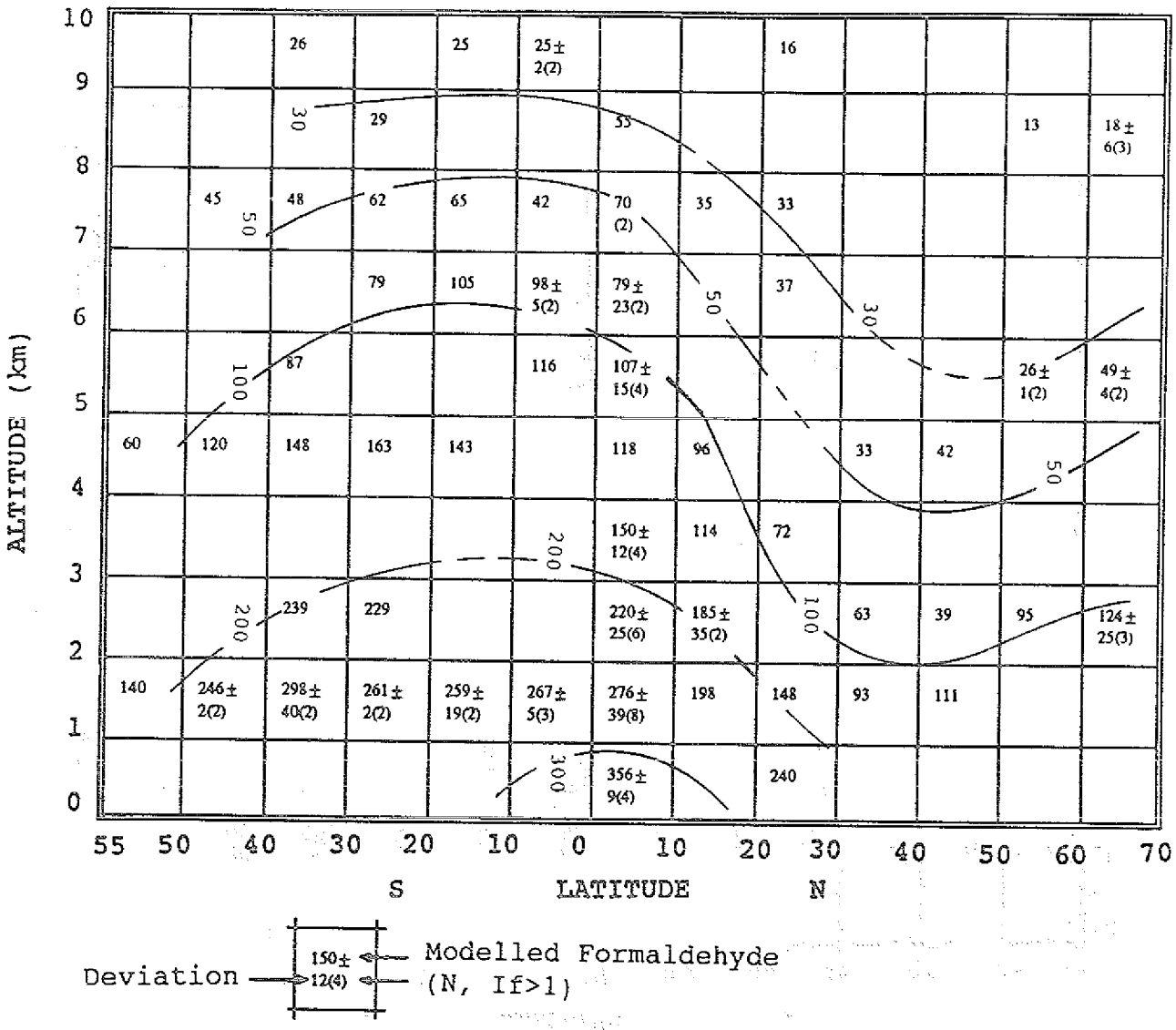

Figure 4.13

Formaldehyde Measured : Model Comparison (in ppt)

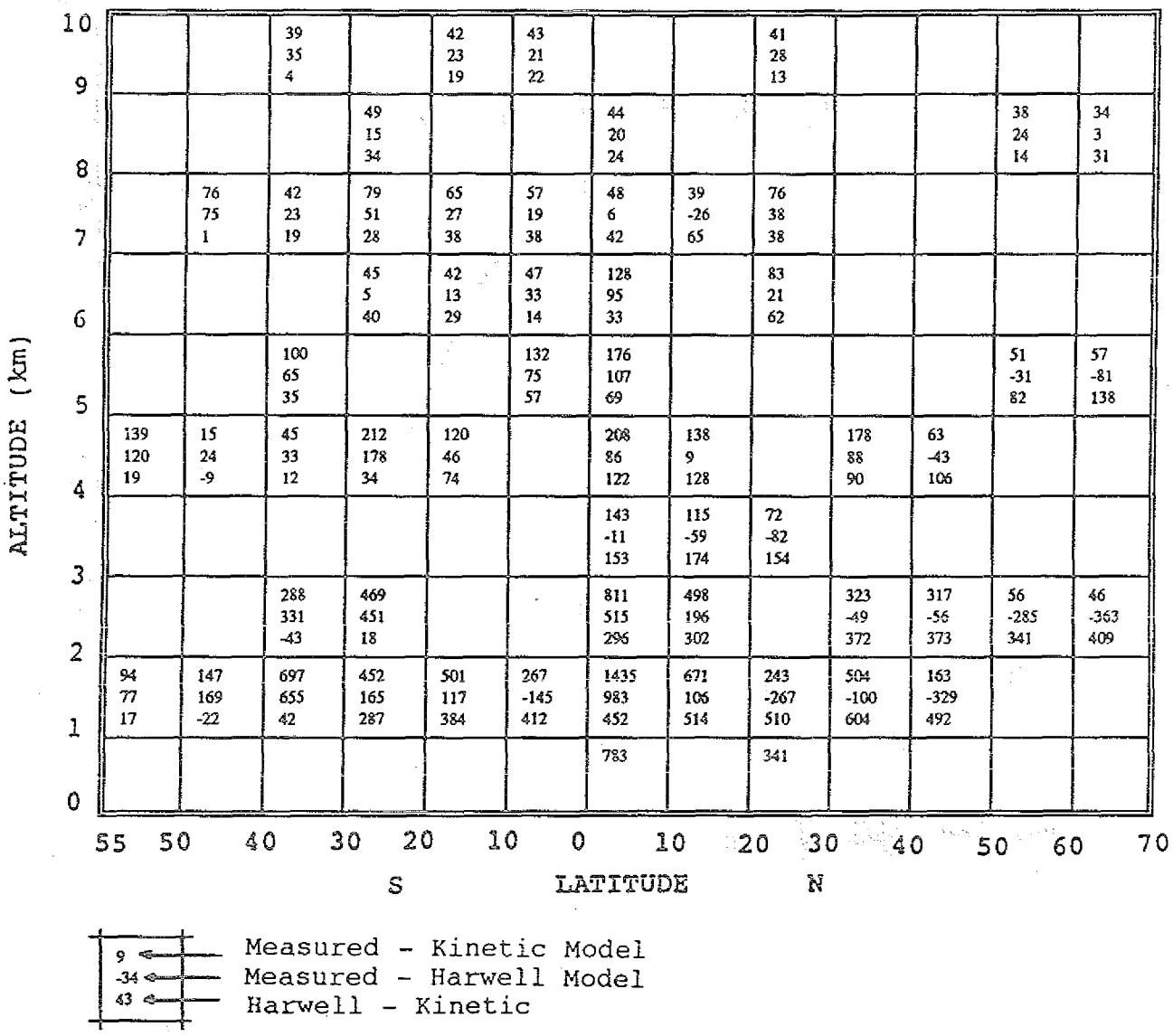

flights. Due to this, slightly larger differences are seen between the northbound segment and the Harwell model, than with the southbound segment (Figure 4.13). In general, however, very good agreement was seen between measured and Harwell modelled HCHO. Agreement between the Harwell model and measurements improved moving northward from Abidjan. As expected, differences between modelled and measured HCHO for the kinetic model (Figure 4.13) are accentuated.

The wind directions show that measured air was predominantly of continental origin for nearly all northbound samples in the southern hemisphere, which could explain the slightly elevated mixing ratios. Southbound samples taken in the southern hemisphere were more of marine origin, and therefore show slightly better agreement with the Harwell model for the southern hemisphere northbound samples.

Better agreement is seen in the northern hemisphere (Abidjan excluded) for northbound flights however. Many of the above-PBL samples taken between 30^{o} N and 40^{o} N (flights 29 and 30) appear to be of marine origin. This is also reflected in the acetaldehyde measurements mentioned below. For comparing measurements with model results it is necessary to remember that wind directions and source regions have a very important role. Understanding the basis of the models, and their limitations is also of utmost importance.

CH_3CHO:

Measurements in the southern hemisphere were mostly of continentally influenced air as shown by westerly to southwesterly wind directions, and were slightly higher than in the southbound flights. Boundary layer measurements in the southern hemisphere (105.9 +/- 24.5, range: 71 to 150.4 ppt, N = 14) were again slightly lower than northern hemisphere values (127 +/- 52.2 ppt, range: 34.2 to 261.6 ppt, N = 28). The mixing ratios are shown to rapidly decrease above the

Figure 4.14

Measured Acetaldehyde in ppt Northbound

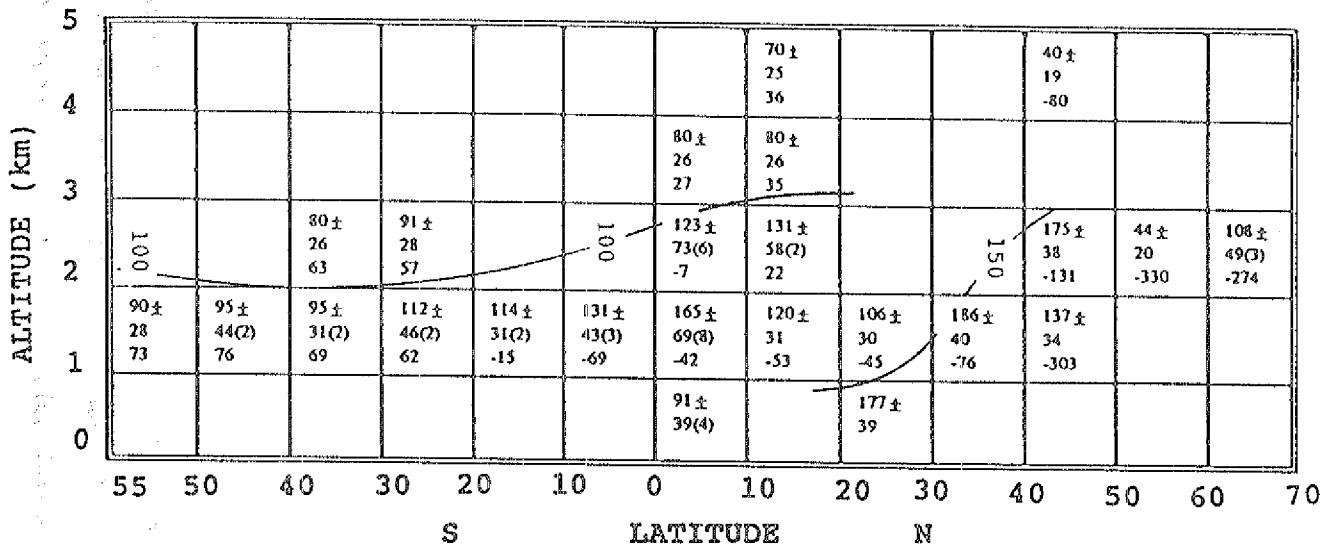

boundary layer to the detection limit (ca. 30 ppt) near 4 to 5 km. Acetaldehyde was shown to increase during the inland flights near Abidjan, and once again northwards. North of Abidjan, air masses in the lower troposphere (0 - 2.0 km) were of continental origin, and indicated similar to slightly higher values than the southbound flights.

As also observed for southbound measurements, the Harwell model tended to overpredict acetaldehyde in the northern hemisphere, and underpredicted acetaldehyde in the southern hemisphere (Figure 4.14). The underprediction is somewhat magnified in the northbound southern hemispheric boundary layer region due to slightly higher continental influences. Differences were accentuated even more during the local flights near Abidjan. Air masses north of Abidjan were of mixed origin, and therefore agreement with modelled results tended to be mixed. In the northern hemisphere, acetaldehyde samples of continentally influenced air tended to show slightly better correlation to the model. Between 28^{o} N and 39^{o} N (flight 29), above-boundary layer samples were mainly of marine origin, which is shown by the rapid decrease in mixing ratios (below detection limits). In this region, the Harwell model overpredicted acetaldehyde by 2 to 3 times. On a global scale, however, there is general agreement between the Harwell model and measurements.

5. Conclusions

The sampling and analysis technique described in this work has been found to be suitable for measuring low mixing ratios of formaldehyde and acetaldehyde and their variations in the free troposphere. The method performed with reasonable efficiency under a very wide range of sampling conditions. The adaptation of cartridges for the collection of aldehydes has enabled simpler and efficient sampling under adverse conditions.

Results of airborne measurements of the distributions of formaldehyde and acetaldehyde in the free troposphere were presented. With the assistance of supporting chemical and meteorological data which was available at this early date, a cursory interpretation of the measurements could be made. General observations indicate that the distribution of formaldehyde is regionally and seasonally dependent, and indicates relationships to major NMHC precursors, source regions, altitude and photolysis rates. Acetaldehyde mixing ratios were highly variable, and higher values were well correlated with air masses of continental origin. Aldehyde mixing ratios were seen to have a great amount of variability in the lower troposphere, then progressively or suddenly declined above the boundary layer depending upon amount of inversion-limited vertical mixing.

Methane-based kinetic models differ from the Harwell model significantly under 6-7 kilometers. Above this elevation, except for episodes of strong vertical transport of NMHCs, methane should dominate HCHO production. The inclusion of NMHC chemistry in the Harwell yielded results for formaldehyde which are much closer to observed values. Modelled values of acetaldehyde also gave results which were similar in magnitude to measured values up to 5 km. With the further development of more complex photochemical models, it

has been shown that many of the long existing incongruencies between measurements and model results can be accounted for. It is shown that models need to include more complete photochemistry which includes the oxidation of NMHCs to at least C_6 in order to achieve better agreement with experimental observations. To this purpose, more complete natural NMHC emission inventory estimates and measurements need to be made. Additional, yet still speculative HCHO sources include Cl-atom initiated NMHC oxidation (Singh and Kasting, 1988) should be included. It is estimated that this mechanism may contribute to HCHO production (by about 30% to that of OH oxidation of NMHCs).

There is a great need for the development and construction of a sampling system which can remove ozone without causing side reactions and is aldehyde passive. Such a system could permit larger sampling volumes in aircraft near the tropopause, or automated stratospheric sampling via balloon or in newly developed stratospheric research aircraft. Ground level quantification of higher carbonyl species such as acetone and propionaldehyde could also be optimized. The study of formaldehyde, total carbonyl content, their variation and lifetimes in tropospheric clouds for the study of global tropospheric/stratospheric carbon and oxidant cycles will possibly remain an important research topic for years to come.

6. Appendix

Additional information obtained during the previously mentioned measurement campaigns is listed in chronological order in this section.

6.1 August 1990 OH-Campaign in Jülich

Date	Time	Julian Date	Cart.	HCHO	CH3CHO	Temp. C	Wind Dir.	Wind Speed
	UT	UT	Number	ppb	ppb	20 Meters	120 Meters	100 Meters
300790	10:00	211.42	1	1.1	0.28	25.1	159.5	1.63
300790	10:51	211.44	2	1.32	0.31	25.5	208.33	1.63
300790	11:01	211.46	3	1.5	0.39	25.73	221	2.5
300790	11:52	211.48	4	1.55	0.43	25.83	311.67	1.67
300790	12:01	211.5	5	1.36	0.38	26.5	307.67	1.47
300790	12:51	211.52	6	1.3	0.29	26.73	295.67	2.43
300790	13:01	211.54	7	1.39	0.32	27.1	203	1.57
300790	13:51	211.56	8	1.22	0.37	27.37	172	1.67
300790	14:01	211.58	9	1.35	0.39	27.27	197	2.13
300790	14:51	211.6	10	1.39	0.38	27.7	268.67	1.6
300790	15:01	211.63	11	1.24	0.32	27.6	299.33	2.53
300790	15:51	211.65	12	1.35	0.25	27.2	341.33	1.73
300790	16:01	211.67	13	1.3	0.31	27.27	219	1.63
300790	16:51	211.69	14	1.32	0.27	27.13	299.67	1.77
300790	17:02	211.71	15	1.41	0.28	26.87	340	1.63
300790	18:00	211.75	16	1.09	0.12	26.2	347.75	1.4
300790	19:00	211.79	17	0.96	0.09	24.68	53	1.48
300790	20:00	211.83	18	1.1	0.1	23.23	85.75	3.08
300790	21:00	211.88	19	1.03	0.11	20.55	96.5	2.9
300790	21:57	211.91	20	1.12	0.12	20	112	3.03
300790	23:00	211.96	22	0.99	DL	19.13	143.75	4.25
310790	0:00	212	23	0.67	DL	17.6	231.25	2.43
310790	1:00	212.04	24	0.73	DL	17.78	268.25	2.08
310790	2:00	212.08	25	0.88	DL	17.18	269.75	1.85
310790	3:00	212.13	26	0.55	DL	16.18	276.75	2.98
310790	4:00	212.17	27	0.85	0.09	15.97	275	3.87
310790	5:00	212.21	28	0.85	0.12	16.3	289.5	3.55
310790	6:00	212.25	29	1.13	0.22	17.73	272.25	1.73
310790	7:00	212.29	30	1.2	0.4	19.75	216.25	0.83
310790	8:00	212.33	31	2.32	0.54	22.8	172.67	1.03
310790	9:00	212.38	32	2.17	0.7	25.23	248.33	0.8
310790	10:00	212.42	34	2.11	0.71	26.58	31	1.13
310790	11:00	212.46	35	2.47	0.96	27.78	36.25	1
310790	12:00	212.5	36	2.48	1.04	28.83	20.75	1.58
310790	13:00	212.54	37	2.03	1.36	28.85	335.25	2.23
310790	15:00	212.63	40	1.68	0.69	29	333	3.25
310790	16:00	212.67	41	2.34	0.73	28.7	341.5	3.28
310790	18:00	212.75	43	1.93	0.6	27.1	353	3.3
310790	20:00	212.83	46	2.17	0.45	23.25	357	1.53
310790	21:00	212.88	47	2.14	0.39	22.35	8.25	2.85
310790	22:00	212.92	48	1.44	0.43	22.48	25.25	3.83
10890	1:00	213.04	51	1.27	0.35	17.1	52.75	1.88
10890	2:00	213.08	52	1.32	0.36	17	61	0.93
10890	5:00	213.21	56	1.24	0.46	16.08	99.5	0.4
10890	6:00	213.25	57	2.16	0.85	18.2	273	0.98
10890	7:00	213.29	58	1.74	0.65	21.53	271	0.25
10890	7:51	213.31	59	2.08	0.74	23.57	213.67	0.33
10890	8:00	213.33	60	1.83	0.51	25.07	328	0.97
10890	8:50	213.35	62	1.62	0.64	26.03	127.33	2
10890	9:47	213.39	64	1.83	0.69	26.73	127.67	2.3
10890	10:50	213.44	66	1.84	0.77	27.77	125	2.27
10890	11:25	213.47	67	2.01	0.8	28.43	113.67	2.6
10890	12:01	213.5	68	2.4	1.31	28.93	231.67	2.97
10890	14:00	213.58	71	2.11	1.25	29.55	347	2.95
10890	16:00	213.67	73	1.74	0.69	28.78	263.75	2.33
10890	18:00	213.75	75	1.66	0.4	27.6	93.5	1.68
10890	20:00	213.83	77	1.39	0.15	23.63	15.25	5.6

10890	21:00	213.88	79	1.37	0.28	22.88	26.75	6.83
10890	21:50	213.9	80	1.22	0.12	22.9	39.67	7
10890	22:00	213.92	81	1.24	0.16	22.4	42	4.47
10890	22:05	213.94	82	1.3	0.17	22.8	54.67	4.27
10890	23:01	213.96	83	1.01	0.11	21.07	60.67	2.5
10890	23:50	213.98	84	1.1	0.15	19.5	75.67	1.2
20890	0:01	214	86	0.68	0.1	18.6	83.67	1.03
20890	0:51	214.02	87	0.7	0.1	17.7	70	1.83
20890	1:00	214.04	88	0.81	0.1	17	55	1.43
20890	1:50	214.06	89	0.89	0.15	16.4	70	1.1
20890	2:01	214.08	90	0.67	0.12	16	71.33	1.83
20890	2:53	214.11	91	0.63	0.14	15.53	68.67	1.87
20890	3:03	214.13	92	0.72	0.28	15.17	75	2.93
20890	3:52	214.15	93	0.59	0.127	15	72	2.43
20890	4:02	214.17	95	0.65	0.1	15	83.33	3.2
20890	4:50	214.19	96	0.62	0.12	14.83	92	3.37
20890	5:01	214.21	97	0.63	0.14	15.27	96.67	3.4
20890	6:02	214.25	99	1.06	0.31	18.93	112	3.6
20890	6:51	214.27	101	1.88	0.39	20.7	114	3.67
20890	7:02	214.29	102	1.62	0.38	21.73	107.67	3.2
20890	8:00	214.33	104	2.22	0.75	23.37	90	3
20890	9:00	214.38	103	2.44	1.04	24.98	86.5	3.75
20890	12:00	214.5	107	2.91	0.91	30.43	90.75	3.9
20890	13:05	214.56	108	3.16	2.1	32.18	81.25	2.6
20890	14:00	214.58	109	2.43	1.3	32.5	75.33	3.43
20890	16:05	214.69	112	1.65	0.18	31.33	70	4.03
20890	17:01	214.71	113	1.77	0.24	30.93	71.33	4.17
20890	17:51	214.73	114	1.45	0.21	30.33	53	4.73
20890	18:01	214.75	116	1.48	0.22	29.7	53.33	5.43
20890	18:51	214.77	117	1.15	0.16	29	55	5.47
20890	19:01	214.79	118	1.49	0.19	28.13	51	6.63
20890	19:51	214.81	119	1.41	0.19	27.47	62.33	4.57
20890	20:01	214.83	120	1.83	0.22	27.03	65.67	5.43
20890	20:51	214.85	121	1.57	0.21	26.57	67	6.13
20890	22:01	214.92	125	1.58	0.28	23.6	93	4.47
20890	23:01	214.96	127	1.45	0.21	23.4	106	6.57
30890	0:01	215	129	1.5	0.24	23.3	111.67	6.63
30890	1:01	215.04	131	1.44	0.2	22.07	107	6.57
30890	2:51	215.1	135	1.42	0.23	21.1	109.67	6.5
30890	3:01	215.13	136	1.23	0.28	20.53	116	7.13
30890	3:51	215.15	137	1.18	0.21	20.37	118.67	6.13
30890	4:01	215.17	138	1.02	0.19	20.17	122.33	6.47
30890	4:51	215.19	140	1.15	0.21	20.3	120	6.47
30890	5:01	215.21	141	1.29	0.28	20.77	115.67	6.6
30890	6:01	215.25	143	1.19	0.24	21.47	110	6.3
30890	6:51	215.27	144	0.99	0.18	22.17	108	5.87
30890	7:01	215.29	145	1.26	0.27	23.03	181.33	4.47
30890	7:06	215.32	146	1.49	0.44	24.23	98.33	3.43
30890	8:05	215.35	147	2.06	0.11	25.93	93.25	2.85
30890	9:01	215.38	148	3.27	0.57	27.4	95	2.7
30890	9:51	215.4	150	2.58	0.42	28.73	91.67	2.3
30890	10:03	215.42	151	3.51	0.57	29.73	83.67	2.6
30890	11:00	215.46	152	2.76	0.42	31.13	80.25	3.25
30890	11:51	215.48	153	4.09	0.77	31.4	82.67	3.77
30890	12:02	215.5	154	4.57	0.64	31.77	86	3.33
30890	12:51	215.52	155	4.71	0.72	32.23	86.33	3
30890	13:01	215.54	157	3.87	0.64	32.73	112.33	2.93
30890	13:52	215.56	158	2.91	0.42	32.93	113	3.03
30890	14:02	215.58	160	3.4	0.7	33.2	87.33	2.37

30890	14:51	215.6	159	2.92	0.55	33.37	85.33	2.33
30890	16:03	215.68	164	4.53	0.78	32.53	75.33	3.33
30890	18:00	215.75	167	7.2	0.86	31.15	83	3.88
30890	20:00	215.83	170	5.44	0.49	28.18	83.5	4.35
30890	21:00	215.88	171	6.51	0.71	24.48	100.75	4.03
30890	22:00	215.92	172	4.59	0.36	22.53	108.25	4.5
30890	23:00	215.96	173	5.35	0.42	22.6	139	4.23
40890	0:00	216	174	4.48	0.31	21.15	173.25	2.73
40890	2:00	216.08	176	4.16	0.55	20.98	163.25	4.48
40890	4:00	216.17	178	3.86	0.41	20.7	157	4.2
40890	6:00	216.25	181	3.66	0.68	22.55	147.5	3.3
40890	7:00	216.29	182	5.23	1.33	24.43	161.75	2.23
40890	7:51	216.31	183	4.78	1.17	25.9	183	1.4
40890	8:01	216.33	184	5.54	1.21	27.77	225	0.97
40890	8:50	216.35	186	5.6	1.15	29.4	242.33	0.77
40890	9:51	216.4	188	6.8	2.03	31.67	265.67	2.97
40890	11:00	216.46	190	6.77	1.98	33.45	257	2.33
40890	11:51	216.48	191	7.16	1.89	33.8	225.67	2.43
40890	12:01	216.5	192	4.54	0.55	34.1	274.33	2.17
40890	13:00	216.54	193	4.98	0.58	34.43	322	1.95
40890	14:00	216.58	194	6.05	2.28	34.88	283	2
40890	16:01	216.67	197	5.85	1.26	34.27	262.33	3.13
40890	16:43	216.71	198	4.14	0.88	33.6	280.67	3.77
40890	18:02	216.75	201	4.49	0.76	32.03	259	2.83
40890	18:51	216.77	202	6.36	1.16	31.03	262.33	3.33
40890	19:02	216.79	203	5.27	0.75	29.9	264.33	3.23
40890	20:01	216.83	206	5.63	0.83	27.57	245.33	5.2
40890	22:00	216.92	208	5.01	0.69	25.33	272	5.53
50890	0:00	217	210	5.11	0.66	22.8	277.67	5.3
50890	2:00	217.08	213	4.72	0.9	21.2	259.67	2.2
50890	3:00	217.13	214	4.51	0.82	19.88	248.25	2.05
50890	4:00	217.17	215	3.14	0.47	18.5	223.75	2.78
50890	5:00	217.21	216	4.7	1.12	18.75	249.25	2.08
50890	6:00	217.25	217	4.64	1.46	20.53	290.33	1.5
50890	7:00	217.29	218	6.04	1.26	22.95	248.5	1.8
50890	8:00	217.33	219	5.59	1.24	25.6	266.5	4.25
50890	10:00	217.42	222	6.39	1.56	25.25	285.5	6.18
50890	12:07	217.5	224	5.47	1.76	25.43	308	5.5
50890	14:00	217.58	226	5.27	1.72	25.9	311	6.85
50890	15:00	217.63	227	4.75	1.58	24.6	311.25	8.38
50890	16:00	217.67	228	3.99	0.98	23.95	311	7.75
50890	17:00	217.71	229	2.92	0.8	22.38	329.75	8.53
50890	18:00	217.75	230	2.99	0.83	19.98	326.25	8.7
50890	19:00	217.79	232	2.26	0.54	18.95	318.25	6.78
50890	20:01	217.83	233	2.76	0.66	18.27	322	6.87
50890	21:00	217.88	234	2.41	0.56	17.3	317.33	7.07
50890	22:00	217.92	235	2.5	0.55	16.4	300.5	5.7
50890	23:00	217.96	236	2.3	0.59	14.97	290.33	5.33
60890	0:00	218	238	2.25	0.62	13.85	312.75	6.5
60890	1:00	218.04	239	2.17	0.65	13	311	5
60890	2:00	218.08	240	2.34	0.54	12.08	305.25	4.4
60890	3:00	218.13	241	1.29	0.27	11.2	307	4.55
60890	4:00	218.17	242	1.37	0.26	10.67	303	4.23
60890	5:00	218.21	243	1.4	0.26	11.13	297	4.07
60890	6:01	218.25	244	3.01	0.69	13.7	273	2.17
60890	11:02	218.46	253	2.65	0.64	16.1	326.67	7.87
60890	12:00	218.5	255	1.99	0.46	14.37	322	5.53
60890	13:03	218.54	256	2.18	0.7	16	342	2.8
60890	14:00	218.58	257	2.1	0.48	15.85	305	4.1

60890	15:05	218.63	258	1.97	0.32	16.03	286.67	4.9
60890	16:02	218.67	259	1.84	0.46	12.87	278.33	3
60890	17:25	218.72	260	1.16	0.17	13.3	307	3.3
60890	18:25	218.76	262	1.05	0.16	13.17	296.67	5.07
60890	19:28	218.8	263	0.84	0.14	13.03	286	4.63
60890	20:26	218.84	264	0.99	0.15	12.63	311	7.73
60890	21:26	218.89	265	0.76	0.11	12.17	306.67	5.87
60890	22:26	218.93	266	0.59	0.08	11.2	306.67	3.77
60890	23:04	218.96	267	0.79	0.1	10.53	296.33	4.7
70890	0:02	219	268	0.81	0.1	10.83	292.33	4.1
70890	1:02	219.04	269	0.99	0.16	10.8	286	3.87
70890	2:00	219.08	270	0.73	0.12	10.43	278.67	3.47
70890	3:00	219.13	272	0.81	0.15	10.37	273	3.3
70890	4:05	219.17	273	0.81	0.13	10.13	272	3.6
70890	5:01	219.21	274	1.42	0.36	10.3	275.33	4
70890	5:15	219.25	275	2.07	0.53	11.8	280	3.5
70890	7:04	219.29	276	2.26	0.64	12.73	286	3.97
70890	8:02	219.33	277	2.98	1.18	14.7	290.67	5
70890	9:02	219.38	278	2.31	1	16.03	311	4.4
70890	9:50	219.4	280	2.08	0.93	16.03	317.67	4
70890	10:00	219.42	281	2.38	1.41	16.23	314.33	3.53
70890	10:50	219.44	281	2.44	1.17	16.5	303.67	3.17
70890	11:26	219.47	282	1.4	0.53	17.1	315.33	3.1
70890	12:25	219.51	284	1.85	0.7	17.27	314.33	3.77
70890	13:01	219.54	285	2.16	1.43	19.17	310	3
70890	13:51	219.56	286	3.28	1.65	19.13	301.67	4.57
70890	14:01	219.58	288	2.93	1.53	19.4	313.33	5.07
70890	14:51	219.6	289	2.01	0.77	19.13	303.67	4.2
70890	15:02	219.63	290	2.41	0.84	19.23	297.67	5.93
70890	16:00	219.67	291	2.55	0.9	19.17	305.67	4.97
70890	16:42	219.71	292	2.46	1.06	18.87	306.67	4.83
70890	17:48	219.73	293	2.44	0.9	18.4	300	5.77
70890	18:00	219.75	294	2.18	0.67	17.95	300.5	4.48
70890	19:00	219.79	296	2.21	0.46	16.05	293.75	3.63
70890	20:00	219.83	297	2.33	0.52	14.35	302.5	3.3
70890	21:00	219.87	298	2.38	0.36	13.4	326	3.8
70890	22:00	219.92	299	2.09	0.33	12.38	342	2.13
70890	23:00	219.96	300	1.97	0.49	11.27	334.33	2.6
70890	24:00	220	302	1.29	0.18	10.57	316	2.73
80890	1:00	220.04	303	1.33	0.29	10.38	302.25	2.68
80890	2:00	220.08	304	1.72	0.41	10.18	297.25	2.25
80890	3:00	220.13	305	1.34	0.45	9.43	275	2.93
80890	4:00	220.17	306	1.54	0.39	9.48	286.75	3.3
80890	5:00	220.21	308	2.09	0.48	9.55	296	3.4
80890	6:03	220.25	309	2.05	0.4	11.17	283.67	2.9
80890	7:02	220.29	310	2.92	0.78	13.83	255.33	1.17
80890	8:00	220.33	311	3.21	1.02	15.88	297	2
80890	9:00	220.38	312	3.22	1.23	17.15	308	2.9
80890	9:50	220.4	313	2.81	1.17	17.63	302	2.73
80890	10:01	220.42	316	2.75	0.7	18.23	300.33	2.9
80890	10:50	220.44	314	2.89	1.01	18.93	301.67	3.53
80890	11:00	220.46	315	3.56	0.9	18.93	301	3.63
80890	11:51	220.48	318	2.47	0.92	19.8	277	3.33
80890	12:01	220.5	319	3.83	0.99	20.43	291	3.87
80890	13:02	220.54	320	2.99	0.74	20.53	276.33	4.07
80890	14:00	220.58	321	3.35	1.37	20.5	301.75	3.85
80890	15:00	220.63	322	2.91	1	20.17	321.67	3.17
80890	16:00	220.67	323	2.9	0.75	20.33	350.33	2.63
80890	17:00	220.71	324	3.74	0.94	19.85	338.25	2.8

80890	18:00	220.75	325	3.53	0.77	19.73	328.5	1.95
80890	19:00	220.79	326	3.2	0.65	17.78	331.5	0.93
80890	20:00	220.83	328	2.6	0.5	15.68	301.75	0.38
80890	21:00	220.88	329	2.72	0.51	14.28	233.25	0.78
80890	22:00	220.92	330	2.71	0.46	13.25	186.75	1.58
80890	23:00	220.96	331	2.41	0.42	12.5	242.25	2.5
90890	0:00	221	332	2.2	0.31	12.05	284.25	3.18
90890	1:00	221.04	334	1.69	0.18	11.95	288	3.4
90890	2:00	221.08	335	1.74	0.23	11.73	306.75	4.08
90890	3:00	221.13	336	2.04	0.22	11.33	303.5	2.95
90890	4:00	221.17	337	2.53	0.34	10.55	259	1.88
90890	5:00	221.21	338	2.26	0.5	10.8	213	2.65
90890	6:00	221.25	340	2.07	0.47	13.35	225.75	2.5
90890	7:02	221.29	341	2.82	0.67	16.8	223.33	1.43
90890	7:20	221.33	342	3.76	1.21	18.97	248	2.1
90890	9:03	221.38	344	4.66	1.39	20.8	278.33	2.43
90890	10:02	221.42	345	3.66	1.01	21.13	303	3.87
90890	11:03	221.46	346	4.48	1.88	22.53	286.67	2.97
90890	12:01	221.5	347	4.22	1.66	23.33	293.67	2.53
90890	13:02	221.54	348	4.76	1.49	24.7	268.33	2.43
90890	14:05	221.59	350	4.52	1.24	24.9	261.67	2.53
90890	16:02	221.67	351	4.44	0.96	25	263.33	2.63
90890	17:00	221.71	352	4.15	0.87	24.7	276.5	2.65
90890	18:00	221.75	353	4.09	0.86	24.03	278	3.15
90890	19:00	221.79	354	3.9	0.64	22.53	261.75	2.75
90890	20:00	221.83	355	2.97	0.39	20.35	218.25	2.08
90890	21:00	221.88	356	3.41	0.57	18.45	227.25	3.5
90890	22:00	221.92	358	3.45	0.38	17.28	240	5.05
90890	23:00	221.96	359	2.84	0.53	17.2	244.5	5.03
100890	0:00	222	360	2.42	0.26	17.33	252	4.98
100890	1:00	222.04	361	2.24	0.28	16.45	265.5	3.73
100890	2:00	222.08	362	2.27	0.29	15.53	238.75	5.28
100890	3:00	222.13	363	2.1	0.22	15.75	244.25	5.33
100890	4:00	222.17	364	2.41	0.44	15.55	265.75	5.63
100890	5:00	222.21	366	2.56	0.36	15.95	255.25	5.23
100890	6:00	222.25	367	2.18	0.36	16.97	259.67	5.3
100890	7:04	222.29	369	2.86	0.77	17.3	264	4.67
100890	8:00	222.33	370	3.09	0.79	17.9	273.33	4.37
100890	9:03	222.38	371	3.54	0.92	18.93	278	3.57
100890	10:08	222.42	372	3.8	0.96	19.7	274.67	2.63
100890	11:28	222.47	373	3.26	0.81	20.43	279.67	2.7
100890	13:26	222.55	374	4.02	1.06	22.5	291.33	3.03
100890	14:03	222.58	375	3.96	0.92	22.83	295	3.47
100890	17:00	222.71	380	3.03	0.7	23.17	317	2.93
100890	18:02	222.75	381	3.93	0.86	22.17	331.33	3.23
100890	19:01	222.79	382	3.09	0.47	20.5	236	0.53
100890	20:00	222.83	383	3.56	0.55	18.83	36.67	0.73
100890	21:00	222.88	384	2.84	0.48	17.23	98.67	1.43
100890	22:00	222.92	385	2.89	0.45	16.23	107.33	1.93
100890	23:00	222.96	386	2.56	0.2	15.77	138.67	2.87
110890	0:03	223	387	2.03	0.273	15.27	141	3.87
110890	1:00	223.04	388	3.01	0.24	15.7	135	4.6
110890	2:02	223.08	390	2.88	0.42	16.13	132.33	4.93
110890	3:00	223.13	391	2.97	0.32	16.87	133.67	5.03
110890	4:02	223.17	392	2.61	0.29	15.93	161.33	3.6
110890	5:02	223.21	393	2.2	0.37	16.17	178.67	2.33
110890	6:02	223.25	394	2.85	0.64	17.4	193	1.27
110890	7:02	223.29	395	2.75	0.45	19.17	167	2.27
110890	8:00	223.33	396	3.6	0.72	21.47	162	2.03

110890	9:02	223.38	397	4.76	0.9	24	196	1.2
110890	11:50	223.48	399	4.93	1.07	26.85	248.5	3.9
110890	12:01	223.5	401	5.97	1.26	27.6	257	3.37
110890	12:50	223.52	402	4.6	1.2	28.13	223.33	3.13
110890	13:00	223.54	403	6.09	1.5	28.27	227.33	2.73
110890	14:00	223.58	405	4.37	0.99	28.63	240.67	3.43
110890	14:50	223.6	406	4.62	1.18	29.07	248.33	3.33
110890	15:01	223.63	408	4.32	1.09	29	243	2.6
110890	16:01	223.67	410	4.6	1.01	29.1	253.5	2.75
110890	16:51	223.69	411	4.68	0.96	29	260	2.33
110890	17:02	223.71	412	4.54	0.8	28.53	264	1.7
110890	17:53	223.73	414	4.13	0.71	28.27	283.33	2.3
110890	18:00	223.75	415	4.09	0.63	27.4	327.33	1.47
110890	18:50	223.77	416	3.29	0.48	26.27	222.67	0.93
110890	19:00	223.79	417	5	0.69	25	42.67	1.2
110890	19:50	223.81	418	5.5	0.73	23.73	67.67	1.43
110890	20:00	223.83	419	4.97	0.74	23.25	98.5	2.85
110890	20:51	223.85	420	4.48	0.6	22.63	97.67	2.5
110890	21:00	223.87	422	3.2	0.38	21.67	95	2.33
110890	21:53	223.9	423	3.83	0.51	20.43	174.67	1.57
110890	22:04	223.92	424	3	0.39	20.33	81.67	1
110890	22:54	223.94	425	3.78	0.64	19.5	102	1.77
110890	23:00	223.96	426	2.52	0.29	18.4	125.67	1.5
110890	23:58	223.98	427	3.6	0.55	18.07	125.67	2.17
110890	0:00	224	428	3.37	0.48	17.75	121	1.9
120890	0:50	224.02	430	2.95	0.41	16.97	128.33	1.5
120890	1:24	224.04	431	2.96	0.39	16.8	128.33	2.27
120890	1:56	224.06	432	1.92	0.23	16.77	163.33	2.37
120890	2:00	224.08	433	1.88	0.17	16.63	159.67	2.47
120890	2:51	224.1	434	2.81	0.27	16.4	180.33	2.27
120890	3:02	224.13	436	2.53	0.16	15.43	210.67	0.87
120890	3:51	224.15	437	2.65	0.37	15.6	206	0.77
120890	4:02	224.17	438	1.95	0.23	15.3	183.67	0.93
120890	4:53	224.19	439	2.06	0.25	15.1	184.33	2
120890	5:01	224.21	440	2.11	0.36	15.83	192.67	2.13
120890	5:48	224.23	442	1.83	0.33	17.15	195	2.5
120890	6:00	224.25	443	3.25	0.76	18.67	206	3.63
120890	6:48	224.27	444	2.63	0.51	20.37	210	2.77
120890	7:00	224.29	445	3.65	1.03	21.63	213.33	1.03
120890	7:50	224.31	446	3.36	0.88	22.63	217.67	0.67
120890	8:00	224.33	447	4.69	1.37	24.03	225.67	0.3
120890	8:48	224.35	448	4.72	1.25	25.3	283.67	0.33
120890	9:00	224.37	450	4.17	1.09	26.57	321.33	0.87
120890	9:23	224.4	451	4.03	1.41	27.77	333.67	1.7
120890	10:00	224.42	452	5.63	1.86	28.4	346.67	1.17
120890	10:27	224.45	453	5.53	1.45	30	340	1.5
120890	11:03	224.48	454	5.81	1.98	31.17	288.67	1.93
120890	12:01	224.5	455	3.95	1.3	31.47	253	1.33
120890	12:51	224.52	456	5.78	1.99	31.77	79	1.7
120890	13:01	224.54	458	5.16	1.69	32.3	204.33	3.3
120890	13:51	224.56	459	4.75	1.42	32.47	247	2.8
120890	14:00	224.58	460	4.79	1.37	32.5	278	2.77
120890	14:53	224.61	461	4.79	1.27	32.8	259.33	3.43
120890	15:03	224.63	465	4.81	1.44	32.77	262.67	3.37
120890	15:50	224.65	462	4.64	1.12	32.6	268.67	2.13
120890	16:00	224.67	464	4.38	1.04	32.53	262.33	2.33
120890	16:50	224.69	466	3.76	0.85	32.27	248	2.73
120890	17:00	224.71	467	5.02	0.96	31.73	217.67	0.67
120890	17:50	224.73	468	4.8	0.76	30.83	218.33	2.7

120890	18:00	224.75	469	4.77	0.73	29.87	23	2.53
120890	18:50	224.77	471	2.97	0.49	28.47	18.67	4.43
120890	19:00	224.79	472	5.02	0.72	26.77	9	5.4
120890	19:50	224.81	473	5.03	0.63	26.1	33	4.3
120890	20:01	224.83	474	4.6	0.52	25.57	41	1.63
120890	20:51	224.85	475	3.93	0.51	24.8	85.33	1.83
120890	21:00	224.88	476	4.26	0.57	22.87	79.67	2.47
120890	21:50	224.9	477	3.05	0.36	22.73	71.67	3.13
120890	22:00	224.92	478	3.72	0.42	21.83	94	3.93
120890	22:50	224.94	479	3.64	0.45	21.77	110	3.03
120890	23:00	224.96	481	2.62	0.3	21.7	134.33	3.57
130890	0:00	225	482	2.76	0.26	22.28	197.75	5.35
130890	1:00	225.04	483	2.3	0.44	25.28	225	6.08
130890	2:00	225.08	484	1.4	0.25	24.58	229.5	8.3
130890	3:00	225.13	485	1.59	0.32	23.8	227	6.03
130890	3:10	225.17	486	1.81	0.36	23.4	231.67	8.1
130890	5:00	225.21	487	2.27	0.52	23.28	235.25	6.35
130890	6:00	225.25	489	2.28	0.48	23.33	237.5	5.45
130890	6:17	225.29	490	2.25	0.6	24.3	278.67	2.7

	A	B	C	D	E	F	G	H	I	J	K
1	Wind			HCHO					CH3CHO		
2	Direction	High	Low	Average	Std. Dev.	N	High	Low	Average	Std. Dev.	N
3	N\NE	5.1	0.8	2.8	1.6	17	1.1	0.1	0.5	0.3	17
4	NE\E	7.2	0.6	2.4	1.7	44	2.1	0.1	0.5	0.5	44
5	E\SE	6.5	0.6	2.9	1.3	51	0.9	0.1	0.4	0.2	51
6	SE\S	5.2	0.9	2.4	1.3	19	1.3	< 0.1	0.4	0.2	18
7	S\SW	5.5	1.2	2.9	1.2	35	1.7	0.2	0.6	0.4	35
8	SW\W	6.8	0.7	3.84	1.7	63	2.1	<0.1	0.9	0.5	60
9	W\NW	6.4	0.6	2.6	1.4	106	1.8	<0.1	0.7	0.5	105
10	NW\N	5.6	1.1	2.8	1.1	36	1.9	0.1	0.7	0.4	36

6.2 Summer - Winter 1990 Eifel Test Flights

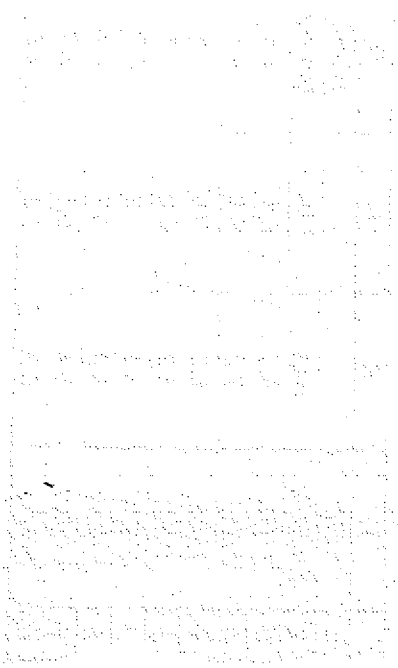

Date	Local Time	Local Time	Altitude	HCHO	Temperature	Wind	Cloud Amount	Cartridge
	Start	End	(km)	(ppt)	Celsius	Direction	% in-cloud	Number
11.6.90	11:28	11:48	1.5	880	2.5	315	0	1
11.6.90	11:51	12:11	1.5	1040	3.5	315	0	2
11.6.90	12:15	12:35	1.5	970	3.0	315	0	3
19.6.90	11:30	11:50	1.5	620	6.0	240	100	1
19.6.90	11:53	12:13	1.5	480	5.0	240	100	2
19.6.90	12:25	12:45	3.1	780	-3.5	240	50	3
19.6.90	12:48	13:03	3.1	500	-4.0	240	100	4
19.6.90	13:11	13:31	3.1	1100	-3.0	240	0	5
25.8.90	15:49	16:04	4.3	310	-10	270	50	1
25.8.90	16:06	16:26	3.5	470	0	270	100	2
25.8.90	16:29	16:49	3.5	310	0	270	100	3
25.8.90	16:51	17:11	3.5	305	0	270	50	4
25.8.90	17:22	17:37	1.5	570	14	270	100	5
7.11.90	10:39	10:59	3.4	600	-4.0	340	0	1
7.11.90	12:43	12:58	1.8	1270	3.0	340	0	8
7.11.90	13:00	13:15	1.8	840	3.0	340	0	9
7.11.90	13:22	13:36	1.5	550	-2.0	340	100	10

6.3 1991 Tropoz-II Flights

Date	Flight	Altitude	Altitude min.	Altitude max.	Cart.	Start Time	End Time	HCHO	CH3CHO	Amb. Temp.	Amb. Press.	Latitude	HCHO D.L.	Ozone
	Number	Km.	km	km	Number	UT	UT	ppt	ppt	Celcius	hPa		ppt	ppb
9.1.91	1	1.4	0.7	3.0	2	8:50	9:00	274	137	4.5	839	48.5	31	42.7
9.1.91	1	4.6	4.4	6.1	1	9:01	9:06	105	40	-13	606	48.6	102	38.3
9.1.91	1	8.4	8.4	8.4	5	9:20	9:40	51	0	-48	327	50.8	46	53.8
9.1.91	1	5.3	3.9	8.2	4	10:17	10:26	84	0	-24	523	55.0	77	71.7
9.1.91	2	2.0	1.3	4.4	9	12:15	12:22	151	44	-3	865	55.8	64	38.2
9.1.91	2	5.6	5.0	8.2	11	12:22	12:35	70	0	-24	560	56.4	64	61.7
9.1.91	2	2.4	0.8	5.3	10	14:13	14:21	180	80	-10	884	63.7	50	48.8
10.1.91	3	2.0	1.3	3.7	26	10:24	10:29	109	91	-9	874	64.0	71	31.4
10.1.91	3	5.3	4.7	8.0	23	10:30	10:42	141	0	-31	523	63.8	66	33.7
10.1.91	3	8.9	8.6	10.0	22	10:44	11:14	55	0	-61	307	64.1	47	85.4
10.1.91	3	8.4	6.1	10.0	25	11:15	11:37	54	0	-46	331	65.0	51	76.9
10.1.91	3	8.7	8.4	9.4	17	11:38	12:08	50	0	-61	333	66.0	47	72.7
10.1.91	3	5.7	4.4	9.3	19	12:09	12:29	70	0	-35	598	66.6	61	76.2
10.1.91	3	2.1	1.5	3.1	20	12:30	12:40	223	153	-20	839	66.8	33	47
11.1.91	5	2.8	2.1	6.9	28	15:35	15:45	140	0	-10	744	53.0	68	37.7
11.1.91	5	5.7	3.4	10.5	31	16:45	16:59	90	0	-21	533	46.1	77	59.4
11.1.91	6	3.1	1.8	5.2	33	21:18	21:27	191	75	-13	704	44.5	71	45
11.1.91	6	7.0	6.2	9.0	39	21:29	21:45	55	0	-32	422	44.3	49	43.6
11.1.91	6	5.5	4.1	8.3	37	23:02	23:15	107	40	-1	527	33.8	85	45.4
11.1.91	6	2.0	1.3	3.3	38	23:16	23:23	280	53	5	814	33.0	77	32.4
12.1.91	7	1.0	0.7	2.3	57	18:15	18:20	535	93	19	923	32.2	64	37.1
12.1.91	7	7.5	6.9	8.7	58	18:33	18:44	53	0	-10	393	30.5	52	30.9
12.1.91	7	8.4	8.4	8.4	50	20:10	20:41	43	0	-22	342	19.0	40	32.7
12.1.91	7	6.1	5.1	8.4	49	20:43	20:57	101	0	-3	486	16.7	80	44.6
12.1.91	7	2.1	1.3	3.3	54	20:59	21:06	508	60	16	808	16.3	53	37.2
15.1.91	8	1.3	0.6	2.2	65	15:10	15:15	326	68	17.7	873	16.1	72	30.9
15.1.91	8	4.0	3.5	5.8	63	15:18	15:27	247	0	0	623	15.7	77	48.8
15.1.91	8	7.1	6.3	8.9	61	15:28	15:44	105	0	-10.5	414	14.9	82	38.4
15.1.91	8	6.0	4.7	8.9	64	16:24	16:31	149	0	1	494	11.3	137	41.1
15.1.91	8	1.5	0.6	3.4	68	16:32	16:38	422	94	21	862	10.8	82	39.8
15.1.91	9	0.8	0.3	1.4	71	18:31	18:36	615	46	21	920	10.8	79	31.1
15.1.91	9	3.5	2.5	5.2	75	18:38	18:47	135	0	90	653	10.8	72	35
15.1.91	9	6.7	6.3	8.1	74	18:49	19:02	101	0	-10	429	10.1	89	27.4

Date	Flight	Altitude	Altitude min.	Altitude max.	Cart.	Start Time	End Time	HCHO	CH3CHO	Amb. Temp.	Amb. Press.	Latitude	HCHO D.L.	Ozone
	Number	Km.	km	km	Number	UT	UT	ppt	ppt	Celcius	hPa		ppt	ppb
15.1.91	9	8.7	8.6	9.4	72	19:05	19:41	50	0	-26	318	8.4	47	42.6
15.1.91	9	6.1	4.7	9.9	76	20:25	20:34	142	0	-4	480	3.7	125	40
15.1.91	9	1.9	1.3	3.2	70	20:36	20:42	1970	70	23	808	3.4	80	50.3
16.1.91	10	1.9	1.5	3.5	82	16:38	16:44	614	173	20.5	817	3.5	96	18
16.1.91	10	4.7	4.4	6.1	81	16:46	16:54	221	57	2	570	3.2	99	14.2
16.1.91	10	7.0	6.8	7.7	84	16:56	17:22	157	0	-13	413	2.1	44	31.2
16.1.91	10	2.1	0.6	4.4	78	17:51	17:57	784	27	22	810	-1.8	76	30.9
16.1.91	11	0.7	0.5	1.5	94	20:09	20:17	1250	50	25	926	-2.2	47	23.6
16.1.91	11	1.5	1.5	1.5	87	20:19	20:28	439	50	16	846	-2.1	41	18.5
16.1.91	11	3.4	2.6	5.5	93	20:30	20:39	240	40	13	676	-2.3	74	20.4
16.1.91	11	9.8	9.7	10.2	85	21:05	21:45	55	0	-36	271	-6.2	54	29.4
16.1.91	11	3.5	3.0	4.3	91	22:19	22:27	202	0	8	587	-10.7	68	29.8
16.1.91	11	1.5	0.9	3.0	88	22:28	22:39	418	33	20	845	-11.4	41	24.2
16.1.91	11	0.4	0.2	0.9	86	22:40	22:45	313	60	23	964	-11.9	93	14.9
18.1.91	12	1.1	0.4	2.7	99	16:03	16:10	381	54	19	904	-12.3	73	16.1
18.1.91	12	4.3	3.7	6.1	95	16:12	16:21	195	0	5.1	597	-13.1	127	23.1
18.1.91	12	7.3	6.7	8.8	98	16:23	16:39	115	0	-11	395	-14.2	96	23.7
18.1.91	12	3.5	3.0	4.0	101	17:57	18:03	370	0	10.4	663	-21.1	60	32
18.1.91	12	2.9	2.9	3.1	97	18:05	18:15	356	42	11	711	-21.9	104	24.1
18.1.91	13	0.9	0.3	2.6	107	20:28	20:35	242	58	17	905	-23.7	79	17.5
18.1.91	13	3.9	3.3	5.5	108	20:36	20:45	106	0	8	625	-24.4	91	36.2
18.1.91	13	6.8	6.1	8.7	109	20:47	21:05	85	0	-9	421	-25.7	73	30
18.1.91	13	9.4	9.2	10.0	111	21:08	21:47	64	0	-31	286	-28.7	65	38.2
18.1.91	13	3.8	3.6	5.1	106	22:00	22:07	151	0	0	629	-32.0	122	36.8
18.1.91	13	2.6	2.6	2.6	105	22:09	22:22	393	93	8.3	729	-32.8	53	34.8
21.1.91	14	1.3	0.9	2.7	116	13:17	13:24	690	105	12	876	-33.6	83	28.3
21.1.91	14	4.3	3.6	5.9	117	13:25	13:33	195	0	0	600	-34.3	147	39.5
21.1.91	14	1.8	1.1	3.8	113	14:48	14:54	237	41	5	825	-41.2	96	19.3
21.1.91	15	1.0	0.4	2.9	158	17:11	17:18	390	95	9	912	-41.6	92	13.1
21.1.91	15	4.4	4.1	5.9	156	17:20	17:29	220	0	-7	596	-42.3	143	18.9
21.1.91	15	5.0	3.3	9.5	153	19:42	19:51	156	0	-20	577	-55.3	138	42.2
21.1.91	15	2.4	1.7	4.5	159	19:53	20:00	214	75	-50	767	-55.3	91	17.9
21.1.91	15	4.1	3.9	5.2	160	20:02	20:14	285	0	-15	615	-54.4	77	39.9

Date	Flight	Altitude	Altitude min.	Altitude max.	Cart.	Start Time	End Time	HCHO	CH3CHO	Amb. Temp.	Amb. Press.	Latitude	HCHO D.L.	Ozone
	Number	Km	km	km	Number	UT	UT	ppt	ppt	Celcius	hPa		ppt	ppb
22.1.91	16	1.1	0.5	2.9	120	12:44	12:50	234	90	2	884.2	-52.9	87	15.2
22.1.91	16	4.5	4.3	5.9	124	12:52	12:57	199	0	-20	569	-52.3	200	29.8
22.1.91	16	1.5	0.6	3.3	126	13:57	14:04	360	118	13	839.8	-46.0	89	16.3
22.1.91	17	1.2	0.6	2.0	133	16:21	16:29	427	71	18	872.1	-45.8	61	13.7
22.1.91	17	4.1	3.1	5.9	128	16:31	16:40	135	0	-5	597	-45.5	104	38.5
22.1.91	17	7.1	6.8	8.2	134	16:42	16:55	121	0	-28	397.5	-44.6	107	36.2
22.1.91	17	2.1	0.6	4.5	129	18:28	18:38	527	80	15	799.9	-35.1	83	31.1
23.1.91	18	1.0	0.4	2.7	138	13:50	13:58	980	102	20	911.8	-34.8	59	36.6
23.1.91	18	4.1	3.4	5.8	137	13:59	14:07	193	0	0	614.8	-34.6	108	38.0
23.1.91	18	7.1	6.6	8.9	141	14:09	14:22	90	0	-20	410.6	-33.9	95	34.1
23.1.91	18	9.4	9.2	10.1	143	14:24	14:50	65	0	-40	287.6	-32.3	58	31.4
23.1.91	18	5.9	4.6	8.8	139	14:53	15:01	187	0	-15	494.1	-30.7	137	35.4
23.1.91	18	1.4	0.5	2.5	140	15:03	15:07	1010	87	18	869.5	-30.2	104	32.0
23.1.91	19	1.6	0.5	4.1	145	17:14	17:24	685	136	18	850.2	-29.9	50	26.7
23.1.91	19	6.0	5.3	8.0	147	17:27	17:41	124	0	-10	480.6	-29.1	70	33.1
23.1.91	19	8.9	8.5	10.1	151	17:43	18:09	79	0	-30	315.3	-27.2	83	29.3
23.1.91	19	2.1	1.6	3.1	146	18:50	18:57	698	91	15	793.8	-23.0	69	36.9
25.1.91	20	1.1	0.8	2.1	174	13:11	13:17	740	87	18	885.8	-22.7	70	25.0
25.1.91	20	4.0	3.5	6.1	176	13:19	13:28	376	0	3	623.1	-22.2	112	26.5
25.1.91	20	7.2	6.5	8.9	173	13:29	13:44	141	0	-17	404.7	-21.2	105	36.9
25.1.91	20	9.4	9.2	10.1	171	13:46	14:27	67	0	-36	290.4	-18.6	56	40.6
25.1.91	20	6.0	4.1	9.8	175	14:52	15:01	147	0	-7	493	-13.9	160	45.7
25.1.91	20	1.5	0.8	3.0	170	15:02	15:07	875	109	15	852.8	-13.2	170	32.3
25.1.91	21	1.2	0.8	3.0	169	16:35	16:41	644	118	20	890	-12.7	89	26.2
25.1.91	21	4.2	4.0	5.7	168	16:43	16:49	263	0	-1	602.6	-12.1	131	33.5
25.1.91	21	7.0	6.4	9.0	164	16:51	17:07	131	0	-15	416	-11.0	96	45.5
25.1.91	21	9.4	9.3	10.1	167	17:09	17:50	62	0	-38	288.3	-8.1	58	48.3
25.1.91	21	6.1	4.6	9.4	165	17:58	18:07	106	0	-10	487.5	-4.7	95	37.9
25.1.91	21	1.7	1.0	3.5	166	18:08	18:14	426	99	18	829.5	-4.1	80	29.1

Date	Flight	Altitude	Altitude min.	Altitude max.	Cart.	Start Time	End Time	HCHO	CH3CHO	Amb. Temp.	Amb. Press.	Latitude	HCHO D.L.	Ozone
	Number	Km	km	km	Number	UT	UT	ppt	ppt	Celcius	hPa		ppt	ppb
25.1.91	22	1.5	0.7	3.2	189	20:19	20:27	580	150	18	858.4	-3.5	65	26.1
25.1.91	22	5.1	4.2	7.0	188	20:29	20:42	248	0	-7	541	-2.6	78	27.8
25.1.91	22	7.9	7.6	9.1	186	20:44	20:58	99	0	-23	361.2	-1.2	96	33.2
25.1.91	22	2.5	1.5	3.1	184	21:26	21:33	309	34	15	750.2	2.1	72	22.0
25.1.91	22	3.6	2.8	5.7	181	21:34	21:43	288	0	0	656.9	1.7	91	28.4
25.1.91	22	7.0	6.4	8.8	177	21:45	22:00	134	0	-15	417.1	1.2	99	35.8
25.1.91	22	9.6	9.3	10.7	182	22:02	22:43	74	0	-35	281.8	-2.1	75	40.4
25.1.91	22	6.0	4.5	9.7	185	23:12	23:24	183	0	-8	495.9	-7.0	107	57.0
25.1.91	22	1.8	1.0	3.4	183	23:26	23:33	596	145	18	826.3	-7.6	79	35.2
29.1.91	25	0.4	0.2	0.9	209	15:06	15:13	835	65	25	965.6	5.3	69	45.9
29.1.91	25	2.3	1.7	3.9	210	15:14	15:21	706	0	17	766.2	5.5	88	48.6
29.1.91	25	5.3	5.1	6.1	201	15:24	15:38	348	0	-10	515.4	6.5	85	49.9
29.1.91	25	2.3	0.7	3.4	207	15:42	15:51	1840	103	20	764.6	7.7	59	53.4
29.1.91	25	5.9	4.8	6.1	200	15:58	16:16	283	0	-8	550.1	8.7	55	42.9
29.1.91	25	1.7	0.6	2.0	205	16:20	16:29	2430	126	30	824.4	9.5	48	60.6
29.1.91	25	5.5	3.8	6.3	204	16:34	16:47	271	0	-5	578.3	9.0	79	42.5
29.1.91	25	3.6	2.6	5.8	206	17:10	17:17	400	0	0	664.7	6.7	98	41.7
29.1.91	25	1.5	1.5	1.5	203	17:19	17:26	1210	90	21	839.5	6.1	67	58.1
29.1.91	25	0.9	0.6	1.5	208	17:28	17:34	1160	79	23	908	5.6	81	48.1
30.1.91	26	0.8	0.3	2.3	218	15:01	15:07	1080	92	23	924.4	5.3	69	46.2
30.1.91	26	3.8	3.3	5.6	216	15:09	15:18	262	0	0	629.8	5.9	78	32.0
30.1.91	26	6.1	6.3	6.4	217	15:20	15:35	207	0	-10	463.6	7.1	57	44.5
30.1.91	26	2.9	1.6	4.0	215	15:39	15:47	964	120	12	725.7	8.5	62	50.8
30.1.91	26	0.5	0.4	0.7	220	15:49	15:58	1480	128	35	944.8	9.1	38	54.6
30.1.91	26	1.8	1.9	3.3	221	16:02	16:10	1200	196	20	812.6	9.2	66	51.7
30.1.91	26	1.6	0.6	1.6	222	16:11	16:16	1390	171	30	834.2	9.2	80	51.1
30.1.91	26	1.8	1.5	3.2	211	16:17	16:24	1950	261	20	815.3	9.3	70	56.9
30.1.91	26	1.1	0.6	1.3	212	16:25	16:31	2430	222	30	879.8	9.3	61	73.1
30.1.91	26	2.3	1.5	4.2	213	16:35	16:42	1370	217	16	771.2	8.9	74	56.4

Date	Flight	Altitude	Altitude min.	Altitude max.	Cart.	Start Time	End Time	HCHO	CH3CHO	Amb. Temp.	Amb. Press.	Latitude	HCHO D.L.	Ozone
	Number	Km	km	km	Number	UT	UT	ppt	ppt	Celcius	hPa		ppt	ppb
30.1.91	26	6.1	5.1	8.8	214	16:44	17:10	207	0	-20	469.8	7.6	48	46.4
30.1.91	26	7.3	7.0	7.8	265	17:12	17:28	101	0	-15	389.6	6.5	76	62.4
30.1.91	26	3.8	2.9	5.9	266	17:29	17:36	220	80	5	639.6	6.2	94	44.2
31.1.91	27	1.2	0.3	3.6	232	9:33	9:44	1660	125	15	749.9	5.5	38	49.2
31.1.91	27	4.5	4.7	6.1	226	9:46	10:02	326	0	-5	573	6.2	51	42.5
31.1.91	27	1.6	0.5	3.5	225	10:03	10:11	1420	127	20	843.7	6.9	45	44.4
31.1.91	27	2.0	1.4	3.9	229	10:12	10:19	998	142	15	801.9	7.3	64	50.8
31.1.91	27	5.5	4.7	7.3	227	10:20	10:31	231	0	-11	512.8	7.8	80	46.8
31.1.91	27	8.2	7.7	9.5	230	10:32	10:53	99	0	-24	345.9	8.5	79	46.7
31.1.91	27	2.5	1.9	5.5	233	12:27	12:37	748	165	5	761.1	14.4	59	44.2
31.1.91	28	1.3	0.4	3.7	234	14:33	14:43	869	120	13	883.6	15.1	38	37.0
31.1.91	28	4.7	4.7	6.5	237	14:45	15:09	233	70	-14	569.7	16.7	37	41.4
31.1.91	28	2.2	1.1	3.2	235	15:11	15:16	644	97	17	791.2	18.0	84	38.4
31.1.91	28	3.4	2.5	5.8	238	15:17	15:28	229	80	-5	686.6	18.7	66	47.0
31.1.91	28	7.0	6.3	8.9	240	15:29	15:44	73	0	-30	414.9	19.9	80	46.7
31.1.91	28	9.6	9.4	10.2	241	15:45	16:21	56	0	-45	282.4	22.6	42	49.0
31.1.91	28	6.4	5.0	9.6	239	16:36	16:46	117	0	-29	464.7	26.7	98	53.1
31.1.91	28	1.8	0.9	3.6	242	16:47	16:54	391	106	12	834	27.5	62	42.5
1.2.91	29	0.9	0.4	2.2	250	10:27	10:32	581	177	12	931.9	28.1	85	44.7
1.2.91	29	3.9	3.6	5.7	248	10:34	10:41	144	0	-14	638.4	28.7	119	45.8
1.2.91	29	7.0	6.2	8.8	247	10:42	10:55	108	0	-32	421.6	29.6	95	42.8
1.2.91	29	2.4	1.1	5.1	245	12:15	12:26	386	0	0	785.5	38.2	60	49.3
1.2.91	30	1.5	0.8	3.1	252	14:29	14:36	598	186	4	893.2	38.9	83	39.6
1.2.91	30	4.7	4.2	6.2	255	14:37	14:44	211	0	-22	568.1	39.3	119	46.8
1.2.91	30	2.7	2.0	4.8	258	16:23	16:30	356	175	-10	743.4	48.0	94	47.0

Literature

Adewuyi, Y.G., S.Y. Cho, R.P. Tsay, and G.R. Carmichael, Importance of formaldehyde in cloud chemistry, Atmos. Environ., 18, 2413-2420, 1984

Altshuller, A.P., Nonmethane organic compound to nitrogen oxide ratios and organic composition in cities and rural areas, J. Air Poll. Control Asso., 39, 936-943, 1989

Altshuller, A.P., Review: Natural volatile organic substances and their effect on air sampling in the United States, Atmos. Environ., 17, 2131-2165, 1983

Altshuller, A.P., and S.P. McPherson, Spectrophotometric analysis of aldehydes in the Los Angeles atmosphere, J. Air Poll. Control Assoc. 13, 109-111, 1963

Arlander, D.W., Measurements of organic acids and their precursors in the remote marine troposphere, MSc. Thesis, College of Engineering, Washington State University, May 1988

Arlander, D.W., D.R. Cronn, J.C. Farmer, F.A. Menzia, and H.H. Westberg, Gaseous oxygenated hydrocarbons in the remote marine troposphere, J. Geophys. Res., 16391-16403, 1990

Arnts, R.R., and S.B. Tejada, 2,4-Dinitrophenylhydrazine-coated silica gel cartridge method for the determination of formaldehyde in air: Identification of an ozone interference, Environ. Sci. Technol., 23, 1428-1430, 1989

Atkinson, R., Gas-phase tropospheric chemistry of organic compounds: A review, Atmos. Environ., 24A, 1, 1-41, 1990

Atkinson, R., and W.P.L. Carter, Kinetics and mechanisms of the gas-phase reactions of ozone with organic compounds under atmospheric conditions, Chem. Rev., 84, 437-470, 1984

Bächmann, K., H. Bauer, and W. Schmied, Determination of aldehydes and carboxylic acids in atmospheric samples, Fresenius Z. Analy. Chem., 333, 715, 1989

Beasley, R.K., C.E. Hoffman, M.L. Rueppel, and J.W. Worley, Sampling of formaldehyde in air with coated solid sorbent and determination by high performance liquid chromatography, Analy. Chem., 52, 1110-1114, 1980

Burrows, J.P., G.K. Moortgat, G.S. Tyndall, R.A. Cox, M.E. Jenkins, G.D. Hayman, and B. Veyret, Kinetics and mechanism of the photooxidation of formaldehyde, 2. Molecular modulation studies, J. Phys. Chem., 93, 2375-2382, 1989

Calvert, J.G., The homogeneous chemistry of formaldehyde generation and destruction within the atmosphere, Federal Aviation Agency Report No. FAA-EE-80, 153-190, 1980

Carlier, P., P. Fresnet, V. Lescoat, S. Pashalidis, and G. Mouvier, Formaldehyde background levels over the Atlantic Ocean during the Polarstern crossing from Bremerhaven to Rio Grande Do Sul, in Physico-Chemical Behaviour of Atmospheric Pollutants, Varese Symposium 1989, ed. G. Restelli and G. Angeletti, Kluwer Academic Publishers, 1990

Carlier, P., H. Hannachi, and G. Mouvier, The chemistry of carbonyl compounds in the atmosphere - A review, Atmos. Environ., 20, 2079-2099, 1986

Chameides, W.L., and D.D. Davis, Aqueous-phase source of formic acid in clouds, Nature, 304, 427-429, 1983

Chapman, E.G., D.S. Sklarew, and F.S. Flickinger, Organic acids in springtime Wisconsin precipitation samples, Atmos. Environ., 20, 1717-1725, 1986

Cofer, W.R., III, R.A. Edahl, Jr., A new technique for collection, concentration and determination of gaseous tropospheric formaldehyde, Atmos. Environ., 20, 979-984, 1986

Dasgupta, P.K., S. Dong, H. Hwang, H-C. Yang, and Z. Gensa, Continuous liquid phase fluorometry coupled to a diffusion scrubber for the determination of atmospheric formaldehyde, hydrogen peroxide, and sulfur dioxide, Atmos. Environ., 22, 949-964, 1988

Drummond, J.W., D.H. Ehhalt, and A. Volz, Measurements of nitric oxide between 0-12 km altitude and 67^{o} N to 60^{o} S latitude obtained during STRATOZ-III, J. Geophys. Res., 93, 15831-15841, 1988

Druzik, C.M., D. Grosjean, A. Van Neste, and S.S. Parmer, Sampling of atmospheric carbonyls with small dnph-coated c-18 cartridges and liquid chromatography analysis with diode array detection, Inter. Jour. Environ. Analy. Chem., 38, 495-512, 1990

Ehhalt, D.H., J. Rudolph, F. Meixner, and U. Schmidt, Measurements of selected C_2 - C_5 hydrocarbons in the background troposphere: Vertical and latitudinal variations, J. Atmos. Chem., 3, 29-52, 1985

Ehhalt, D.H., Free radicals in the atmosphere, Free Rad. Res. Comm., Vol. 3, No. 1-5, pp. 153-164, Harwood Academic Publishers GmbH, 1987

Ehhalt, D.H. and J. W. Drummond, NO_x sources and the tropospheric distribution of NO_x during STRATOZ-III, in Tropospheric Ozone, I.S.A. Isaksen (ed.), D. Reidel Publishing Company, 217-237, 1988

Eichman, R., G. Ketseridis, G. Schebeske, J. Hahn, P. Warneck, and C. Junge, n-Alkane studies in the troposphere - I. Gas and particulate concentrations in north Atlantic air, Atmos. Environ., 13, 587-599, 1979

Finlayson-Pitts, B.J., J.N. Pitts, II., Atmospheric chemistry: Fundamentals and experimental techniques, John Wiley and Sons, Inc., N.Y., 1986

Fung, K., and D. Grosjean, Determination of nanogram amounts of carbonyls as 2,4-dinitrophenylhydrazones by high-performance liquid chromatography, Analy. Chem., 53, 168-171, 1981

Galloway, J.N., G.E. Likens, W.C. Keene, and J.M. Miller, The composition of precipitation in remote areas of the world, J. Geophys. Res., 87, 8771-8786, 1982

Graedel, T. The kinetic photochemistry of the marine troposphere, J. Geophys. Res., 84, 273-286, 1979

Grosjean, D., Formaldehyde and other carbonyls in Los Angeles ambient air, Environ. Sci. Technol., 16, 254-262, 1982

Grosjean D., and K. Fung, Collection efficiencies of cartridges and microimpingers for sampling of aldehydes in air as 2,4-dinitrophenylhydrazones, Analy. Chem., 54, 1221-1224, 1982

Grosjean, D., Atmospheric chemistry of toxic contaminants. 2. Saturated aliphatics: Acetaldehyde, dioxane, ethylene, glycol ethers, propylene oxide, J. Air Waste Manage. Assoc. 40, 1522-1531, 1990a

Grosjean, D., Gas-phase reaction of ozone with 2-methyl-2-butene: Dicarbonyl formation from Criegee biradicals, Environ. Sci. Technol., 24, 1428-1432, 1990b

Guenier, J.P., P. Simon, J. Delcourt, M.F. Didierjean, C. Lefevre, and J. Muller, Air-sampling of aldehydes-applications of chromatographic determination of formaldehyde and acetaldehyde, Chromatographia, 18, 137-144, 1984

Harris, G.W., G.I. Mackay, T. Iguchi, L.K. Mayne, and H.I. Schiff, Measurement of formaldehyde in the troposphere by tunable diode laser spectroscopy, J. Atmos. Chem., 8, 119-137, 1989

Hauser, T.R., and R.L. Cummins, Increasing sensitivity of 3-methyl-2-benzothiazolone hydrazone. Test for analysis of aliphatic aldehydes in air, Analy. Chem., 36, 679-681, 1964

Horowitz, A., C.J. Kershner, and J.G. Calvert, J. Phys. Chem., 86, 3094, 1982

Horowitz, A., J.G. Calvert, J. Phys. Chem., 86, 3105, 1982

Hough, A.M., The development of a two-dimensional global tropospheric model, 1, The model transport, Atmos. Environ., 23, 6, 1235-1261, 1989

Hough, A.M., Development of a two-dimensional tropospheric model: Model chemistry, J. Geophys. Res., 96, 7325-7362, 1991

Johnson, J.E., R.H. Gammon, J. Larson, T.S. Bates, S.J. Oltmans, and J.C. Farmer, Ozone in the marine boundary layer over the Pacific and Indian Oceans: Latitudinal gradients and diurnal cycles, J. Geophys. Res., 95, 11847-11856, 1990

Johnson, L., B. Josefsson, P. Marstorp, and G. Eklund, Determination of carbonyl compounds in automobile exhaust and atmospheric samples, Intern. Jour. Environ. Analy. Chem., 9, 7-26, 1981

Keene, W.C., J.N. Galloway, and J.D. Holdren, Measurement of weak organic acidity in precipitation from remote areas of the world, J. Geophys. Res., 88, 5122-5130, 1983

Kirschmer, P., Aldehydmessungen in der Aussenluft, Staub - Reinhaltung der Luft, 49, 263-266, 1989

Kleindienst, T.E., P.B. Shepson, C.M. Nero, R.R. Arnts, S.B. Tejada, G. I. Mackay, L.K. Mayne, H.I. Schiff, J.A. Lind, G.L. Kok, A.L. Lazrus, P.K. Dasgupta, and S. Dong, An intercomparison of formaldehyde measurement techniques at ambient concentrations, Atmos. Environ., 22, 9, 1931-1939, 1988

Kuwata, K., M. Urebori, H. Yamasaki, Y. Kuge, and Y. Kiso, Determination of aliphatic aldehydes in air by liquid chromatography, Analy. Chem., 55, 2013-2016, 1983

Lazrus, A.L., K.L. Fong, and J.A. Lind, Automated fluorometric determination of formaldehyde in air, Analy. Chem., 60, 1074-1078, 1988

Lelieveld, J., and P.J. Crutzen, Influences of cloud photochemical processes on tropospheric ozone, Nature, 343, 227- 233, 1990

Lelieveld, J., and P.J. Crutzen, The role of clouds in tropospheric photochemistry, J. Atmos. Chem., 12, 229-267, 1991

Levine, J.S., Global biomass burning: Atmospheric, climatic and biospheric implications, AGU-EOS, 71, 37, 1075-1077, 11 Sept. 1990

Lipari, F., and S.J. Swarin, 2,4-Dinitrophenylhydrazine-coated florisil sampling cartridges for the determination of formaldehyde in air, Environ. Sci. Technol., 19, 70-74, 1985

Liu, S.C., M. Trainer, F.C. Fehsenfeld, D.D. Parrish, E.J. Williams, D.W. Fahey, G. Hübler, and P.C. Murphy, Ozone production in the rural troposphere and the implications for regional and global ozone distributions, J. Geophys. Res., 92, 4191-4207, 1987

Logan, J.A., M.J. Prather, S.C. Wofsy, and M.B. McElroy, Tropospheric chemistry: A global perspective, J. Geophys. Res., 86, 7210-7254, 1981

Lowe, D., The tropospheric distribution of formaldehyde, Ph.D. Dissertation, Universität zu Köln, 1981, Jül-Bericht-1756, KFA Jülich, 1981

Lowe, D., and U. Schmidt, Formaldehyde in the clean troposphere, Second Symposium on the Composition of the Nonurban Troposphere, American Met. Soc., May 25-28, Williamsburg, Va., 288-291, 1982

Marenco, A., M. Macaigne, and S. Prieur, Meridional and vertical CO and CH_4 distributions in the background troposphere (70^{o} N - 60^{o} S; 0 - 12 Km altitude) from scientific aircraft measurements during the STRATOZ-III experiment (June 1984), Atmos. Environ., 23, 185-200, 1989

Matthews, T.G., and T.C. Howell, Solid sorbent for formaldehyde monitoring, Analy. Chem., 54, 1495-1498, 1982

McKeen, S.A., E.-Y.Hsie, M. Trainer, R. Tallamraju, and S.C. Liu, A regional model study of the ozone budget in the Eastern United States, J. Geophys. Res., 96, 10809-10845, 1991

Moortgat, G.K., and P. Warneck, CO and H_2 quantum yields in the photodecomposition of formaldehyde in air, J. Chem. Phys., 70, 3639, 1979

Mopper, K., W.L. Stahovec, and L. Johnson, Trace analysis of aldehydes by reversed-phase liquid-chromatography and precoloumn fluorigenic labeling with 5,5-dimethyl-1,3-cyclohexanedione, J. Chromatogra., 256, 243-252, 1983

Nash, T., The colorimetric estimation of formaldehyde by means of the Hantzsch reaction, J. Biochem., 55, 416-423, 1953

O'Hara, D., and H.B. Singh, Sensitive gas chromatographic detection of acetaldehyde and acetone using a reduction gas detector, Atmos. Environ., 22, 2613-2615, 1988

Otson, R., and P. Fellin, A review of techniques for measurement of airborne aldehydes, The Science of the Total Environment, 77, 95-131, 1988

Penner, J.E., C.S. Atherton, J. Dignon, S.J. Ghan, J.J. Walton, and S. Hameed, Tropospheric nitrogen: A three dimensional study of sources, distributions, and deposition, J. Geophys. Res., 96, 959-990, 1991

Pesez, M., and J. Bartos, Donnees nouvelles de spectrophotometrie ultraviolette en analyse organique fonctionnelle, Analusis, 1, 4, 257-262, 1972

Pierotti, D., Analysis of trace oxygenated hydrocarbons in the environment, J. Atmos. Chem., 10, 373-382, 1990

Platt, U., and D. Perner, Direct measurement of atmospheric CH_2O, HNO_2, O_3, NO_2, and SO_2 by differential optical absorption in the near UV, J. Geophys. Res., 85C, 7453, 1980

Przewosnik, M., Untersuchung der Festphasenderivatisierung von Aldehyden und Ketonen, Diplomarbeit, Universität zu Darmstadt, 1989

Röth, E.P., Description of a one-dimensional model for atmospheric chemistry, Jül-Bericht 2098, KFA Jülich November 1986

Rudolph, J., and D.H. Ehhalt, Measurements of C_2 - C_5 hydrocarbons over the North Atlantic, J. Geophys. Res., 86, 11959-11964, 1981

Rudolph, J., Two-dimensional distribution of light hydrocarbons: Results from the STRATOZ-III experiment, J. Geophys. Res., 93, 8367-8377, 1988

Sawicki, E, and C.R. Sawicki, Aldehydes - Photometric analysis, Vol. 1, Academic Press, London, 283 pages, 1975

Schmidt, U., and D.C. Lowe, Vertical profiles of formaldehyde in the troposphere, Proceedings of the Second European Symposium on Physico-Chemical Behaviour of Atmospheric Pollutants, (ed. B Versino, H. Ott), D. Reidel Publishing Co. Dordrecht , 377-386, 1981

Schmied, W., Entwicklung einer Bestimmungsmethode für Carbonylverbindungen in der Troposphäre, Diplomarbeit, Universität zu Darmstadt, 1988

Schubert, B., U. Schmidt und D.H. Ehhalt, Untersuchungen zum Nachweis und zur Chemie von Formaldehyd und Acetaldehyd in der unteren Troposphäre, Ph.D. Dissertation, Universität zu Köln, 1988, Jül-Bericht 2257, KFA Jülich, Dezember 1988

Shriner, R. L., R.C. Fuson, and D.Y. Curtain, T.C. Morrill, The Systematic Identification of Organic Compounds, Sixth Edition, John Wiley and Sons, Inc., New York., 1980

Singh, H.B., and J.F. Kasting, Chlorine-hydrocarbon photochemistry in the marine troposphere and lower stratosphere, J. Atmos. Chem., 7, 3, 261-285, 1988

Singh, H.B., and P.L. Hanst, Peroxyacetylnitrate (PAN) in the unpolluted atmosphere: an important reservior for NO_x, Geophys. Res. Lett., 8, 941-944, 1981

Smith, D.F., T.E. Kleindienst, and E.E. Hudgens, Improved high-performance liquid chromatographic method for artifact-free measurements of aldehydes in the presence of ozone using 2,4-dinitrophenylhydrazine, J. Chromatogra., 483, 431-436, 1989

Stahovec, W.L., and K. Mopper, Trace analysis of aldehydes by pre-coloumn fluorigenic labeling with 1,3-cyclohexanedione and reversed-phase high-performance liquid-chromatography, J. Chromatogra., 298, 399-406, 1984

Tanner, R.L., A.H. Miguel, J.B. de Andrade, J.S. Gaffney, and G.E. Streit, Atmospheric chemistry of aldehydes: Enhanced peroxyacetyl nitrate formation from ethanol-fueled vehicular emissions, Environ. Sci. Technol., 22, 1086-1034, 1988

Tejada, S.B., Evaluation of silica gel cartridges coated in-situ with acidified 2,4-dinitrophenylhydrazine for sampling aldehydes and ketones in air, Inter. Jour. of Environ. Analy. Chem., 26, 167-185, 1986

Thompson, A.M., Wet and dry removal of tropospheric formaldehyde at a coastal site, Tellus, 32, 376-383, 1980

Vaghjiani, G.L., and A.R. Ravishankara, New measurement of the rate coefficient for the reaction of OH and methane, Nature, 350, 406-409, 1991

Westberg, H., and L. MacGregor, Nonmethane organic carbon concentrations in air masses advected into urban areas in the United States, Atmospheric Sciences Research Laboratory, United States Environmental Protection Agency, Research Triangle Park, NC 27711. Report Nr. EPA/600/53-87/045, 1987

Zafiriou, O.C., J. Alford, M. Herrera, E.T. Peltzer, R.B. Gagosian, and S.C. Liu, Formaldehyde in remote marine air and rain: Flux measurements and estimates, Geophys. Res. Lett., 7, 341-344, 1980

Zhou, X., and K. Mopper, Measurement of sub-parts-per-billion levels of carbonyl compounds in marine air by a simple cartridge trapping procedure followed by liquid chromatography, Environ. Sci. Technol. 24, 1482-1485, 1990

Zimmerman, P.R., R.B. Chatfield, J. Fishman, P.J. Crutzen, and P.L. Hanst, Estimates on the production of CO and H_2 from the oxidation of hydrocarbon emissions from vegetation, Geophys. Res. Lett., 5, 679-682, 1978

FORSCHUNGSZENTRUM JÜLICH GmbH

KFA

Jül-2650
July 1992
ISSN 0366-0885